Investigation of the processes causing the degradation of the sandstone used on the Thorn church based on mineralogical analysis.

Author: J. Kalpoe

BSc. Thesis

Faculty of Civil Engineering and Geoscience, Delft University of Technology, Geo-Engineering

Delft, 2017

Supervisors:
Dr. Ir. D. J. M. Ngan-Tillard
Jack Voncken

Abstract

The rapid degradation of the Thorn-sandstone could be explained by the presence of organics or minerals such as swelling glauconite, oxidized glauconite or non-swelling clays sensitive to hydric variations despite being non-swelling. A variety of tests and observations have been carried out to identify the most likely process of degradation. Conventional optical microscopic observations, XRF and XRD analyses, Methylene Blue tests on rock powder, Methylene Blue staining of thin-sections, and Loss-on-Ignition have been conducted as well as more advanced observations using X-ray micro-computed tomography (micro-CT) and Scanning Electronic Microscopy (SEM). The micro-CT scans allowed the visualization of the grain arrangement in 3D along with the network of micro-fissures spread around within the material. The SEM combined with EDEX measurements allowed the visualization of grains in 2D in great detail along with determining chemical elements at the sub-grain scale. Combined results showed that the Thorn-sandstone consists of quartz grains along with some grains of hematite, rutile or ilmenite. Porosity (excluding fissures) is very low. The grains are tightly packed and surrounded by a very heterogeneous fine-grained brown material. This brown material consists of a mixture of minerals, possibly clays, chlorite , micas, weathered glauconite and feldspar as well as small grains of rutile, hematite or ilmenite. The aforementioned Micro-fissures run through the brown material. The sensitivity of the brown clayey material to water, when exposed to wetting and drying cycles, is likely to explain the degradation of the Thorn-sandstone. Other hypotheses could be formulated to explain the rapid deterioration of the Thorn sandstone.

Preface

This piece of writing represents my Bachelor Thesis corresponding with the conclusion of the Bachelor's degree at the Delft University of Technology. My research was conducted at the Geo-Engineering section of the department of Geoscience and Engineering within the Faculty of Civil Engineering and Geosciences (CiTG).

This thesis is written to obtain insight into the degradation processes which are responsible for the rapid deterioration of the Thorn-Sandstone by usage of mineralogical analysis. By using several different methods results were obtained which made it possible for me to finish my Bachelor's degree.

I would hereby like to express my sincere gratitude to my supervisor Dr. Ir. D. J. M. Ngan-Tillard for giving me the opportunity to be part of this research. Furthermore, I want to thank all other members of staff within the CiTG-faculty (Dr J. Voncken, drs. M. van Tooren, Wim Verwaal, Arno Mulder, and Jens van den Berg) for their contribution to this thesis.

I also want to thank all members of the Dutch Cultural Heritage Agency (drs . H.J. Tolboom**,** Dr. Hans Huisman and Dr. A. van Hoessel) for providing the samples used for testing and for their highly valued advise, analyses and recommendations.

Finally I want to express my sincere and greatest gratitude to my parents, my sister, my girlfriend, my family and friends who have given me the necessary support and motivation during my Bachelor's degree at the Delft University of Technology.

Jash Kalpoe
Delft, 2017

Table of contents

Chapter 1: Introduction

1.1 General

This research concerns the H. Michaël catholic church in the city of Thorn, at the Netherlands-Belgium border. Thorn, known as The White Village due to its large amount of white houses in its city center, was once a miniature principality (website: [1]). Now it is a historical site that attracts many tourists who want to admire Thorn's cobbled streets, the beautiful Abbey Church and the characteristic white houses with their own eyes (website: [1]).

The church walls were made of natural stone. The method of using natural stone as building and construction material is one of the oldest used by humans (Shadmon, 1996). More than 5000 years ago the first natural stone structures were built in Malta (Cassar, 2002), and possibly even earlier, like the carved T-shaped stone pillars at Göbekli Tepe site, Turkey (Schmidt, 2000). Most natural stone variations are prone to damage and decay in time due to their sensitivity to the environment (Winkler, 1997). Part of the façade of the 11th-CE church in Thorn was built using a particular sandstone. This stone is now deteriorating rapidly: It fractures along sedimentary planes, and at the surface in multiple directions. The walls of the church used to be plastered. The problems with this stone probably started when the plaster layer on the church walls was removed. Recently a church with a similar problem in Liëge, Belgium, has been re-plastered for having the same problem. Through Mr. Hendrik Tolboom, specialist in building-stone, Dr. Ir. Hans Huisman, specialist in conservation of cultural heritage at the Dutch Cultural Heritage Agency and Dr. Ir. D.J.M. Ngan-Tillard, engineering geologist at Delft University of Technology, this research project was established to determine what the main reason(s) is (are) for the Thorn-sandstone to fracture at such a high rate.

The sandstone cannot be found anymore in outcrops neither in the Netherlands nor in Belgium. It is however thought to have been quarried in Liëge, Belgium, and to belong to coal-measures sandstones of Carboniferous - Westphalian age which were used on numerous other churches build up until the 13th century (Satijnplus Architecten, 2015).

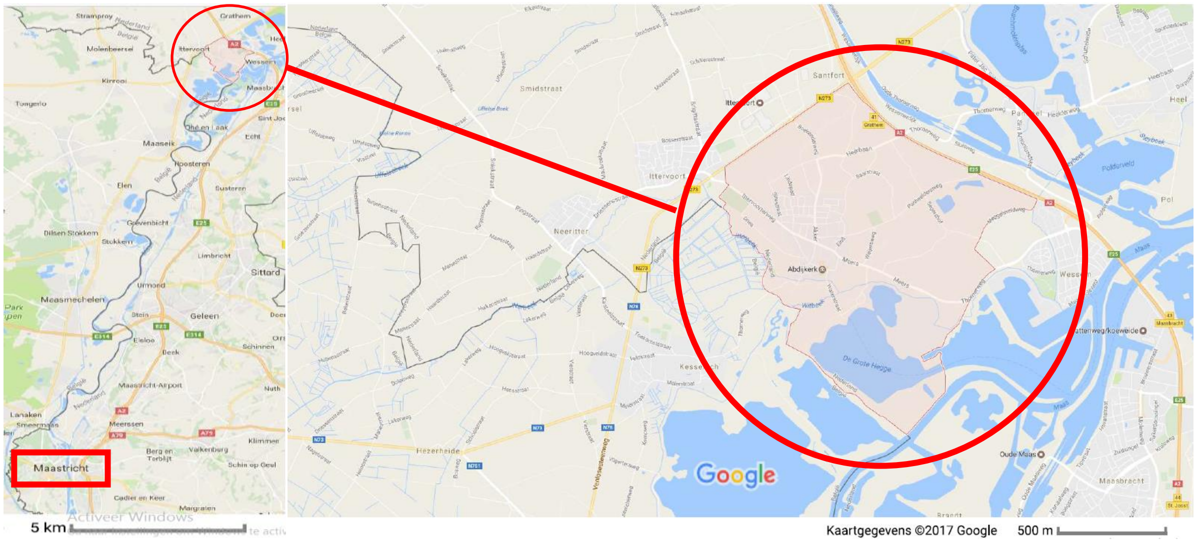

Kaartgegevens ©2017 GeoBasis-DE/BKG (©2009),Google

Figure 1: Thorn, at the border of North-East Belgium and the south of the Netherlands. Source: website [2].

1.2 Goal

Each method, test and technique used in this research has the purpose to obtain information and data regarding the mineralogy and micro-structure of the Thorn-sandstone that can elucidate its susceptibility to degrade. Several hypotheses have been formed to explain this rapid degradation. Each method, test and technique will be described along with their corresponding objectives for rejecting or accepting each hypothesis.

1.3 Hypotheses

H_1: *Coal-measures Sandstone rich in organics*

The first hypothesis of this research is that the Thorn-sandstone contains coal. There are several reasons for this. First, it belongs to a carboniferous coal-measure formation. Second, brown material was visible with the naked eye. The presence of organic material in a sandstone, over time, can cause a significant negative effect on the durability and strength of the corresponding (sand)stone. By determining the presence and subsequently the amount of organic material within the sandstone, this hypothesis can be accepted or rejected.

H_2: *Glauconite Sandstone containing swelling clays*

The second hypothesis is that the Thorn-sandstone is a glauconite sandstone. This hypothesis is supported by the greenish color of the large rock sample. Glauconite is a phyllosilicate that can weather to smectite under temperate climate. Smectite is a swelling clay that swells and shrinks under wetting and drying cycles. It is known that the mineral glauconite forms in marine environments. Such an environment prevailed during the Westphalian in Belgium. Therefore the presence of glauconite in the Thorn-sandstone is considered a possibility. For more information on glauconite, glauconite sandstone and Westphalian glauconitic sandstones in Belgium (Western Europe) please consult appendix A. Pore-size distribution along with mineralogical composition, and in this case, the presence of glauconite, have the ability to influence the durability and thermal behavior of sandstones (Martinec et al., 2010).. By determining the amount of swelling clays in this sandstone, this hypothesis can then be accepted or rejected.

H_3: *Glauconite Sandstone subjected to oxidation*

The third hypothesis is that the Thorn-sandstone contains oxidized glauconitic particles. At first sight brown beds and brown/red colored areas are present on some of the rock samples. This optical property is often associated with the oxidation of iron. To be able to accept or reject this hypothesis several tests must be conducted to determine the presence and the amount of iron and oxygen within the Thorn-sandstone.

H_4: *Sandstone with clayey matrix*

The fourth assumption is that the Thorn-sandstone consists of quartz grains which are surrounded by a clay matrix along some beds. Clays, even non swelling clays, change of volume when exposed to wetting and drying cycles. Moreover, they are weaker when wet and can lead to the degradation of a sandstone. To be able to accept or reject this hypothesis, the presence and amount of these clays should be determined.

1.4 Methodology

The processes causing the rapid deterioration of the sandstone used on the Thorn church walls have been investigated. To do so, different methods for mineralogical analysis have been used, as explained below.

At the start, a literature study has been conducted to obtain the necessary knowledge about the sandstone used on the walls of the Thorn church.

Through Drs. Hendrik Tolboom and Dr. Ir. Hans Huisman of the Dutch Cultural Heritage Agency, large samples along with the corresponding thin-sections of the sandstone have been provided. These rock materials have then been subjected to several analysis methods as stated below.

Methylene Blue adsorption testing, to determine the amount of swelling clays within the sandstone, has firstly been conducted.

After that, microscopic images of several thin-sections were made and analysed to obtain potential optical mineralogical properties corresponding to the selected sections of the sandstone samples.

Third, High resolution X-Ray micro-CT analysis has been conducted on different areas of several rock samples. This to gain a 3-Dimentional insight of the internal structure of the sandstone.

Following this, XRF and XRD analysis were conducted on rock powder of the sandstone to obtain the chemical composition in terms of individual chemical elements and minerals. To know if this rock contains coal, the amount of organic material within the sandstone needed to be determined. To this purpose a Loss-On-Ignition test was conducted on powdered samples of the sandstone.

The seventh method is the SEM (Scanning Electron Microscope) analysis conducted on three thin-sections of the sandstone to gain very precise information regarding the elemental composition of several interesting areas within the thin-sections.

And finally, to determine the difference in degree of absorption of the grains, the method of Methylene Blue staining of a thin-section was conducted.

This concludes the methods used for testing. Hereafter, the obtained results were compared and conclusions regarding the rapid deterioration of the Thorn-sandstone were drawn after which the most plausible hypothesis could be selected.

1.5 Thesis Layout

In this first chapter, the context of the study of the Thorn-sandstone’s rapid degradation has been explained, the goal of the study has been set and four hypotheses capable of explaining the degradation of the Thorn-sandstone have been formed. In Chapter 2, the methodology followed to discard or accept hypotheses will be explained. It is mainly based on mineralogical, chemical and microstructural analysis of Thorn-sandstone samples. The goals and procedures of each analysis or test shall be described. Following this, in Chapter 3, the results obtained from individual tests will be presented after which , in Chapter 4, individual test results will be combined. Chapter 5 contains an evaluation of the four hypotheses. After this a discussion (Chapter 6) and the final conclusion and recommendations (Chapter 7) constitute to the ending of this thesis. Appendices are added to provide more insight regarding separate subjects.

Chapter 2: Goals and procedures of conducted tests

2.1 Methylene Blue Adsorption test (MBA test)

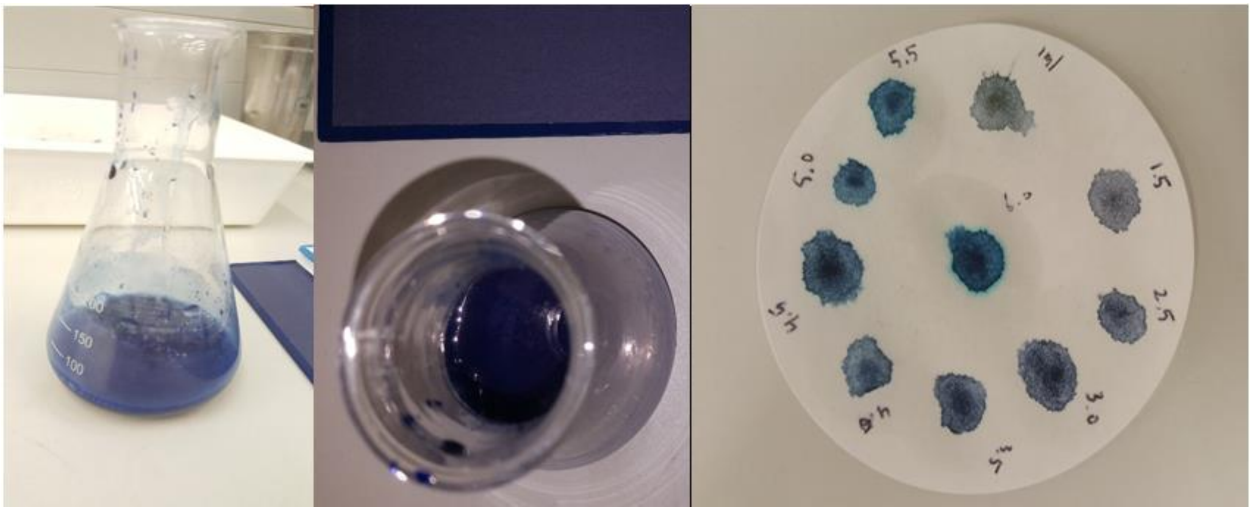

FIGURE 2: MBA ERLENMEYER FLASK (LEFT AND CENTER) AND FILTER PAPER WITH DUST CIRCLES (RIGHT).

2.1.1 Goal

The MBA-test is used to obtain the necessary information regarding the presence and properties of several clay minerals in rocks and soils. The “spot method” test is conducted on ground rock. The MB absorption value is reported in milli-equivalents absorbed by 100 g of ground rock (Verhoef, 1992).

The test has a limitation: it does not provide the percentage of stained minerals inside the rock. For this, methylene blue stained thin-sections are necessary. The MBA-test on ground rock is only indicative of the presence of swelling minerals. It is possible that swelling minerals are only concentrated along a few thin bands and cause rock disintegration by swelling and shrinking while they represent only a small percentage of the rock minerals and therefore do not lead to a high MBA value.

2.1.2 Procedure

The test procedure for the spot test is described below (Verhoef, 1992).
Necessary quantities:

- Concentration of the methylene blue: 0.003 gr/ml.
- Amount of grained (powdered) rock: 2.05 gr
- Amount of demi-water added to rock powder: 30 ml

Start:
First a piece of the rock sample must be powdered to a size of less than 100 micrometers. Approximately 2 grams of powdered rock along with 30 ml demi-water is needed. The powdered rock is mixed with the demi-water in a Erlenmeyer flask to create an aggregate suspension. Then Methylene Blue solution is added to the aggregate suspension. This is done by repeated titration of 0.5ml using a 25ml burette. During this, a magnetic stirrer is used. After each 0.5ml titration the mix in the flask gets stirred for a period of approximately 1 minute. After this a drop of the mix is removed using a glass rod and then cautiously placed on a sheet of filter paper. At first a dark blue circle of dust, containing distinct edge, is visible. This edge is enclosed by a clear water ring. This action is done repeatedly.
When the dust circle edge starts appearing vague and a narrow light blue halo becomes visible, then the suspension in the flask gets stirred for an extra 1 minute. Immediately hereafter another spot test, of the same mix, is done. In case the halo disappears, add more methylene blue. These steps are repeated until a definite permanent light blue halo becomes visible. By writing down the amount of methylene blue added corresponding to each spot on the filter paper, the final and right amount of methylene blue can be obtained. This constitutes to the end-point of the “spot test”. After this calculations can be made which provide a MBA value given in grams per 100 grams (g/100g).

It is also possible to carry out methylene blue tests on a non-coated thin-section. The thin-section is immersed in a Methylene Blue solution, rinsed before being observed under the optical microscope to determine the area-percentage stained by the Methylene blue.

2.2 Optical Microscopic analysis

FIGURE 3: THREE THIN-SECTIONS AND CORRESPONDING ROCK SAMPLE.

2.2.1 Goal

Sometimes minerals are so small that is becomes almost impossible to properly identify them on a macroscopic scale. When this is the case, then it is customary to switch to microscopic analysis. This can be conducted with the usage of an optical polarization microscope. The main function of such a microscope is that it can enhance the view by using different zoom rates. The different zoom rates are coupled to corresponding lenses which provide the user of this particular microscope with a variety of views and imaging options. In combination with a microscopic camera attached to the optical polarization microscope, the aforementioned imaging option can be used. The goal with this analysis is to determine as much optical mineral properties as possible.

2.2.2 Procedure

Instrument Specification:

- Polarization Microscope, Leica DM/LP.
- Transmitted and Reflected light
- Digital microscope camera (Leica)

FIGURE 4: LEICA DM/LP POLARIZATION OPTICAL MICROSCOPE.

It is necessary to prepare minerals before they can be subjected to microscopic examination. This is necessary because microscopic light should be able to have an effect on these minerals. In order to achieve this, the minerals in the rock are buffed to a thin-section with a thickness of 30 microns (0.03mm) - a thickness where most minerals are transparent.

The next step is covering of the thin-section. This is done by using a covering slip after applying Canada-balsam as glue to bond the covering slip. The sample (thin-section) is now ready to be examined.

During microscopic examination a number of properties can be examined that could already be studied macroscopically, such as the color, the cleavage and sometimes the crystal structure. However, the interaction with polarized light also provides other, optical, mineral properties which cannot be studied macroscopically. Each mineral is characterized by a unique combination of optical properties. By using features of the microscope and optical properties of minerals such as: color, interference color, cleavage, angle of cleavage, double refraction, relief, refractive index, crystal structure, extinction and extinction angle, among others, it is possible to determine an accurate indication of the minerals present in the thin-section (Van Tooren, 2012).

The optical polarization microscope uses two types of light:

- Transmitted light: Light coming from a light source below the thin-section. Light waves are sent upwards towards the thin-section and in the direction of the microscopic lens. The transmitted result can then be seen through the lens (Van Tooren, 2012).

- Reflected light: Light coming from a light source above the thin-section. Light waves are sent down toward the thin-section which are then reflected off. This results in reflected beams which can then be seen through the lens (Van Tooren, 2012).

2.3 High resolution X-Ray micro-Computed Tomography

2.3.1 Goal

Thin-sections or polished thin-sections are used in earth science to examine 2-dimensional textures in rocks (Ikeda et al., 2000). Polished thin-sections are often easier to examine because the section surface is equally flat everywhere. For this reason polishing is recommended. To determine 3-dimensional properties of a rock structure, 2-dimensional analysis can sometimes be sufficient. But more often it is not. In many cases the mineral interconnections within a rock structure can significantly indicate information corresponding to the rock origin (Ikeda et al., 2000). X-ray micro-computed tomography (micro-CT) can be used to visualize and quantify the microstructure of a rock in 3D. It allows to visualize grains, pores, and cracks. More dense minerals and minerals with high atomic numbers absorb a larger amount of X-rays. Micro-CT is a non-destructive method (Ikeda et al., 2000) which means that the sample can be re-used after testing. The spatial resolution of a micro-CT scan is about 1000th times smaller than the width of the scanned object. By scanning tiny pieces of the Thorn-sandstone, which is a fine-grained rock, it is possible to visualize the 3D arrangement of grains, pores and cracks in the Thorn-sandstone.

2.3.2 Procedure

X-ray micro-CT is used to obtain tomographic information. This information is given in the form of maps of the internal X-ray linear attenuation coefficient of a sample (Ikeda et al., 2000). For this procedure the Phoenix Nanotom

FIGURE 5: PHOENIX NANOTOM MICRO-CT SCANNER AT THE FACULTY OF GEOSCIENCE (TU DELFT).

micro-CT scanner at the department of Geoscience was used. The 2-dimensional X-ray CT images can be described as 'slices' (Ikeda et al., 2000). The X-ray beam goes through the rock(sample) and creates a 3-dimensional model which presents the internal structure by stacking a sequence of the aforementioned "slices". Having this information makes it possible to determine the position, attenuation and more properties of several minerals within the rock(sample).

2.4 X-Ray Diffraction analysis (XRD)

2.4.1 Goal

X-Ray Diffraction analysis, or XRD, provides a measure for the intensity of crystal diffraction peaks of the minerals, due to the individual chemical compounds, within a rock sample. The rock sample can either be powder, liquid or in solid form. The result, for each compound of interest, is provided in estimated percentages. The goal of using this method of analysis is to gather more information about the chemical compound of the Thorn-sandstone.

2.4.2 Procedure

The procedure of the XRD analysis starts with an XRD-analyzer which measures and stores the intensity of the x-ray beams which are diffracted into different wave patterns by the atoms present in the crystal compounds within the rock sample. This produces multiple diffracted beams. The angle and intensity of these diffracted beams indicate a 3-dimensional density of electrons inside the crystal which correspond to a unique compound. By performing this analysis it is possible to obtain more insight regarding the composition of the Thorn-sandstone.

2.5 X-Ray Fluorescence analysis (XRF)

2.5.1 Goal

X-Ray Fluorescence analysis, or XRF, makes it possible to obtain the amount of chemical elements present (in percentages) in the Thorn-sandstone. This is the main goal of using the XRF analysis. The rock sample can either be powder, liquid or in solid form.

2.5.2 Procedure

Experimental conditions:

For XRF analysis the measurements were performed with a Panalytical Axios Max WD-XRF spectrometer and data evaluation was done with the SuperQ5.0i/Omnian software. This information was provided by Mr. R. Hendrikx of the Faculty of 3mE at the TU Delft.

An x-ray beam, called the “incident beam”, is send through a rock sample by the XRF spectrometer. The different atoms in the rock sample light up and get excited when the x-ray beam reaches these atoms. The degree of atom activity varies with each atom because each atom possesses its own specific wavelength. The x-ray beam going through the rock sample causes back scattering which is saved and displayed using a XRF data viewing computer program. After this the obtained data will be processed to determine the elemental content. Finally this content is converted to mineral content in terms of silica (SiO_2), calcium carbonate ($CaCO_3$) or other minerals .

2.6 Loss-on-Ignition test

FIGURE 6: POWDERED ROCK SAMPLE (LEFT), TWO PORCELAIN DISHES WITH ROCK POWDER (CENTER) AND BURNING OVEN (RIGHT).

2.6.1 Goal

To obtain an indication about the amount of organic material present in the Thorn-sandstone, the Loss-on-ignition test is performed on a piece of rock sample which is powdered before the test.

2.6.2 Procedure

First the individual weight of two empty porcelain dishes is determined. Then the two porcelain dishes are filled with rock powder. Afterwards the weight of each dish containing the rock powder is determined. Finally both dishes containing the rock powder are put in the oven to dry at 105 °C.

LOI-Test at 440 °C

The two porcelain dishes with rock-powder content are put in the oven at 440 °C for four hours. After this, the dishes containing the burned soil are removed from the oven and then cooled off to room temperature. Finally the dishes with the burned soil content are weighed again.

LOI-Test from 440 °C to 550 °C

The porcelain dishes are reheated from room temperature to 550 °C for four hours. After this the dishes containing the burned soil are removed from the oven and then cooled off to room temperature. Then again, the dishes with the burned soil content are weighed.

The difference in weight before and after heating is then calculated which gives an indication about the amount of organic material present in the Thorn-sandstone.

2.7 SEM analysis

2.7.1 Goal

FIGURE 7: THE JEOL JSM-5910LV SCANNING ELECTRON MICROSCOPE.

When optical microscopy is not able to provide sufficient image resolution, high enough magnification or accurate enough information then SEM-analysis can be used (website: [3]). High-resolution and high-depth-of-field images of the rock-sample surface and near-surface can be obtained by using Scanning Electron Microscopy (SEM) (website: [3]). This is a widely used analytical tool because of the greatly detailed images it can provide in a fairly limited amount of time (website: [3]). The SEM can also provide elemental identification of nearly all elements of the periodic table when connected to an auxiliary Energy Dispersive X-ray Spectroscopy (EDX) (website: [3]). In this research the SEM is used to generate high-resolution images of the Thorn thin-sections. The SEM is critical in almost all fields that require characterization of solid materials which is the case in this research.

2.7.2 Procedure

Sample preparation of thin-section 3:

FIGURE 8: AN IMAGE OF THE SAMPLE CHAMBER WITH A THORN-SANDSTONE THIN-SECTION PLACED INSIDE.

Three thin-sections are used for SEM-analysis. The third polished thin-section is made by Jens van den Berg at the TU Delft. This thin-section is cut and then hand polished with silicium-carbide (Carborundum sic powder) of various sizes: on the first polishing table; grain "150", the second polishing table; grain "500" and the third polishing table; grain "1000" (and possibly intermediate grain roughness). Afterwards the thin-sections were polished with the polishing machine for 3-5 min, grain 2 micrometres. The SEM makes use of electrons for imaging and makes it possible to examine the samples at higher magnification and greater depth-of-field compared to an optical microscope (website: [4]). A beam of accelerated electrons, produced by a thermal emission source, in the form of an electron column positioned above the sample chamber is generated by the SEM (website: [5]). Positioned in the SEM column are several electromagnetic lenses which are tasked with focusing of the accelerated electrons into a small beam (website: [4]). When the accelerated electrons reach the sample they decelerate into the solid sample (website: [5]). These electron-sample interactions cause the accelerated SEM beam to dissipate into a variety of signals (website: [5]).

These signals can be in the form of (website: [5]):

- Secondary electrons: which produce SEM images.
- Backscattered electrons (BSE): which produce data that can be used to obtain crystal structures and orientation of minerals.
- Diffracted backscattered electrons: which produce data that can be used to obtain crystal structures and orientation of minerals.
- Photons: which produce data for elemental analysis.

When information regarding the morphology and topography of the rock thin-section is needed, the use of secondary elements is considered to be the most useful (website: [5]). In case the contrast in sample composition needs to be determined, then the usage of backscattered electrons is considered the most useful (website: [5]). Because the energy of the electrons in the SEM beam changes (decreases), they then produce specific x-rays for each element in a mineral (website: [5]). Through this effect it is possible to know which elements are present in the specific area of the sample that is being analyzed. When the produced x-rays interact with the sample, they do not quantitatively nor qualitatively change the sample which means that SEM analysis can be characterized as being a “non-destructive” method of sample analysis (website: [5]). This also means that multiple analysis on the same sample in possible.

Chapter 3: Individual tests results

3.1 Methylene Blue Adsorption test

The value for the methylene blue adsorption test is calculated in grams MB adsorbed by 100 g of powdered rock sample according to the following formula:

$$\boxed{MBA = (c \times p) / (A / 100), \qquad [g/100\ g],} \qquad \text{(Verhoef, 1992)}$$

Parameters:

MBA = methylene blue adsorption value
c = concentration methylene blue solution [g/ml]
A = weight of soil or rock powder [g]
p = amount of methylene blue adsorbed [ml]

The parameter values of the MBA test done are:

c = 0.003 g/ml
A = 2.05 g
p = 5.0 ml

The MBA value is:
MBA = (0.003 x 5.0) / (2.05 / 100) = **0.73** g/100 g

The obtained MBA value of 0.73 qualify the soundness of Thorn-sandstone as acceptable to marginal for rock aggregate (Verhoef, 1992). It does not match any known value in literature that corresponds to a specific type of swelling clay. However, it should be noted that the MBA analysis was done on rock powder of the Thorn-sandstone sample which contains sediment grains along with an unknown brown material. This means that it is also the quartz grains and the brown material that comes into contact with the methylene blue. Knowing that the quartz does not react it must then be stated that this method is less conclusive and less reliable for this specific sandstone.

For this reason, the methylene blue staining of a Thorn-sandstone thin-section was conducted. Staining was limited on the brown material and difficult to observe in all grains. However, results of the methylene blue staining are questionable because the thin-sections were left in the methylene blue solution for too long. This caused the glass to be stained too which reduces the reliability on this thin-section.

3.2 Optical Microscopic analysis

Note: In all microscopic images the approximate average size of the quartz grains (100 micro meter) is used as a scale indication.

The following have been observed through optical microscopic analysis:

- Quartz grains
- Mica grains
- Grains suspected to be Hematite grains
- Cracking in multiple directions
- Largest cracks, parallel to sediment layering
- Large amount of unidentified brown material surrounding grains and along cracks
- Unknown, black voids or grains.

The 3 thin-sections from the block with cross bedding:

FIGURE 9: FROM LEFT TO RIGHT: THIN-SECTIONS 1, 2 AND 3. THESE THIN-SECTIONS WERE MADE FROM THE THORN-SANDSTONE BLOCK IN FIGURE 10.

The thin-sections do not have a coating which leaves them vulnerable to asperities on the pictures. Smearing a film of water on the thin-section does not help. To solve this problem a glass plate needs to be pasted onto the thin-section using Canada balsam. Canada balsam is preferred because it has the same reflection index as glass. The thickness of the thin-sections are more than 30 um (> 30um).

The (quartz) grains are about 100um. The grains on both sides of cracks, following the sedimentation layering, are coated with a unknown brown material. The more coarse grains are surrounded by a smaller amount of this material whereas the smaller grains are surrounded by more.

FIGURE 10: THIN-SECTIONS 1, 2 AND 3 CORRESPOND TO THIS SAMPLE.

The layering is not continuous which may indicate turbulent deposition of this sandstone. The brown material surrounding the grains and along the cracks is visible in all microscopic pictures which were analyzed. As stated earlier, the quantity varies in different areas of all three thin-sections. Several other tests were conducted to aid in determining whether this material could be clay, organics or something else. The zones with high amounts of brown material, mainly zones consisting of smaller grains, correspond to the zones where cracking is found. Under the microscope there is no sight of fractured grains which can indicate that the cracks follow a flowing pattern around the grains.

Examination of thin-section 1:

FIGURE 11: THIN-SECTION 1.

Thin-section 1 was cut perpendicular to the layering within a stone taken from the Thorn church. Only the top of the thin-section corresponds to an external surface of the stone. It can be seen that its structure is not parallel to the main layering.

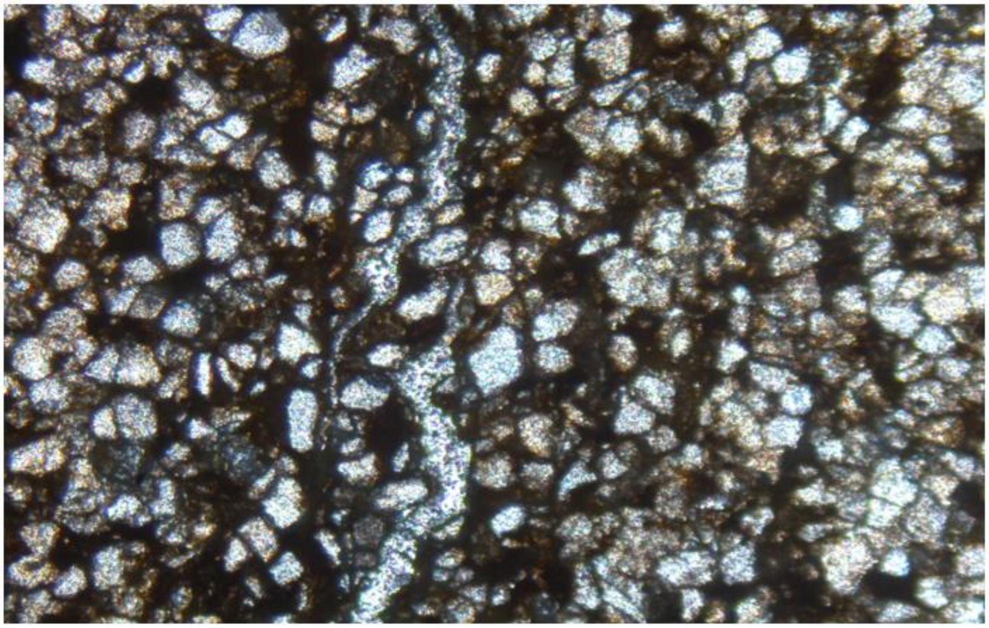

FIGURE 12: ZONES WITH SMALLER GRAINS, SURROUNDED BY BROWN MATERIAL, ARE WHERE CRACKS ARE FOUND.

The smaller cracks look to be in multiple directions whereas the larger cracks are either parallel or perpendicular to the sedimentation layering.

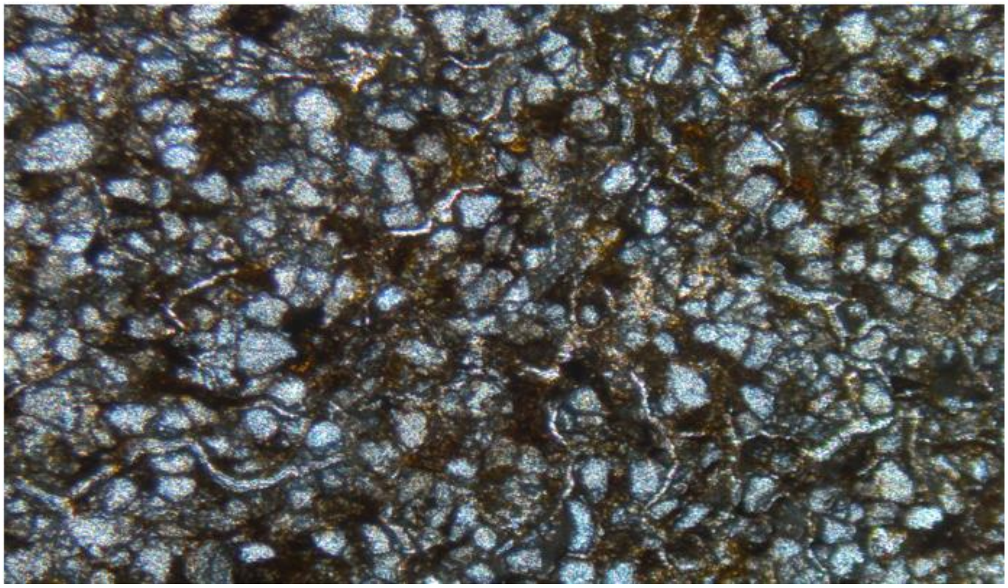

FIGURE 13: LARGE AMOUNT OF SMALL CRACKS IN MULTIPLE DIRECTIONS.

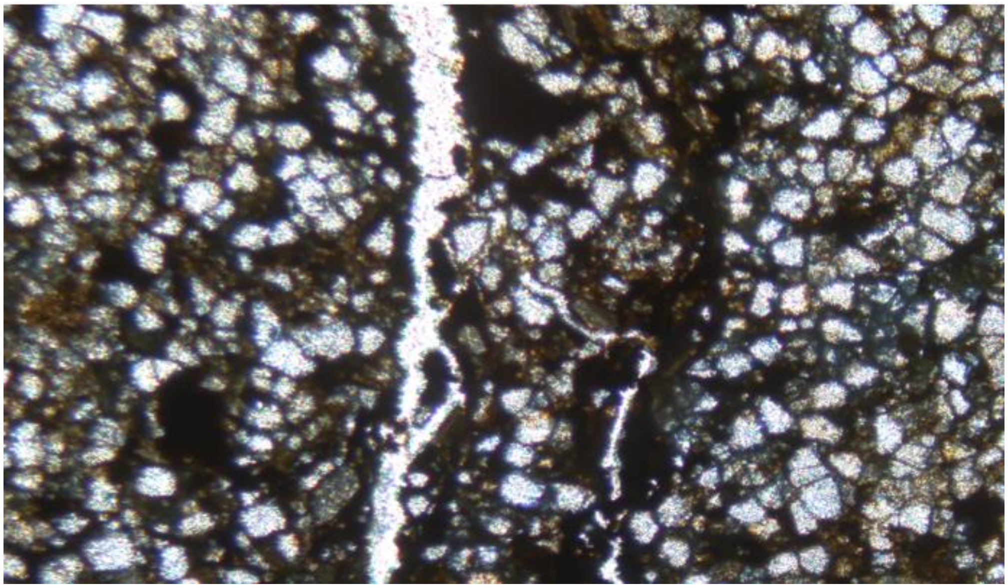

FIGURE 14: LARGE SINGULAR CRACK. THERE IS ALSO BROWN MATERIAL VISIBLE ALONG THE CRACK AND AROUND THE GRAINS.

Step-inclined cracks, which look to cross-cut the sedimentation layers, can also be seen in figure 15.

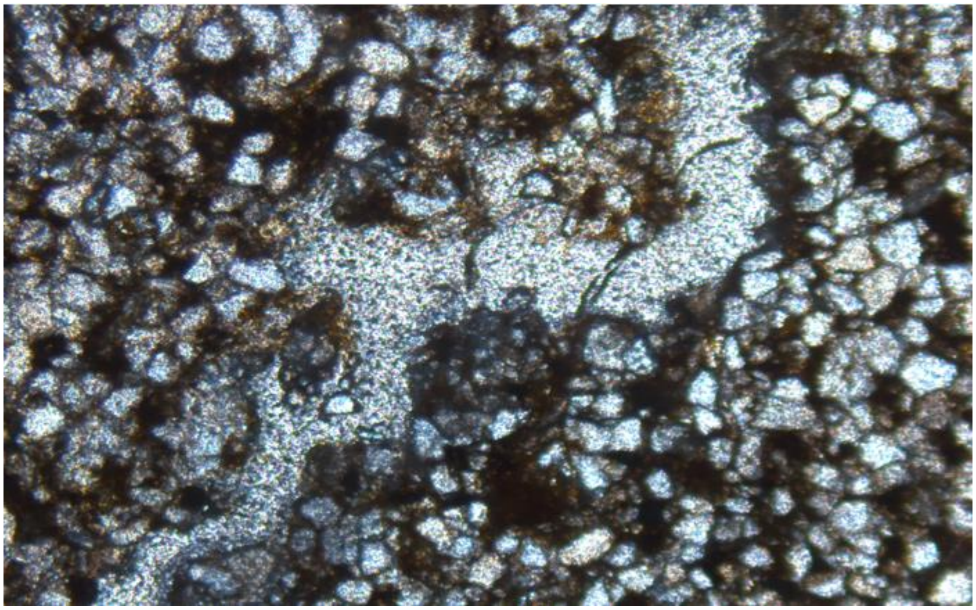

FIGURE 15: BROAD STEP-INCLINED CRACK, DEVELOPED AT THE INTERFACE BETWEEN ZONES WITH DIFFERENT TEXTURES, WHICH FORCES ITS WAY THROUGH SEDIMENTATION LAYERS.

Broad cracks look to have developed at the interface between sedimentation zones with different grain sizes. The cracks can then be seen to end at the cross bedding (see figure 16).

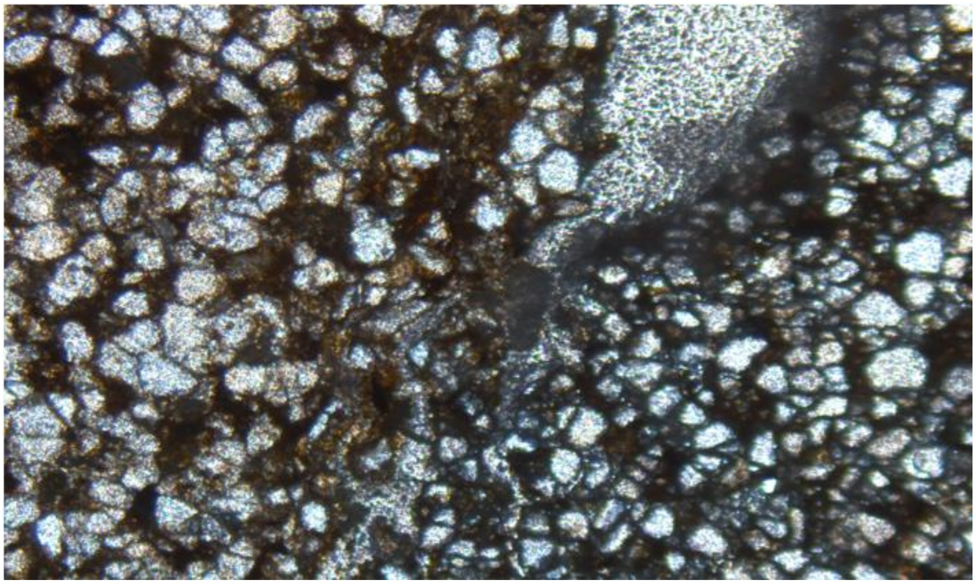

FIGURE 16: COARSER GRAINS (LEFT SIDE OF THE IMAGE) AND LESS COARSE GRAINS (RIGHT SIDE OF THE IMAGE) ARE VISIBLE. CRACKING THEN OCCURS AT THE INTERFACE BETWEEN THESE TWO ZONES.

We also see thinner smaller cracks parallel to the sedimentation layering which converge to a larger crack. Further along the presence of more brown material, forming two bands parallel to one another, results to a bottom set of ripples in which cracks are formed (see figure 17).

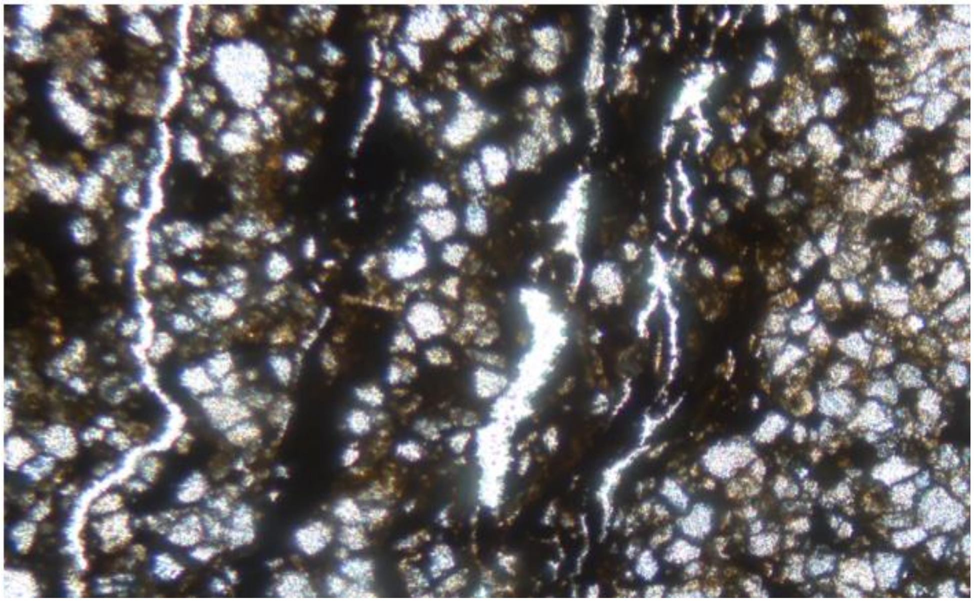

FIGURE 17: SUB-PARALLEL CRACKS VISIBLE. BROWN MATERIAL PRESENT ALONG THE CRACK AND AROUND THE GRAINS.

Examination of thin-section 2:

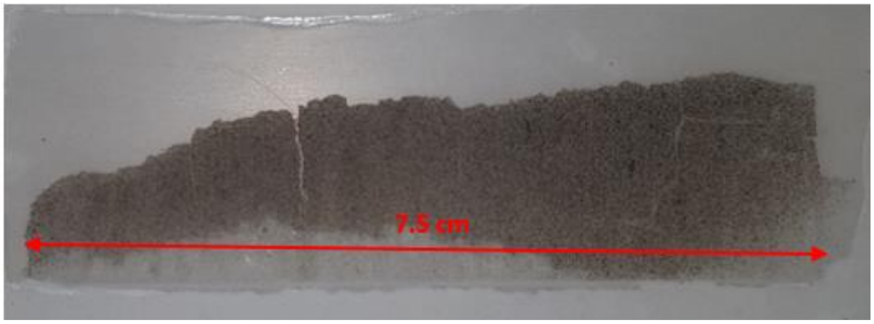

FIGURE 18: THIN-SECTION 2.

Thin-section 2 is cut perpendicular to the layering at the edge of the stone where weathering and cracking are most developed. Several types of cracks were observed. These can be categorized in a main crack parallel to sedimentation layering and many thin cracks connected to each other. The large crack with multiple linked micro-cracks, found near the sample edge, is parallel to the sedimentation and many other thinner cracks (see figure 19).

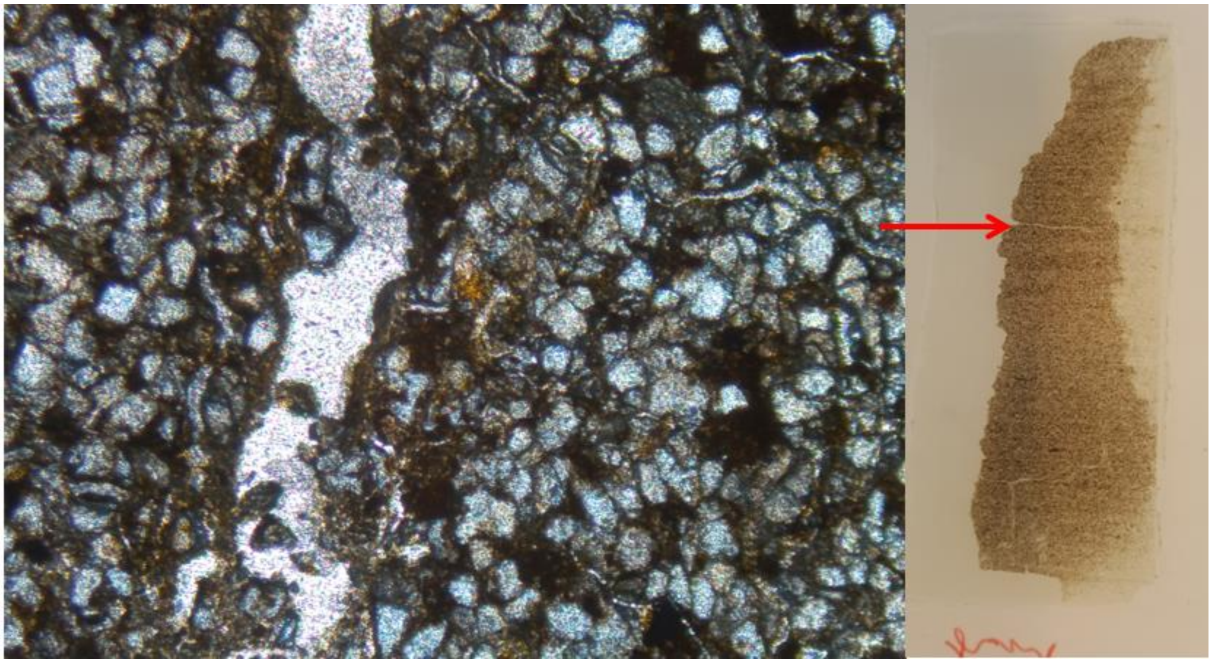

FIGURE 19: LARGE CRACK AT A MORE INWARD POSITION WITHIN THE THIN-SECTION (INDICATED BY THE RED ARROW) ALONG WITH MULTIPLE MICRO-CRACKS. BROWN MATERIAL ALONG THE CRACK ALSO VISIBLE.

In the second organic band multiple cracks parallel to the sample edge can be seen (see figure 21).

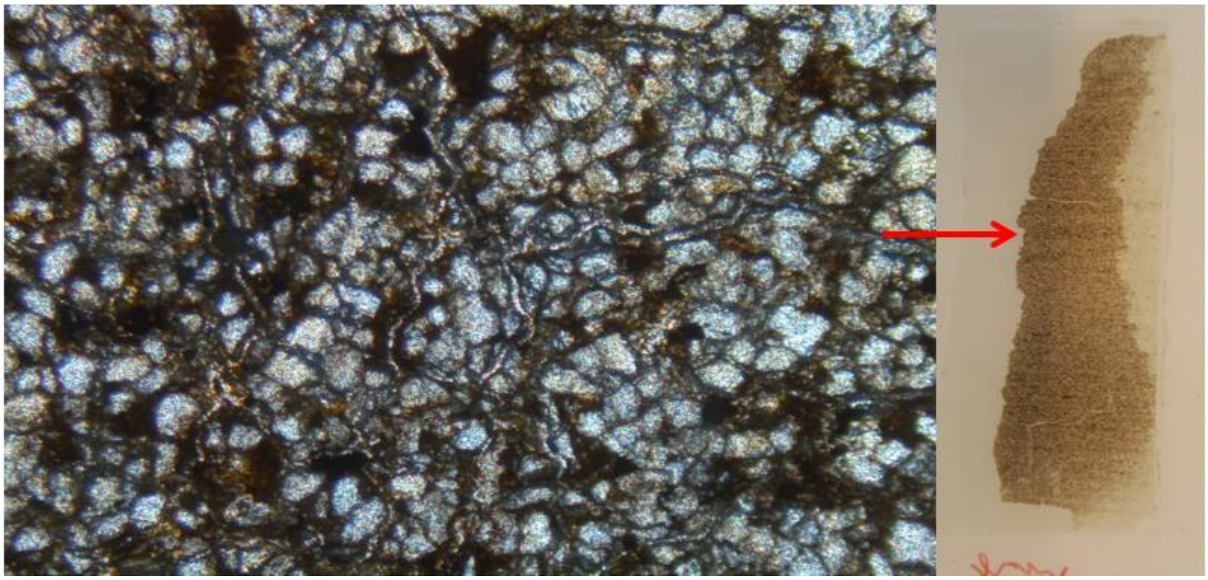

FIGURE 20: THE RED ARROW INDICATES THE FIRST VISIBLE BLACK BAND AND CORRESPONDING MICRO CRACKS.

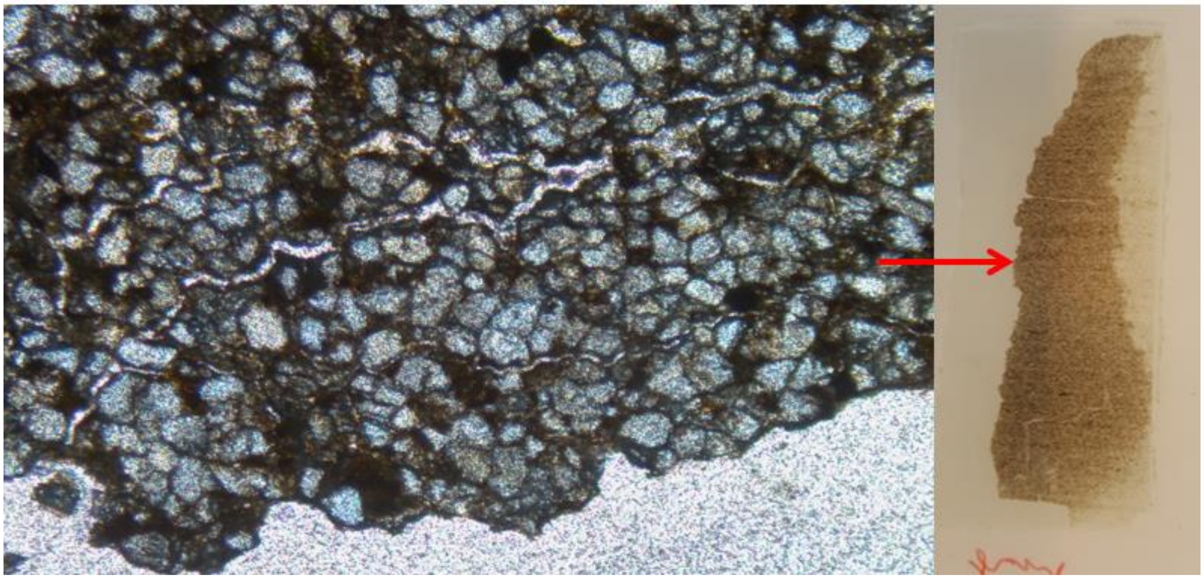

FIGURE 21: THE RED ARROW INDICATES THE SECOND VISIBLE BLACK BAND.

Examination of thin-section 3:

Thin-section 3 is a second thin-section made of the same area of thin-section 2. It is perpendicular to the layering at the edge of the stone where weathering and cracking are most developed. In this thin-section the focus was laid onto the brown material seen under the microscope in a specific area.

Figure 22 shows a large crack visible on the edge of the thin-section going inward, perpendicular to the thin-section edge. This is indicated by the red frame in figure 22. All following pictures are within this area.

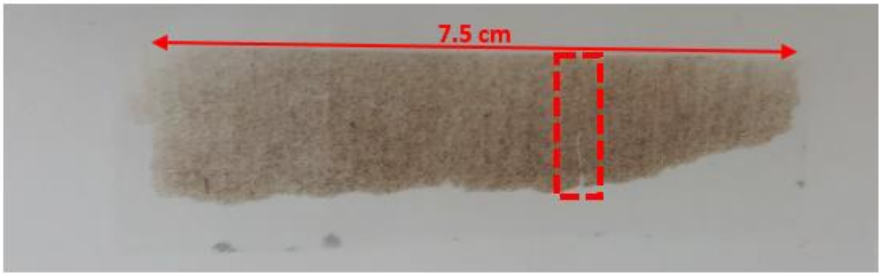

FIGURE 22: THIN-SECTION 3. EXAMINED PART IS INDICATED BY THE FRAME.

Using the optical microscope we again see the brown material concentrated in certain areas as well as around the grains. Mica's are also visible.

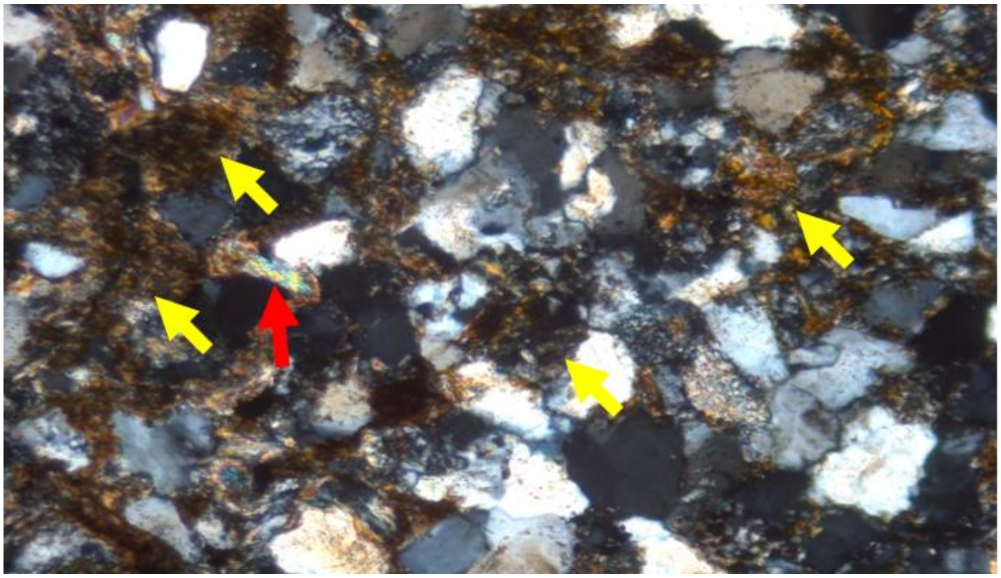

FIGURE 23: THIS PICTURE, TAKEN UNDER NORMAL LIGHT, IS OF AN AREA WITHIN THE RED FRAME IN FIGURE 22. MICA'S (RED ARROW), QUARTZ GRAINS AND BROWN MATERIAL (YELLOW ARROWS) ARE VISIBLE. THE BROWN MATERIAL SURROUND THE GRAINS AND IS ALSO CONCENTRATED IN SOME AREAS.

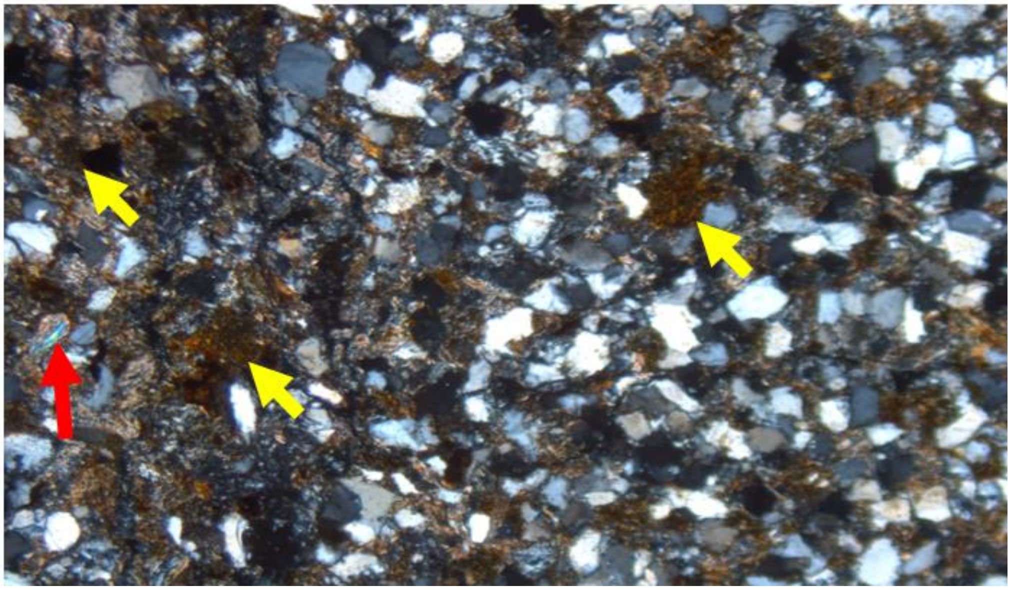

FIGURE 24: MICA (RED ARROW) AND BROWN MATERIAL (YELLOW ARROWS) VISIBLE.

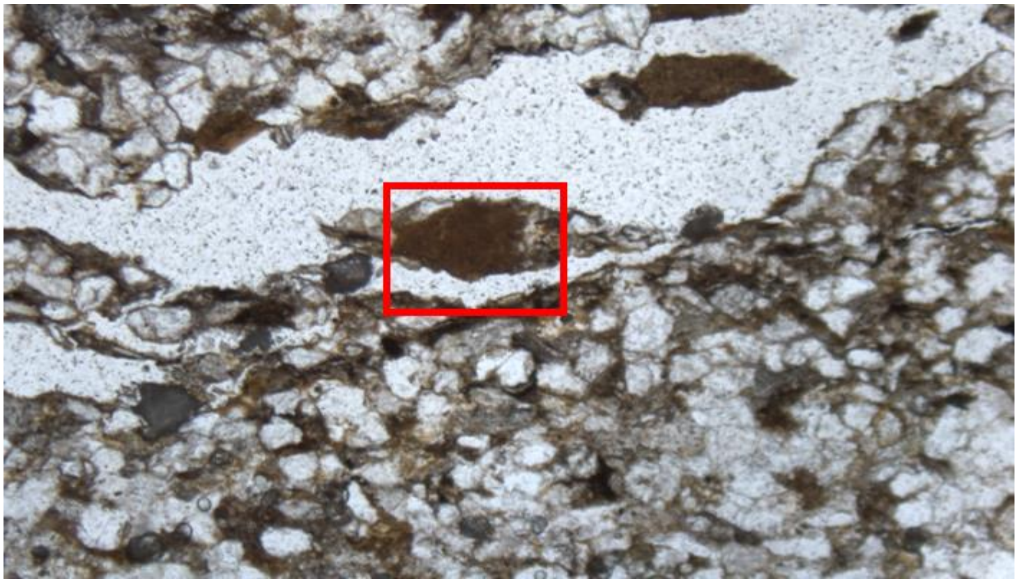

FIGURE 25: IN THIS PICTURE, TAKEN UNDER NORMAL LIGHT, THE AREA CONTAINING THE BROWN MATERIAL OF INTEREST IS INDICATED BY THE RED FRAME. FIGURE 26 GIVES A ZOOM ON THIS SPECIFIC AREA.

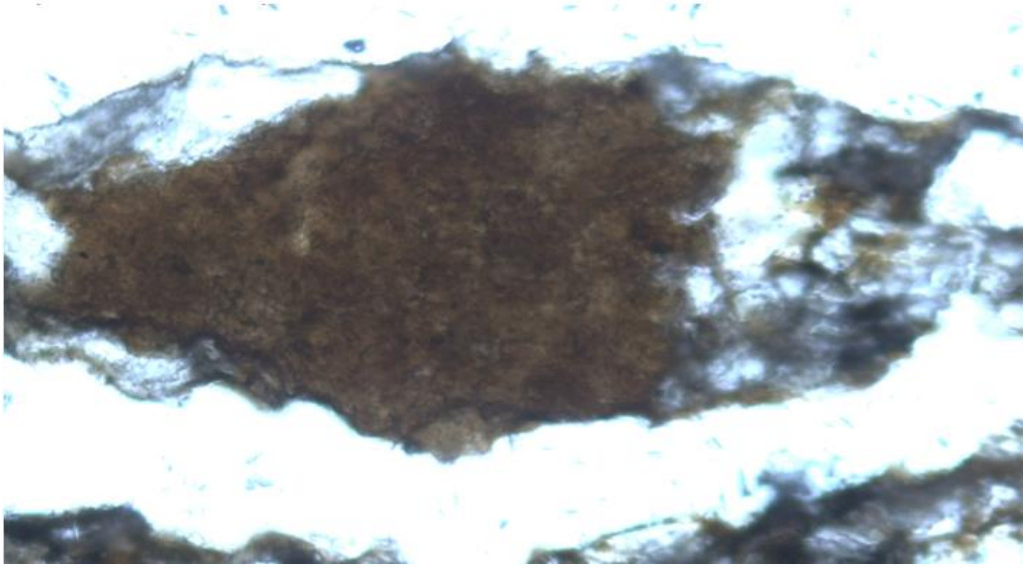

FIGURE 26: IN THIS IMAGE THE AREA INDICATED BY THE RED FRAME IN FIGURE 25 IS ZOOMED IN. THE BROWN MATERIAL OF INTEREST IS VISIBLE AND LOOKS TO BE CONSISTING OF SMALL AGGREGATES.

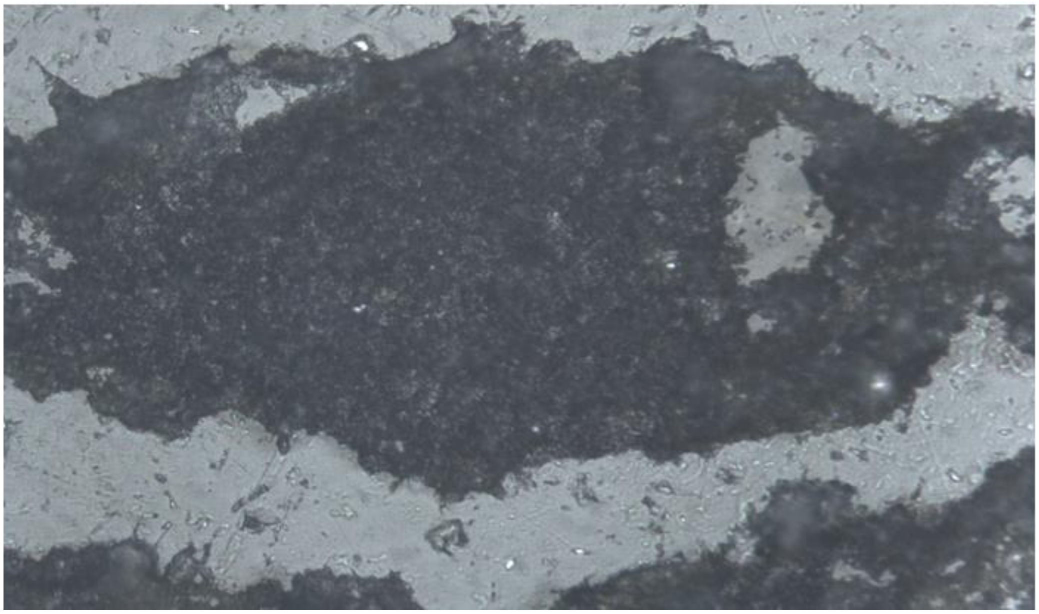

FIGURE 27: THIS IS THE SAME AREA DISPLAYED IN FIGURE 26, HOWEVER, TAKEN UNDER REFLECTED LIGHT. BY DOING SO IT CAN BE CONCLUDED THAT, UNDER THIS LIGHT, THE BROWN MATERIAL ALSO STAYS DARK COLORED. THIS MEANS THAT IT CANNOT BE AN IRON-OXIDE OR ANOTHER SPECIFIC MINERAL. THE HETEROGENEITY OF THE BROWN MATERIAL IS ALSO VISIBLE.

Besides the quartz grains, mica’s, cracks and large amount of brown material other minerals were also observed. This is illustrated in the following images. However, it is not possible, solely through optical analysis, to be sure what exact mineral is present. To determine this, SEM-analysis could perhaps provide the necessary information regarding the composition of the minerals.

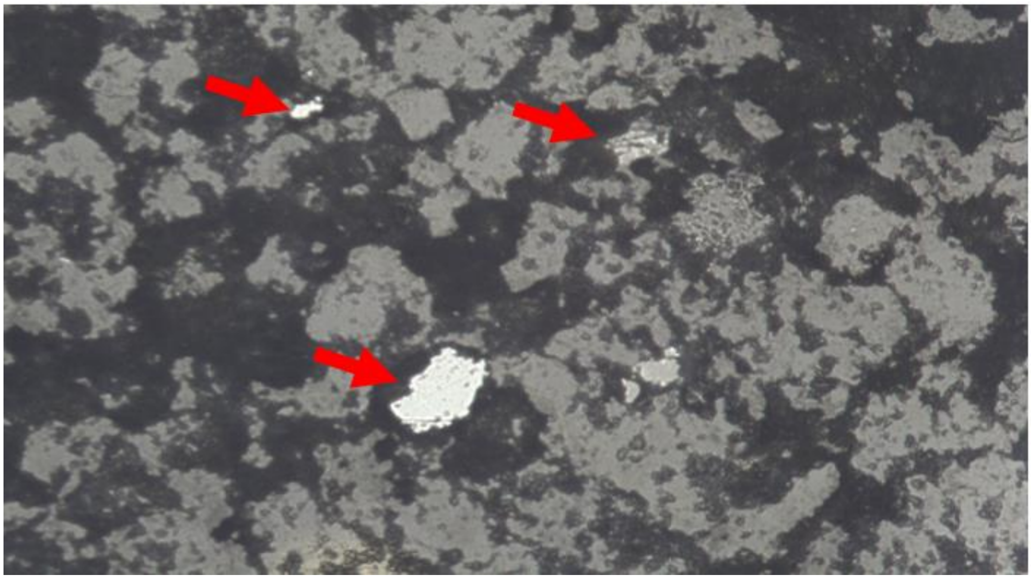

FIGURE 28: IN THIS IMAGE, TAKEN UNDER REFLECTED LIGHT, THREE GRAINS (RED ARROWS) OF AN UNKNOWN MINERAL ARE VISIBLE. TO KNOW WHICH MINERAL IS PRESENTED MORE ANALYSIS IS NEEDED.

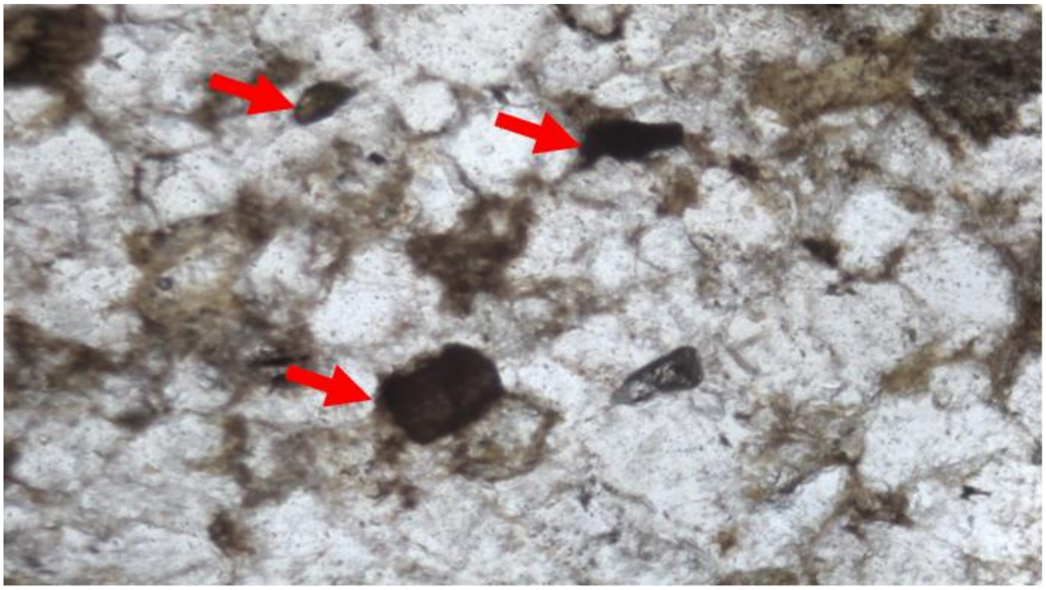

FIGURE 29: THIS IS THE SAME AREA DISPLAYED IN FIGURE 28, HOWEVER, TAKEN UNDER NORMAL LIGHT. THIS SHOWS THAT THE UNKNOWN MATERIALS ARE VISIBLE AS OPAQUE (RED ARROWS).

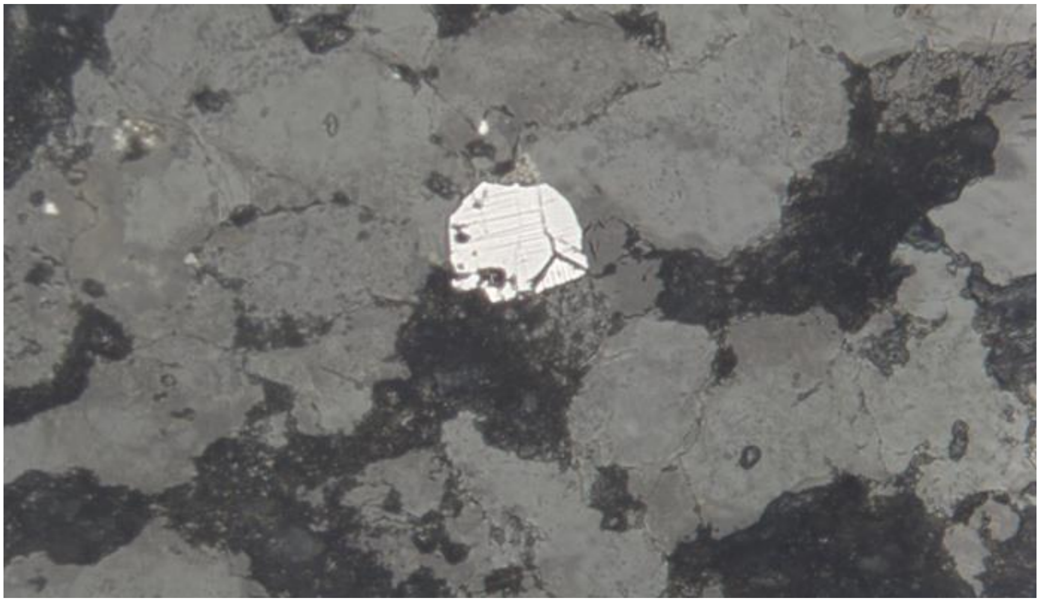

FIGURE 30: THIS IMAGE SHOWS AN UNKNOWN GRAIN UNDER REFLECTED LIGHT (CENTER). LAMINAR TWINNING BOUNDARIES ARE VISIBLE. THIS IS A KNOWN PROPERTY OF HEMATITE. TO BE SURE WHETHER THIS CAN BE A HEMATITE GRAIN MORE ANALYSIS ON THIS GRAIN IS NEEDED.

Also seen on some microscopic images were large, almost black, spots/grains (see figure 31 and figure 32). To know if these are voids (pores) or some other minerals, optical microscopy only does not seem enough. Further analysis is required to also determine the composition of this observation.

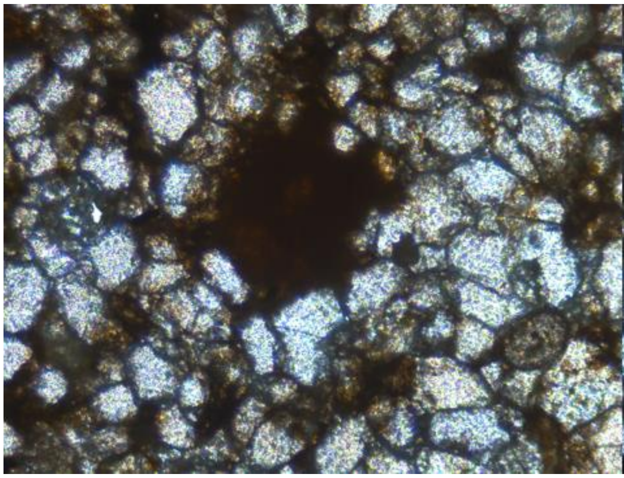

FIGURE 31: BLACK SPOT APPEARING UNDER NORMAL MICROSCOPIC LIGHT (CENTER). BROWN MATERIAL BETWEEN GRAINS IS VISIBLE.

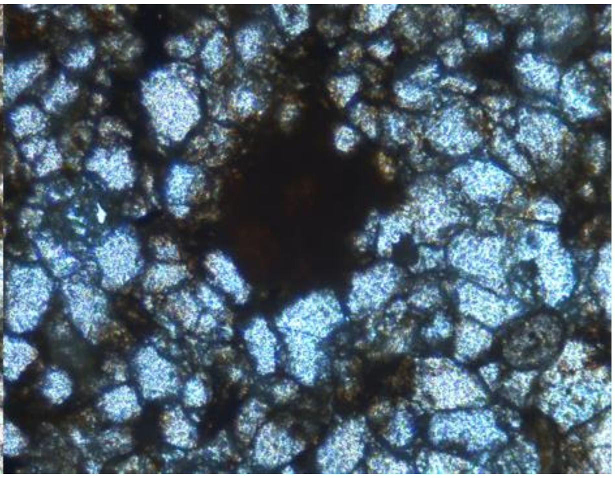

FIGURE 32: BLACK SPOT APPEARING UNDER REFLECTED MICROSCOPIC LIGHT (CENTER). BROWN MATERIAL BETWEEN GRAINS IS VISIBLE.

Solely with optical microscopic analysis we do not have enough information about the mineral content of the Thorn-sandstone, especially with regards to the unknown brown material and black spots. More analysis seems to be a necessity. The earlier proposed SEM-analysis may provide more information.

3.3 High resolution X-Ray micro-Computed Tomography

The following images are from micro-CT scans performed on several different samples of the Thorn-sandstone at the Faculty of Civil Engineering and Geoscience, department of Geo-Engineering at the Delft University of Technology. Thorn-samples used for micro-CT scanning are given in appendix B.

Figure 33 shows micro-CT images of the weathered part of a drilled core. Parallel sedimentation layering including cracks are visible.

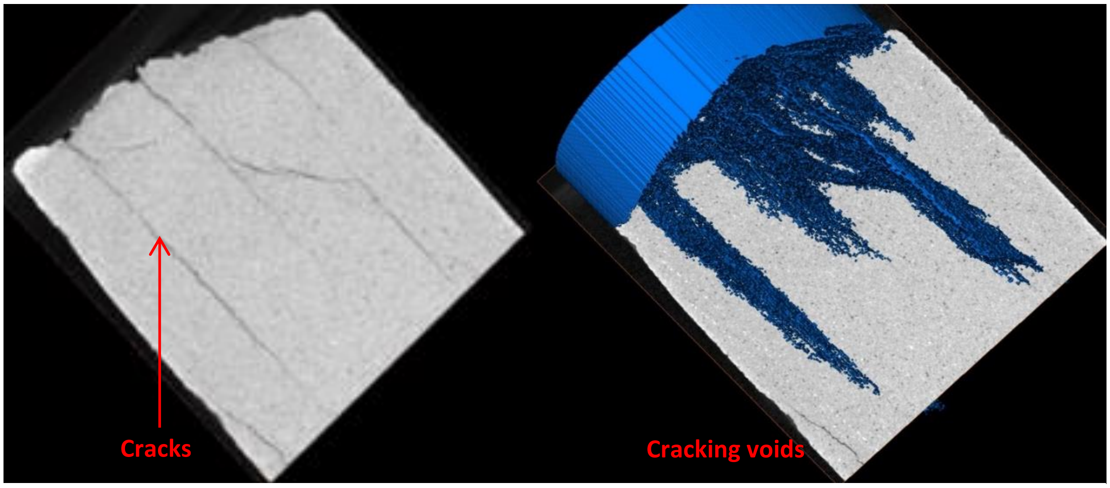

FIGURE 33: SCAN OF B3-1 TOP. SEVERAL PARALLEL SEDIMENTATION LAYERING VISIBLE INCLUDING (MICRO) CRACKS (LEFT). CRACKING VOIDS INDICATED ON THE RIGHT.

The following images are taken from a sub-sample cut from the weathered edge of sample 8 that corresponds to the thin-section made from sample 3. The scanned area is indicated by the red frame.

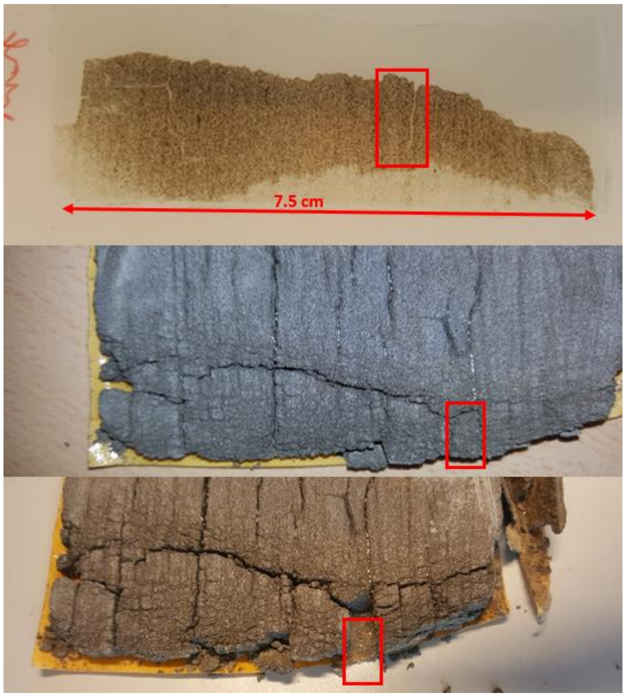

Figure 34: Thin-section obtained from sample 3 (see table 1, appendix C). Sub-sample area indicated by the red frame. Scale of the boxed is approximately 8mm x 5mm.

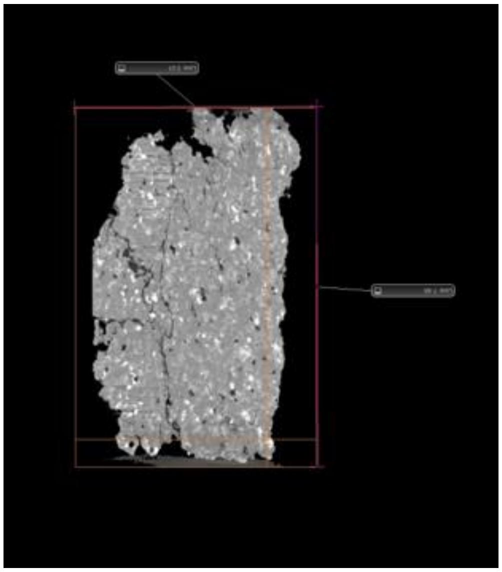

Figure 35: Gray Quartz grains along with other highly attenuating grains are visible. Scale: approximately 8mm x 5mm.

Several micro-CT scans are presented below to illustrate the microstructure of the Thorn-sandstone in 3D. Observations made are described in the captions of the figures.

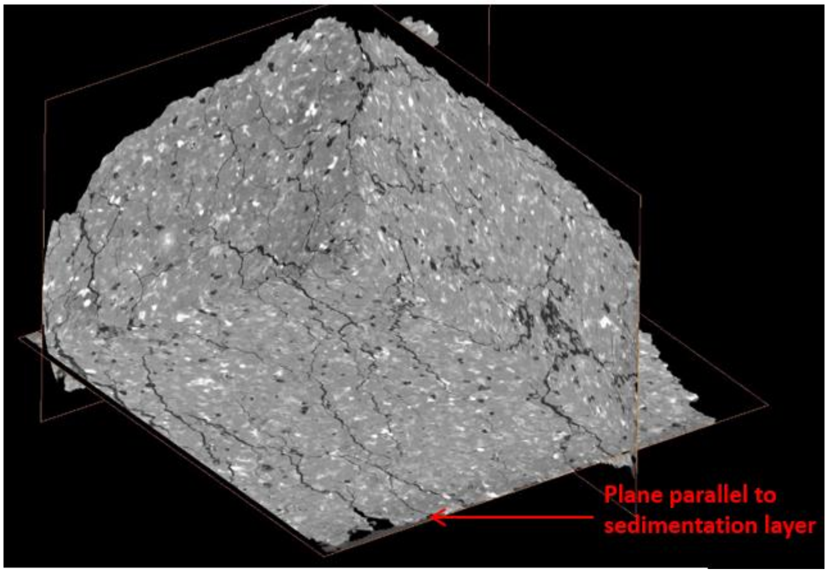

Figure 36: Internal structure of the above mentioned sub-sample in 3-dimensions.

The cracks observed through optical microscopic analysis can also be seen in the micro-CT images. This is shown in figure 37.

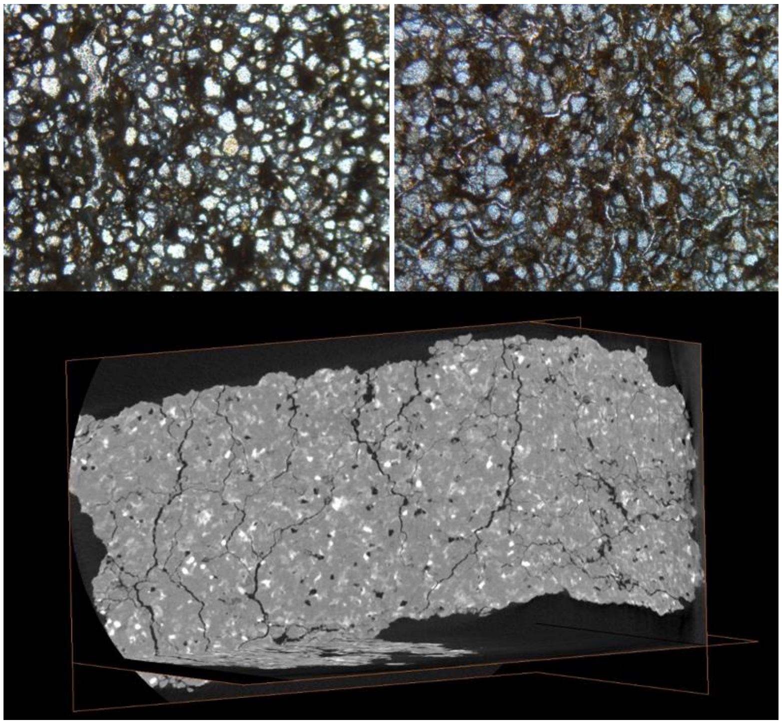

FIGURE 37: MULTIPLE CRACKING IN SEVERAL DIRECTIONS. HIGHER (ALMOST WHITE) AND LOWER (ALMOST BLACK) ATTENUATING GRAINS ARE ALSO VISIBLE.

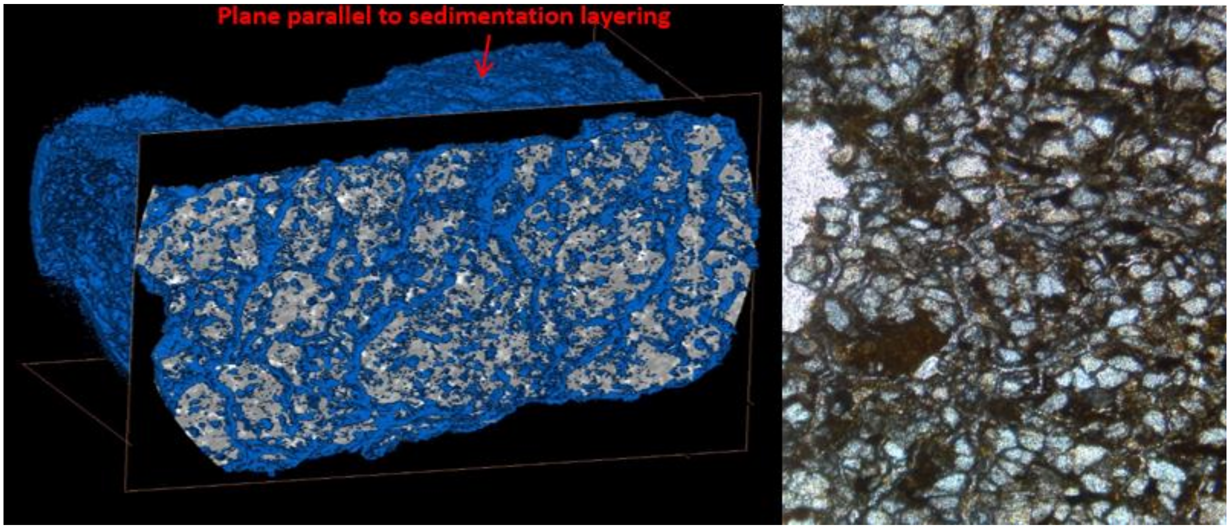

FIGURE 38: MULTIPLE CRACKING IN ALL DIRECTIONS. MICRO-CT IMAGE (ON THE LEFT) AND OPTICAL MICROSCOPIC IMAGE OF THE SAME AREA (ON THE RIGHT).

A high resolution scan (0.0015 x 0.0015 x 0.0015 mm^3 voxel) was done on a selected area of the previous sub-sample. Very light colored, almost white, spots on micro-CT images indicate highly attenuating particles. This can be seen in figure 39.

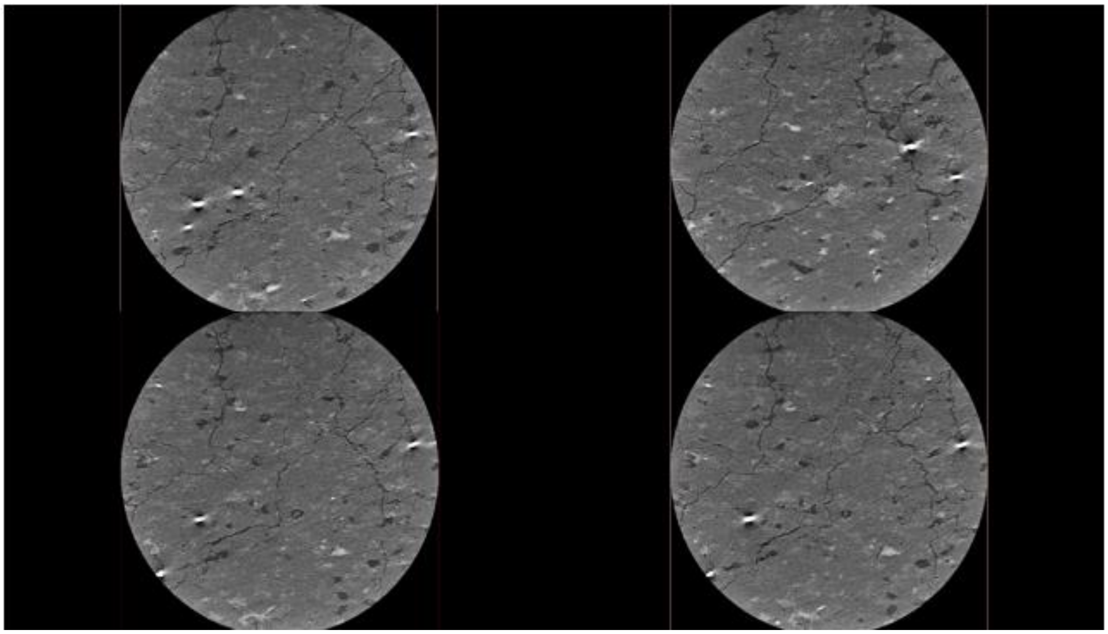

FIGURE 39: HIGHLY ATTENUATING PARTICLES (ALMOST WHITE).

The next scan was done on another sub-sample taken from sample 8 (see table 1, appendix B). This was then reconstructed into the shape of a flat cylinder (dimension: diameter: 3.61 mm, height: 1.74 mm. Resolution: 0.00175 mm) (see figure 40).

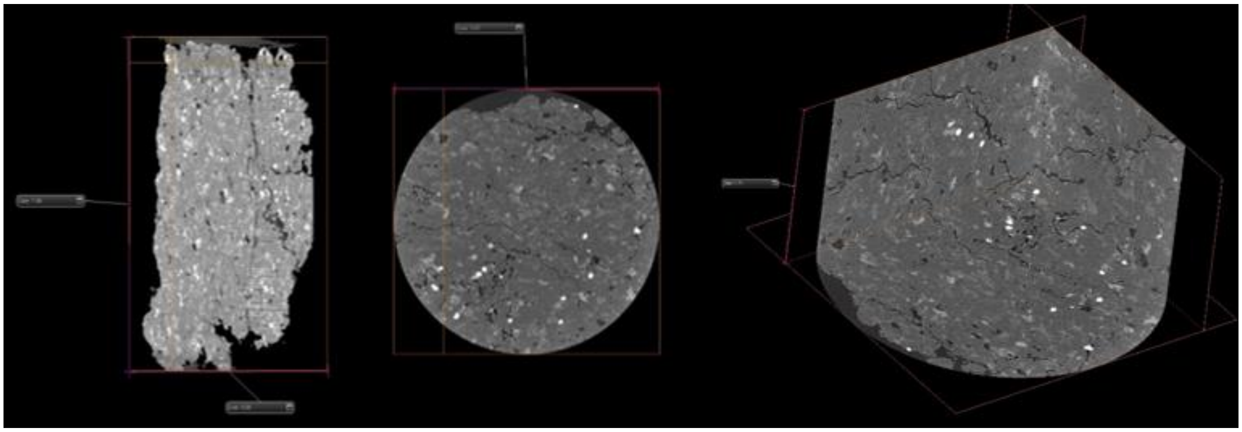

FIGURE 40: SUB-SAMPLE (LEFT) AND CORRESPONDING FLAT CYLINDER (CENTER AND RIGHT).

The next micro-CT scan is done on a platy sub-sample of the brown cross-bedded zone at the top of sample 8 (see figure 41). Dimension of the sub-sample is 1.20cm x 0.75cm. The images display the micro-cracking and the highly attenuating particles (figure 42 and 43).

FIGURE 41: PLATY SUB-SAMPLE.

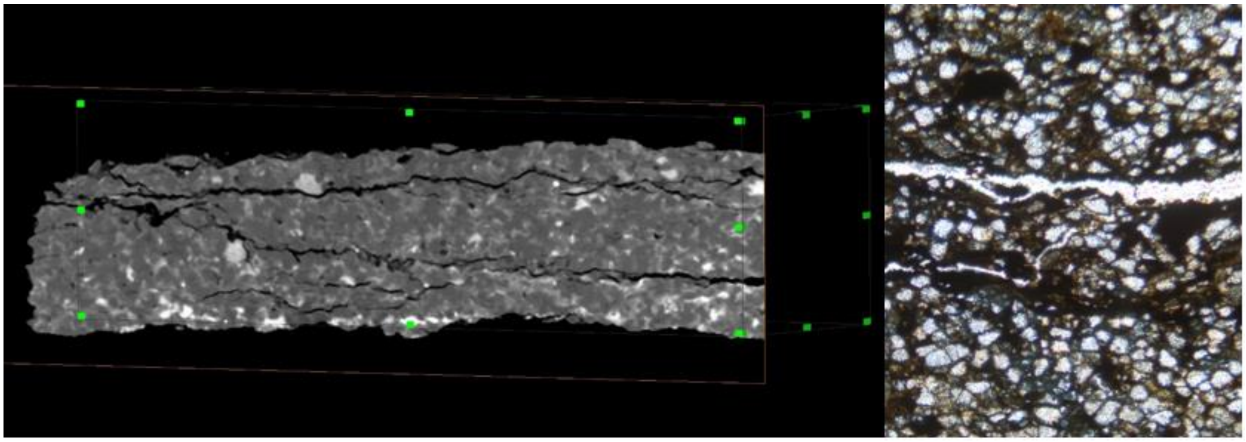

FIGURE 42: MICRO-CT (LEFT) AND OPTICAL MICROSCOPIC (RIGHT) IMAGES OF PARALLEL CRACKS WITHIN THE PLATY SUB-SAMPLE.

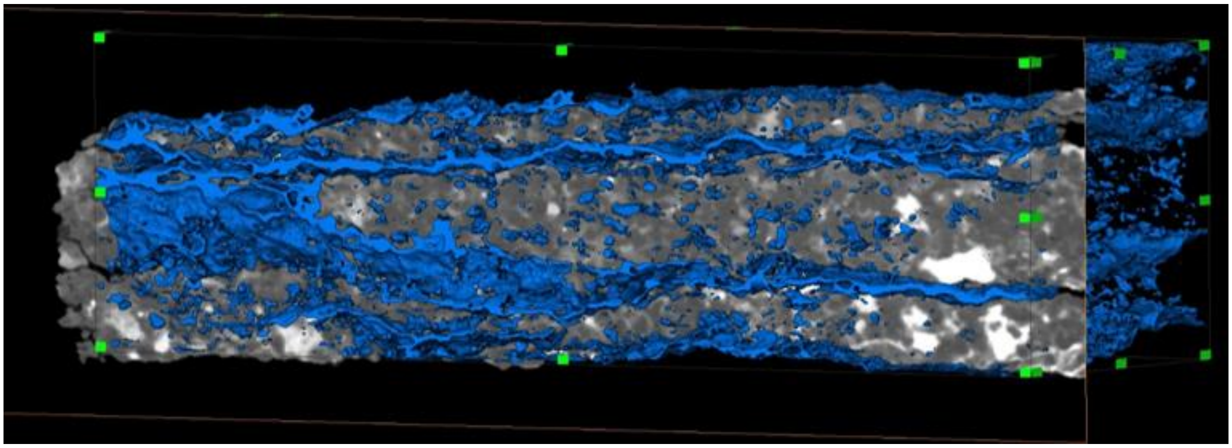

FIGURE 43: PARALLEL CRACKING VOIDS WITHIN THE PLATY SUB-SAMPLE.

Further analysis and testing is required to determine if the high attenuating grains are connected to the dark spots visible on the optical microscopic images as shown in figure 44.

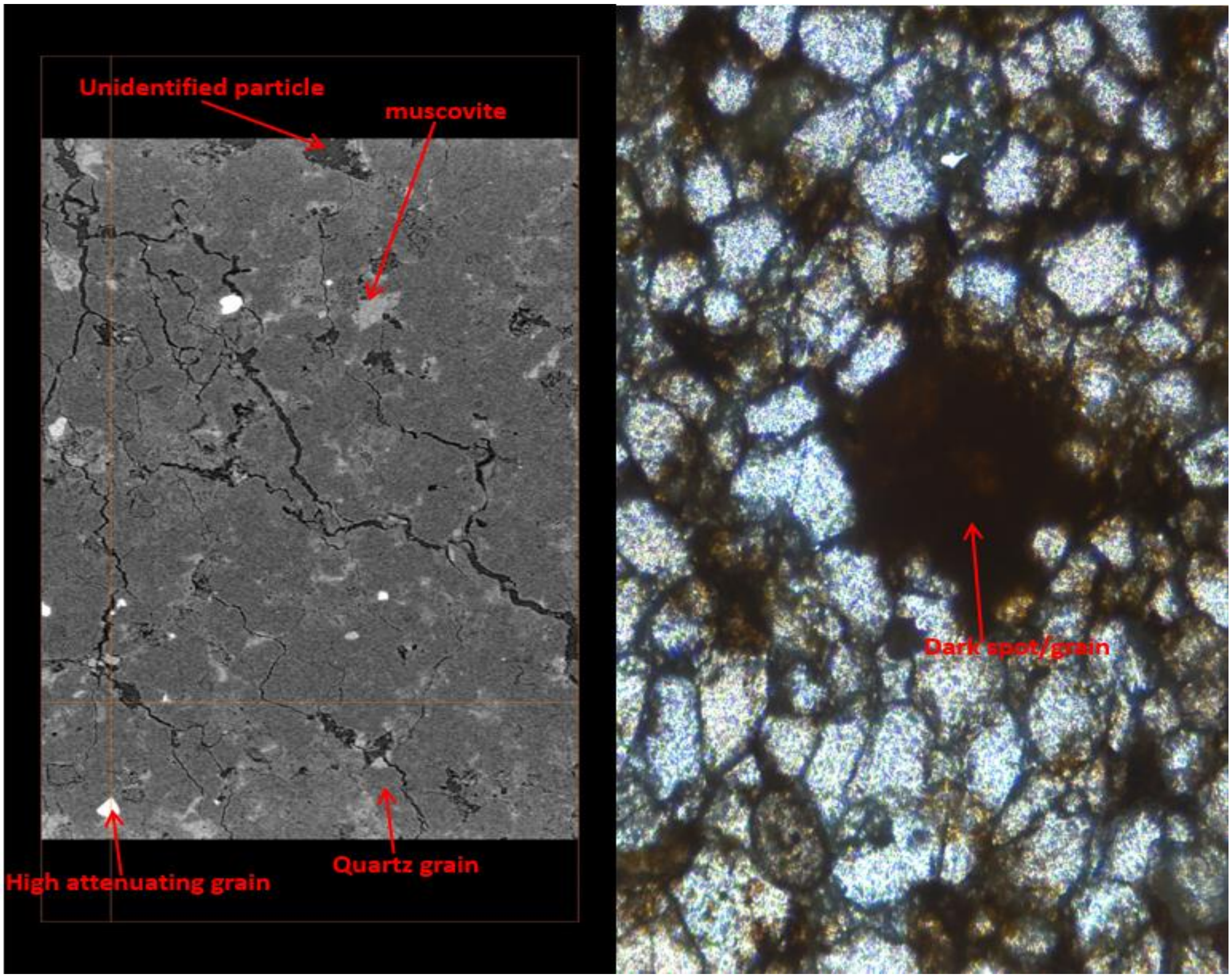

FIGURE 44: HIGHLY ATTENUATING GRAINS ON MICRO-CT IMAGE (LEFT) AND DARK SPOT ON OPTICAL MICROSCOPIC IMAGE (RIGHT).

Analysis of the micro-CT scans of the Thorn-sandstone shows the presence of several different grains. These grains are tightly packed. Their boundaries are not always fully visible, even at the most detailed micro-CT scan (voxel size: 1.75b micro meters). Often, a denser (more attenuating) material seems to coat the grains. This material looks heterogeneous since it has variable grey values. It does not only surround but also forms grains. This material seems to be spread around the quartz grains in more or less the same way as the unknown brown material visible in optical microscopic images. Furthermore, highly attenuating and almost white grains are visible. Naming these particular grains is not yet possible. More information is required. Also, black particles with angular edges can be seen. They might be voids filled with unidentified material or filled in with the resin used to impregnate the rock for producing thin-sections. For more micro-CT images, see appendix B.

3.4 X-Ray Diffraction analysis (XRD)

The XRD analysis only indicated quartz, chlorite and micas. The quartz and micas are visible on the thin-sections observed with the optical microscope while only a few grains of chlorite have been identified. The XRD results do not elucidate the nature of the brown material. It should be noted that the XRD that has been conducted is not tuned to detect clays. Also, minerals present in amounts less than 5% are not detected.

3.5 X-Ray Fluorescence analysis (XRF)

The XRF-analysis indicates quartz, aluminum and iron dominate in the Thorn-sandstone. Aluminium and iron are assumed to be present in the form of oxides. Also a significant amount of potassium, magnesium, titanium, sodium, calcium, phosphorus, and fluor is present. Traces of elements like zirconium, zinc, lead are found. The analysis cannot show the presence of organic material. The results of the XRF do not provide sufficient insight into the mineralogy of the brown material. To be able to name the minerals present more analysis is needed. SEM-analysis should provide this information. For the XRF results, see appendix C.

3.6 Loss-on-Ignition test

The detailed calculations and results of the Loss-on-Ignition test are given in appendix D. After heating the rock-powder to 440 ^{o}C during four hours and then, after calculating the OM-value, reheating to 550 ^{o}C for another four hours the OM-values are 1.65% and 1.68%. The mass loss between 440 ^{o}C and 550 ^{o}C are only 0.26% and 0.22%. These values indicate a very small amount of mass loss which indicate the quasi-absence of organic material (and clays) in the Thorn sandstone. As the brown material concentration is low in the Thorn sandstone, one cannot conclude that the brown material is inorganic and does not contain clay.

3.7 SEM Analysis

3 thin-sections were used for the SEM-analysis session at the Rijksmuseum in Amsterdam:

- Thin-sections 1 and 2, prepared by the Cultural Heritage Agency of the Netherlands, also observed earlier under the optical microscope.
- Thin-section 3, prepared at the TU Delft.

Analysis of thin-sections 1 and 2 was focused on zones highlighted with an arrow in figure 45 and 46. Thin-section 3 was analyzed as a whole, as indicated in figure 47.

FIGURE 45: THIN-SECTION 1 WITH INDICATION ARROW.

FIGURE 46: THIN-SECTION 2 WITH INDICATION ARROW.

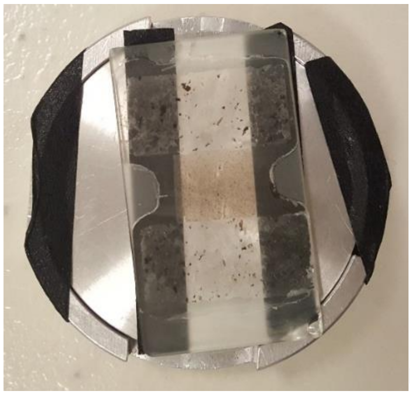

FIGURE 47: SAMPLE PREPARATION OF THIN-SECTION 3.

Some grains were subjected to the EDEX analysis. The results of the EDEX analysis on grains have been clustered based on their brightness with respect to the brightness of quartz grains. For the results, see appendix E1. Many grains which are not quartz grains contain carbon, oxygen, sodium, magnesium, aluminum, silicium, potassium, iron in diverse proportions.

A few grains also contain fluor, titanium, zirconium, lead, phosphorus, sulfur, chlorine, copper, chrome and manganese. A table of all elements found in specific parts of the thin-sections, during SEM-analysis, can be found in appendix E2. An elemental map of a part of thin-section 3, C2(19), was produced (Van Hoessel, 2016). The map shows the variation of elemental composition in grains contained in an area with a resolution of 512 x 384 pixels. Quartz grains can be easily distinguished. However, it is not obvious to figure out the minerals out of which non-quartz grains are made based on their elemental composition. Unsuccessful trials have been made by guessing the number of oxygen in the minerals and assuming that grains are made of feldspars, micas or clays. See appendix F for chemical formulas of these minerals and elements. Elemental-color maps of section C2(19), in the center of thin-section 3, are given underneath in figures 48 to 53. This part was chosen because it containes all elements of interest (Al, K, F, Mg, Si, Ti and Fe). The following are properties of section C2(19):

Name: C2(19) Data Type: Counts Image Resolution: 512 by 384 Image Pixel Size: 1.77 µm	Map Resolution: 512 by 384 Map Pixel Size: 1.77 µm Acc. Voltage: 20.0 kV Magnification: 140

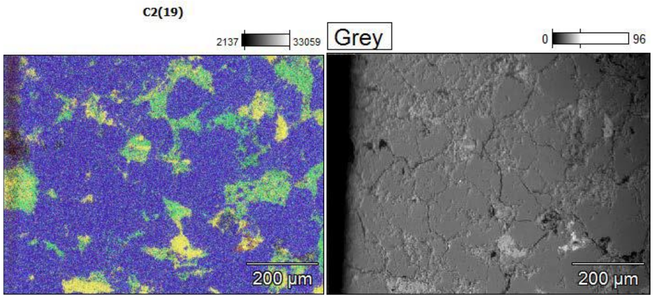

FIGURE 48: COLOR MAP (LEFT) COMPARED TO GREY SCALE (RIGHT).

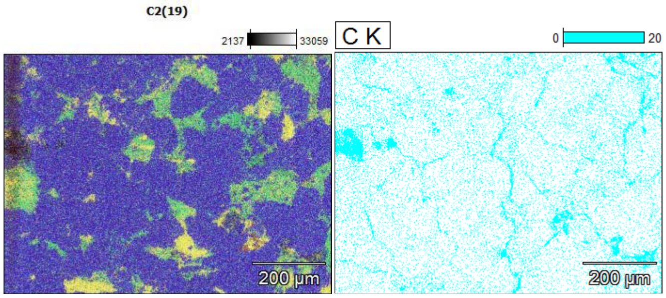

FIGURE 49: CONCENTRATED AREAS OF C AND K WITHIN C2(19).

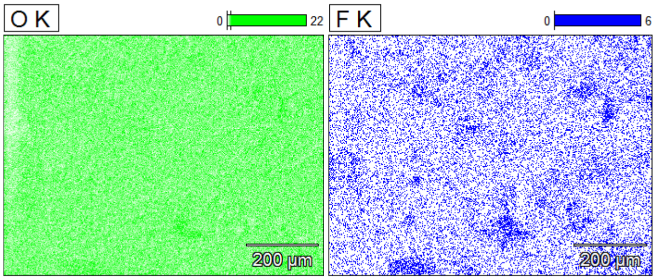

FIGURE 50: CONCENTRATED AREAS OF O, F AND K WITHIN C2(19).

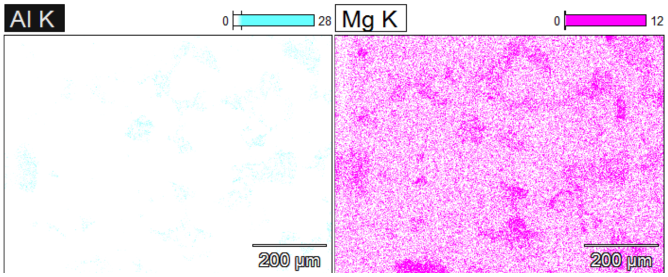

FIGURE 51: CONCENTRATED AREAS OF MG, AL AND K WITHIN C2(19).

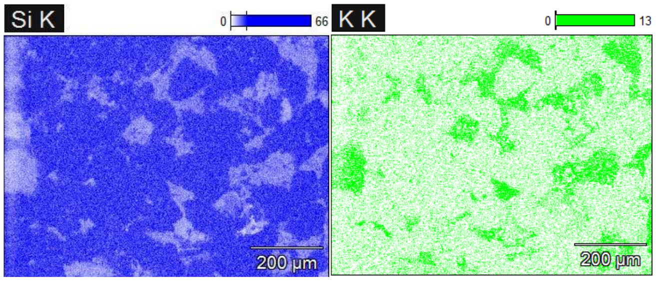

FIGURE 52: CONCENTRATED AREAS OF SI AND K WITHIN C2(19).

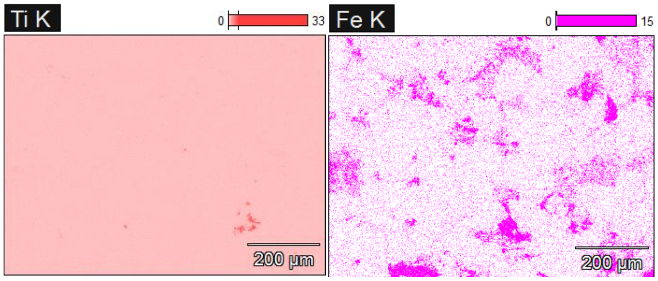

FIGURE 53: CONCENTRATED AREAS OF TI, FE AND K WITHIN C2(19).

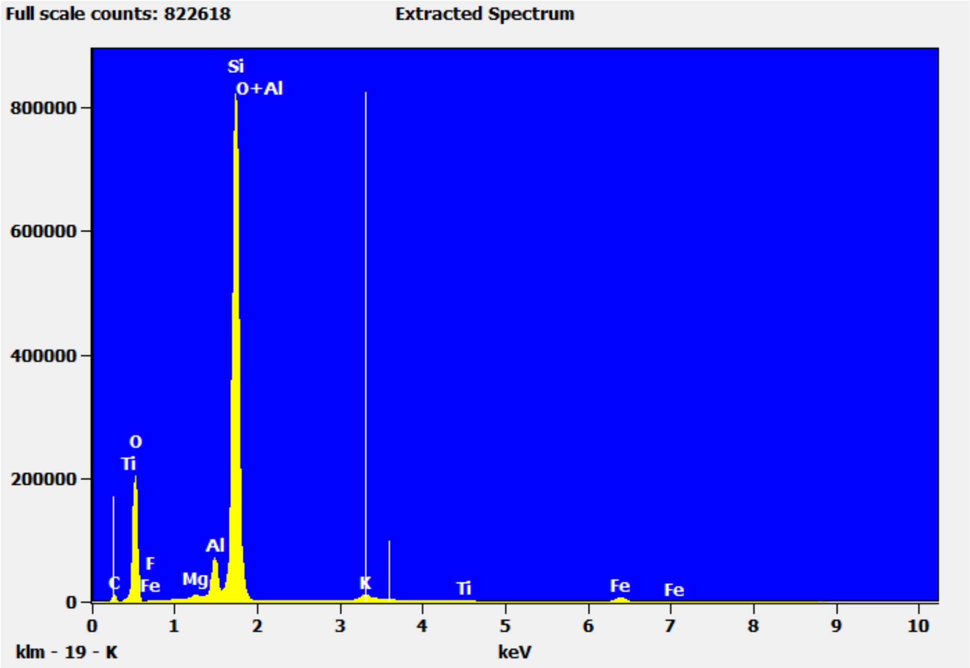

FIGURE 54: ELEMENTAL MAP SHOWING THE PRESENCE AND AMOUNT OF VARIOUS INTERESTING ELEMENTS IN SECTION C2(19). TI, AL,SI, K AND FE AMONG OTHERS.

Chapter 4: Combination of individual test results

An MBA value of 0.73 was obtained which indicates that the Thorn-sandstone has an acceptable to marginal soundness when used as rock aggregates. Since the result is obtained for 2g of powdered rock, including non-reactive grains like quartz grains, we cannot conclude on the absence of swelling clays. Furthermore, the staining of a thin-section did not provide reliable results.

Through optical microscopic analysis of the thin-sections quartz grains, mica’s, and some other materials are found. The other materials were more difficult to identify. Brown material surrounding quartz grains and several black spots were also unidentifiable.

With micro-CT scanning of several (sub-) samples quartz grains were recognizable. Additionally, there is a significant amount of higher attenuating material which looks to be either forming grains in between quartz grains or coating these quartz grains. This material is more or less spread like the unidentified brown material seen earlier in the optical microscopic images. Some very bright grains, that attenuate highly on X-rays, are also visible. Unfortunately, this info is not sufficient enough to be able to know the names of these materials.

The XRD analysis only indicated quartz, chlorite and mica's but given that the chlorite minerals were not observed frequently during optical microscopic analysis, the results of the XRD is considered uncertain. The test was conducted at the faculty of 3mE where the database used to derive mineral names from X-ray diffracted beams does not contain many clay minerals. To recognize clay minerals, several treatments to the material are necessary for correct XRD analysis. These include treatments like exposure to different temperatures and saturation, with Glycol for example. Moreover the XRD cannot detect minerals present in amounts less than 5%.

The XRF analysis indicated the presence of mainly quartz, aluminum and iron, a significant amount of potassium, magnesium, titanium, sodium, calcium, phosphorus, and fluor along with traces of elements like zirconium, zinc, lead. The Thorn-sandstone was reduced to powder for the test. The XRF analysis cannot reveal the presence of organic material. The absence of a significant amount of organics in the Thorn sandstone is supported by the Loss-on-Ignition test. Due to the low concentration of the brown material in the Thorn sandstone, it cannot be concluded that the brown material is inorganic.

To be able to name the unknown substances more elemental analysis, through SEM-analysis, is done per grain rather than for a powdered bulk in which grains are mixed.

From the SEM-results, it appears that the brown material between the grains is not amorphous but heterogeneous at the detailed scale. It probably contains clays and may be chlorite, micas, weathered glauconite, feldspar as well as very small grains of rutile, hematite or ilmenite. Clay mineralogy is complex and multiple but most of the elements identified with XRF and SEM can be found in clays. Additionally all elements present in glauconite [$(K,Na)(Fe^{3+},Al,Mg)_2(Si,Al)_4O_{10}(OH)_2$], belonging to the group of micas, have been identified. At this point however, not enough micas have been observed under the optical microscope.

Larger grains containing iron (and no titanium), titanium (and almost no iron) or both iron and titanium were observed during SEM-analysis. These grains could possibly be hematite [Fe_2O_3], rutile [TiO_2] or ilmenite [$FeTiO_3$] based on the presence of Fe and Ti. Such grains are not uncommon in sandstones, especially when parent rocks are of igneous origin.

During the SEM-session P-Si minerals were noticed. These are probably zircon due to the Zr-P peak overlap (Van Hoessel, 2016). Some grains do contain phosphorus rather than zircon. They are a lot darker than the Zr grains on the SEM-images (Van Hoessel, 2016). Grains containing phosphorus could be small fossil fragments - e.g. from (fish) bones or coprolites - or secondary calcium phosphates (phosphorite-like material). They could possibly be apatite grains [$Ca_5(PO_4)_3(F,Cl, OH)$]. The presence of fluor (SEM) might indicate that this is the case (Huisman, 2016).

Identifying minerals based on their chemical composition from EDEX or XRF is difficult. There are quite a number of relevant minerals to choose from (various feldspars, micas and clay minerals, combined with secondary minerals like iron-oxides and various carbonates), more than the number of relevant chemical elements. This means that there are too many degrees of freedom to make “hard” identifications. Because of this we keep the possibility of having apatite in the Thorn-sandstone and assume material containing Ca and P (and F) are connected to fossils. We conclude that the brown material is an heterogeneous mixture of clays, micas, chlorites and feldspars. Weathering of the mixture would cause its discoloration into brown material.

Chapter 5: Evaluation of Hypotheses

5.1 H_1: Coal-measures Sandstone rich in organics.

Not enough organics have been found to retain this hypothesis. However, due to the low concentration of brown material around the sandstone grains, it cannot be concluded that the brown material is inorganic.

5.2 H_2: Glauconite Sandstone containing swelling clays

Even if every element out of which glauconite is made of has been identified, too few micas have been observed under the microscope. The hypothesis that the Thorn sandstone is a Glauconite Sandstone is rejected despite the greenish grey color of the Thorn-sandstone. Glauconite can weather to Smectite, a swelling clay under temperate climate. The MBA value measured on powder of the Thorn sandstone does not exclude the presence of (swelling) clays in the brown material; the brown material being present in low concentration in the Thorn sandstone. Unfortunately, the Methylene Blue staining on thin sections was not properly conducted to reject or accept the hypothesis of a brown material rich in swelling clays..

5.3 H3: Glauconite Sandstone subjected to oxidation

The presence of iron oxides is anticipated from the XRF results. Iron oxides are expected to occur in the form of large grains as well as in the form of amorphous brown material based on the optic microscopic analysis. This point is confirmed by the EDEX analysis. The iron oxides could be goetite, lepodocrocite, ferrihydrite, and probably many others. They could be hydrated or deshydrated. If the low LOI value measured on the rock powder could be extrapolated to the brown material present in the low concentration in the Thorn sandstone, the iron oxides would have to be dehydrated. The origin of the iron is unclear. It could have precipitated in the rock in situ before quarrying or after quarrying. In this latter case, iron would result from the weathering of some minerals. The assumption that the Thorn Sandstone is a Glauconite Sandstone that has been subjected to oxidation cannot be rejected nor accepted.

5.4 H4: Sandstone with clayey matrix

This hypothesis cannot be accepted nor rejected. The XRD results do not point at clays but these were not correctly conducted and analyzed to detect clays. The MBA spot test does not indicate a large amount of swelling clays in the Thorn sandstone and MBA staining of a thin-section was not conclusive. However, results from the SEM and XRF do not contradict this hypothesis: in the material surrounding the quartz grains, a heterogeneous material formed consisting of very small grains. Some of these grains contain all chemical elements that can be found in clays.

Chapter 6: Discussion

The obtained results, ranging in significance and certainty, are not conclusive enough and are thus open to discussion. Although a large amount of chemical elements which are characteristically present in clays have been found through testing, it has not been possible to name specific minerals. Elements like phosphorus, fluor, titanium and zirconium along with more common elements like calcium, iron, silicon, among others, have been identified. They can be related to the formation of the Thorn sandstone rather than to its degradation.

Phosphorus within the system may be a possibility due to the presence of fossilized organisms with phosphorus bearing bones. Just as phosphorus, fluor and titanium are not uncommon in certain clays and micas. Zirconium containing grains, usually of detrital origin, are also present.

It is for that reason that these grains can account for the high attenuating particles found on the micro-CT scans.

Marine invasions:

Marine invasions were a regular occurrence during the Westphalian (Dusar, Paproth, Streel & Bless, 2000). These conditions can cause detrital sediments when pre-existing rocks are rubbed away or weathered by, in this case, the force of water. Detrital ilmenite or rutile are therefore not uncommon if igneous rocks are part of the provenance area of the sandstone. The presence of titanium and iron provides the possibility for ilmenite and rutile to be present. The interpretation of having ilmenite and rutile may therefore explain the detrital origin of the Thorn-sandstone. Zirconium containing grains are very heavy and would be visible on micro-CT scans in the form of highly attenuating particles.

By assuming a detrital environment makes it difficult to exclude apatite as a detrital grain. Apatite inclusions, containing elements like phosphorus, fluor and calcium, in rock fragments can therefore be a possibility. Because it was not possible to name this mineral (apatite) with high certainty this theory is also open to discussion.

Chapter 7: Conclusion and Recommendations

In this thesis the processes which are causing the degradation of the Thorn-sandstone are investigated. Several criteria were used to distinguish the interesting parts of the provided samples. A series of tests were conducted to determine the mineralogical content, elemental content, organic content and swelling potential of the Thorn-sandstone. Four theories can be formulated as to why the sandstone currently undergoes such rapid degradation. These theories, given as hypotheses, have been examined by analyzing the micro-structure of several samples of the Thorn-sandstone and argue the presence of coal, glauconite, oxidized glauconite and a clay-matrix within the Thorn-sandstone. No significant amount of organics (coal) were found which is also the case for the presence of swelling clays in the Thorn sandstone. However, it needs to be noted that the brown material is present in low concentration in the Thorn sandstone. As a result, it cannot be excluded that the brown material contains (swelling) clays and organics; the main constituent of the Thorn sandstone being inactive quartz grains. Methylene blue staining on thin sections was not done properly. The absorption potential of the brown material could not be checked. Iron(-oxide) are present in the brown material in an amorphous form. They could be or not related to the oxidation of glauconite. The theory of a sandstone with a clay-matrix, given as hypothesis 4, has proven to be the most likely based on the obtained results. These results partly support but also disprove this hypothesis. The heterogeneous clayey matrix found in several grains contains a vast variety of elements generally present in clays. Because the amount of each element, within several different grains, could not be identified it is impossible to classify the grains and to name the minerals. This difficulty is expected due to the complex mineralogy of clays. Due to the many degrees of freedom to make hard identifications it is concluded that it cannot be said with significant certainty whether the observed minerals in the brown material are specific clay minerals glauconite, rutile, hematite, or ilmenite. What can be said is that the brown material is a mixture of clay minerals, fine crystalline micas and perhaps even chlorite as well as amorphous (iron) oxides. For this reason it can be said that this research, though it provides some insight into the Thorn-sandstone, does not answer the question as to why the Thorn-sandstone is rapidly degrading at this rate. The findings show that the Thorn-sandstone is degrading through multi-directional fracturing which could be connected to the exposure of clayey minerals to wetting- and drying cycles.

Recommendations:

Conducting analysis on more Thorn-sandstone samples covering a wider area of the church-façade may be a way to obtain more unknown mineralogical information not present in the current samples. This information may then possibly be used to recognize patterns which characterize the internal structure of this sandstone. Also, to obtain better mineralogical insight into the sandstone, XRD analysis with proper sample preparation for clay mineral identification is recommended.

It is not excluded that other hypotheses should be formulated to explain the degradation of the thorn sandstone.

References

1. Cassar, J. (2002). Deterioration of the Globigerina Limestone of the Maltese Islands. In: Siegesmund, S., Weiss, T., Vollbrecht, A. (Eds.), Natural Stones, Weathering Phenomena, Conservation Strategies and Case Studies: Geological Society, London, Special Publications, 205, 33–49.
2. Dusar, M., Paproth, E., Streel M. & Bless M. J. M. (2000). Palaeogeographic and palaeoenvironmental characteristics of major marine incursions in northwestern Europe during the Westphalian C (Bolsovian). Geologica Belgica, 3(3-4), 331–347.
3. Ikeda, S., Nakano, T. & Nakashima, Y. (2000). Three-dimensional study on the interconnection and shape of crystals in a graphic granite by X-ray CT and image analysis. Mineralogical Magazine, 64(5), 945–959.
4. Martinec, P., Vavro, M, Ščučka, J. & Maslan, M. (2010). Properties and durability assessment of glauconitic sandstone: A case study on Záměl sandstone from the Bohemian Cretaceous Basin (Czech Republic). Eng. Geol. doi:10.1016/j.enggeo.2009.08.005.
5. Schmidt, K. (2000). Göbekli Tepe, southeastern Turkey a preliminary report on the 1995–1999 excavations. Paléorient 26(1), 45–54.
6. Shadmon, A. (1996). Stone: An Introduction, 2nd ed. Intermediate Technology Publications, London.
7. Verhoef, P. (1992). The Methylene blue adsorption test applied to geomaterials.
8. Winkler, E.M. (1997). Stone in Architecture, 3rd revised and extended ed. Springer-Verlag, Berlin.
9. Restauratie R.K. Kerk H. Michaël, Thorn – Herstellen natuursteen basement kerktoren, Satijnplus Architecten, 2015.
10. Dusar, M., Paproth, E., Streel, M., Bless, M. J. M. (2000). Palaeogeographic and palaeoenvironmental characteristics of major marine incursions in northwestern europe during the westphalian C (Bolsovian)
10. ta1900-M&G-Dictaat, M. M. van Tooren, 2012

Personal communication:
1. Van Hoessel, A., 2016. Visit (17/08/2016), email exchange (24/08/2016)
2. Huisman, H., 2016. Visit (17/08/2016), email exchange (02/09/2016)

Websites:

1. [1], http://www.holland.com/global/tourism/article/the-white-village-of-thorn.htm
2. [2], http://bit.ly/2nA4an2 - Google Maps - The city of Thorn, Belgium – (visited: May 2016)
3. [3], https://goo.gl/6ht8u9 - EAG Laboratories - Scanning Electron Microscope (SEM) – (visited: August 2016)
4. [4], https://goo.gl/z1O3X6 - MEE: Materials Evaluation and Engineering, Inc. – Scanning Electron Microscopy (SEM) – (visited: August 2016)
5. [5], https://goo.gl/xV2Qiw - Geochemical Instrumentation and Analysis – Scanning Electron Microscopy (SEM) – (visited: August 2016)
6. [6], http://bit.ly/2netjCt - Imperial College Rock Library – Glauconitic Sandstone – (visited: August 2016)

Appendices

Appendix A – Information regarding glauconite

Glauconite:

Glauconite is a term used for small, rounded, green-to-black pellets and grains mostly found in sedimentary rocks. It has a structure similar to most micas which causes it to be considered a mica-like clay mineral. For this reason glauconite has a complex chemical formula. It has a monoclinic crystal structure and develops at the expense of minerals like biotite and Illite which are more commonly occurring iron-bearing sheet silicates (sandatlas.org/glauconite). The complex chemical formula of clay minerals causes these minerals, such as glauconite, to have similar optical properties (such as morphology and internal structure) and thus making it difficult to distinguish them from one another. Glauconite is also described as a hydrated iron- and potassium-rich (illitic) clay whose composition consists out of intermixtures of expandable (montmorillonitic) and non-expandable (illitic) layers (Triplehorn, 1965).

Diagenesis of biotite or illite in sandstones in shallow water exposed to reducing anaerobic conditions at slow deposition rates can lead to the formation of glauconite minerals within these sandstones. Pyrite, which also needs these reducing conditions to form, may occur together with glauconite for this reason (sandatlas.org/glauconite). However, oxygen may be present in the sandstone due to atomic oxygen-bonds in other compounds. The aforementioned reducing conditions are probably caused by the presence of decaying organic matter which consumes all free oxygen (sandatlas.org/glauconite). This gives an indication regarding the environment of formation of glauconite. Glauconite can have swelling potential due to the compositional varieties this mineral may contain.

Glauconite sandstone:

Glauconite sandstones mostly consist of clastic grains of quartz, siltstone, chert, bioclasts, ooliths, glauconite pellets, cement and smaller amounts of other minerals. In these sandstones the occurrence of glauconite can be in the form of green elongated pellets (up to 0.2mm) or as groups of authigenic crystals within the cement (website [6]). Authigenic crystals are crystals which precipitate from hydrothermal fluids. Glauconite is the only clay mineral within sedimentary rocks which has a authigenic origin, is present in large amounts and is also impurity-free (Triplehorn, 1965). Four important factors are needed for glauconitization of a sandstone to occur: (1) parent silicate material, (2) an iron and potassium source, such as sea water, (3) reducing conditions and (4) time (Triplehorn, 1965). If these factors get the chance to have an impact on said sandstone then glauconitization can be the cause of significant changes in the glauconite pellets (Triplehorn, 1965). These, in general, can be: (1) Increased amount of iron and potassium, (2) smaller amount of expandable material (thus reducing the swelling potential), (3) crystallinity increase (better internal ordering), (4) change of color (light- to dark-green) and (5) better rounding and sorting of pellets (Triplehorn, 1965).

Glauconite in a (Belgian) Westphalian sandstone:

The presence of silicic grains, carbonate-clastic grains along with glauconite minerals in a glauconite sandstone are indicative for slow-rate deposition in a shallow marine environment in combination with, as earlier mentioned, relatively anaerobic conditions (Triplehorn, 1965). These conditions are most common at unconformities such as at the base of marine transgressive sequences (Triplehorn, 1965). By looking at the fragmental nature of the mineral content it is possible to determine the degree of transport prior to deposition. The difference in kind/form, variety and amount of glauconite pallets found makes it possible to use the recognition of these pallets and their degree of transport for environmental determinations and correlations (Triplehorn, 1965). Due to the occurrence of marine invasions during the Westphalian it can be possible to have glauconite in a Belgian Westphalian sandstone.

Marine invasions during the Westphalian:

Marine invasions on the European mainland during the Westphalian, a time with frequent tectonic activity and climate change, are related to the distribution of marine bands and faunal occurrences (Dusar, Paproth, Streel & Bless, 2000). It is these occurrences which make it possible to have glauconite in the Westphalian sandstone of Belgium. There is a close relation between the distribution of marine fauna-beds and distribution of upper delta plain environments (Dusar, Paproth, Streel & Bless, 2000). These delta plain environments contain the perfect circumstances for low velocity deposition to occur. Glauconite deposition would therefore be possible. The sea stayed situated long enough during every marine invasion (Dusar, Paproth, Streel & Bless, 2000). This is suggested by the frequent succession of transgressive-regressive faunal phases in these beds (Dusar, Paproth, Streel & Bless, 2000). This means that the marine invasions should be regarded as significant occurrences during the Westphalian (Dusar, Paproth, Streel & Bless, 2000). Due to these above mentioned Westphalian circumstances of Western Europe it can be a possibility that a glauconite sandstone was formed.

Appendix B – Micro-CT Images

The following images are from micro-CT scans performed on different samples of the Thorn-sandstone at the Faculty of Civil Engineering and Geoscience, department of Geo-Engineering, at the Delft University of Technology. All sandstone samples were provided by the Dutch Cultural and Heritage Agency (RCE).Thorn-samples used for micro-CT scanning are:

TABLE 1: ALL SAMPLES USED FOR MICRO-CT SCANNING.

	Information	Picture
Sample 1	Large block of the Thorn-sandstone. Dimension: (x x)	
Sample 2	Block of the Thorn-sandstone. Dimension: (x x)	
Sample 3	Block of the Thorn-sandstone. Dimension: (x x)	

Sample 4,5,6,7	4 cores: B1,B2,B3,B4; drilled from of sample 1. B1,B2: Vertically drilled B3,B4: Horizontally drilled B1,B2 and B3 broken along sedimentary boundaries. B4 remained whole.	
Sample 8	This thin slab was cut from sample 3. Several parts have been taken out of this sample to perform micro-CT scanning. Dimension: (x x)	

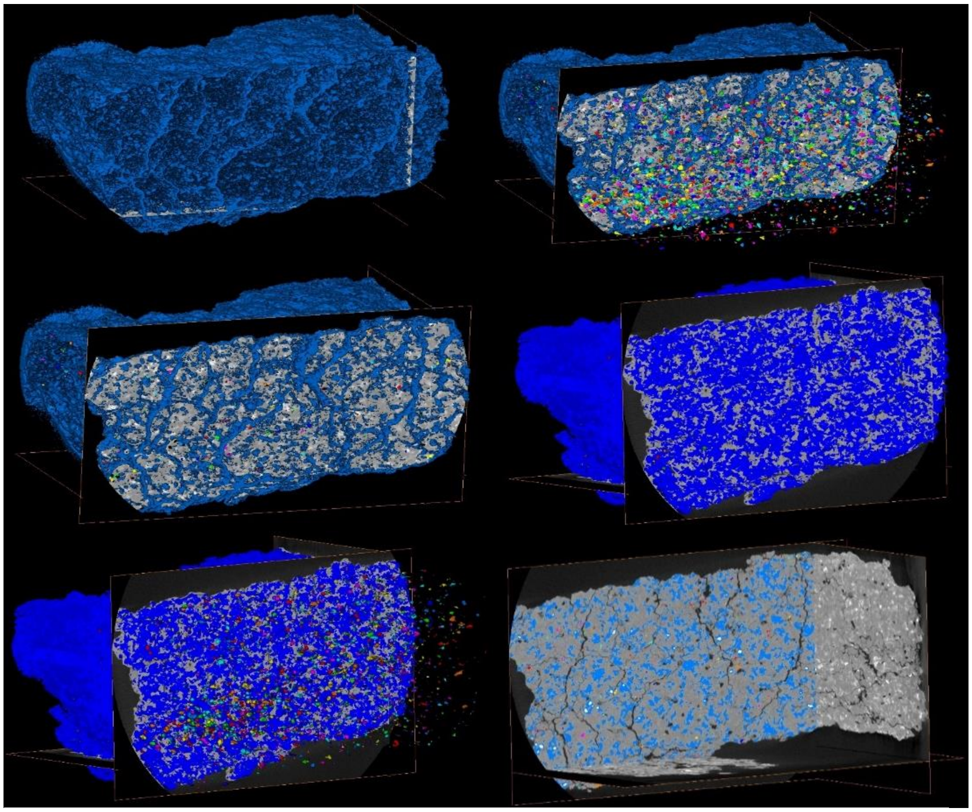

FIGURE 55: MICRO-CT IMAGES SHOWING MULTIPLE FISSURES OR CRACKS. MULTIPLE GRAINS INDICATED IN DIFFERENT COLORS ARE ALSO VISIBLE THROUGHOUT THE SAMPLE.

FIGURE 6: SEVERAL CORES ARE BEING DRILLED FOR MICRO-CT SCANNING.

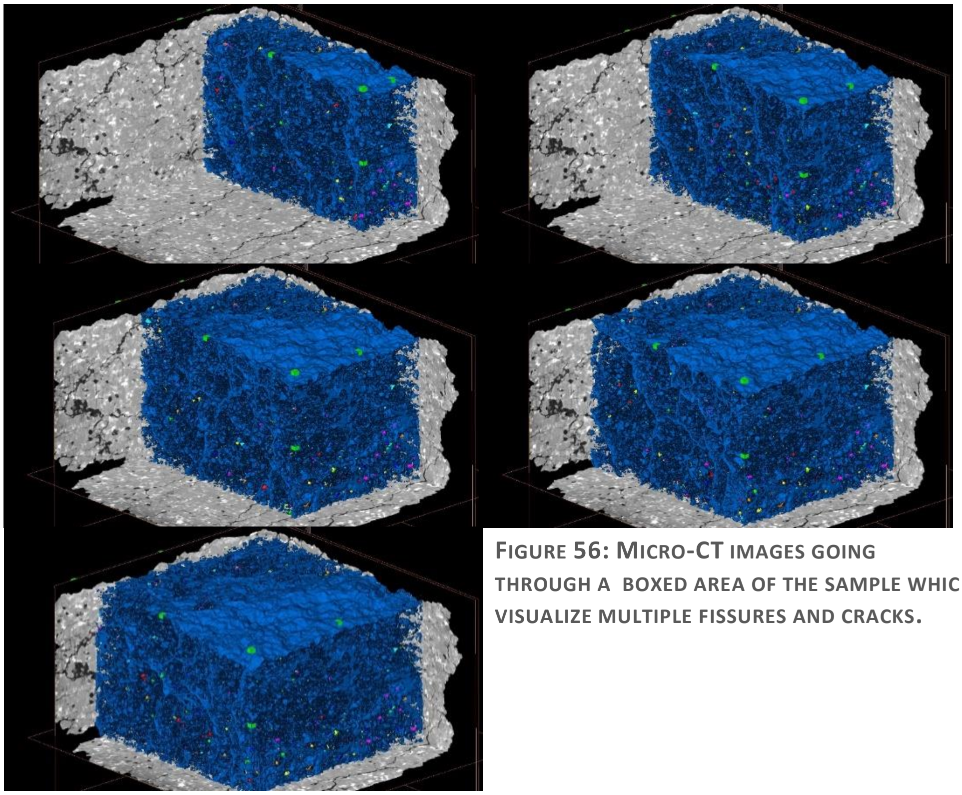

FIGURE 56: MICRO-CT IMAGES GOING THROUGH A BOXED AREA OF THE SAMPLE WHICH VISUALIZE MULTIPLE FISSURES AND CRACKS.

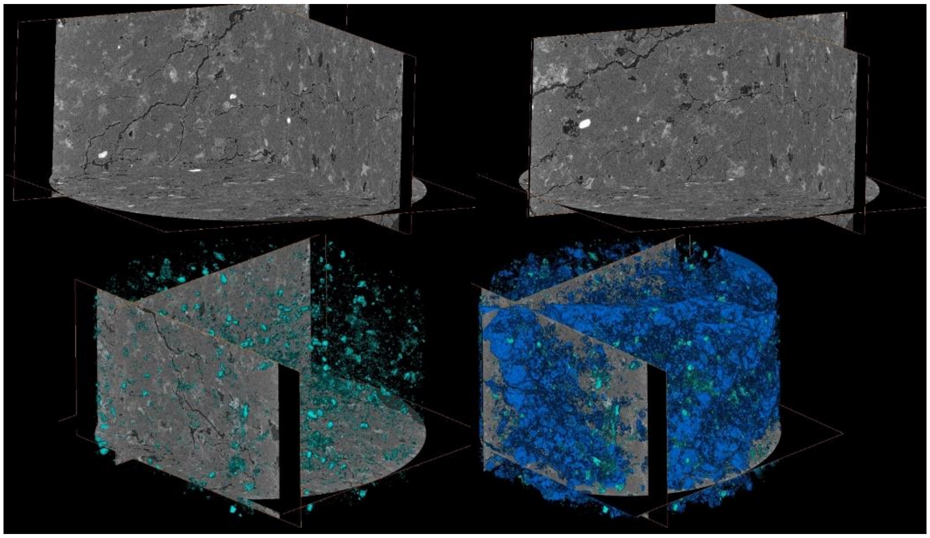

FIGURE 57: MICRO-CT IMAGES SHOWING IN 3D FROM A CIRCULAR SAMPLE IMAGE-CUT. LARGE PARTICLES (LEFT UNDER) AND FISSURES/CRACKS (RIGHT UNDER) ARE VISIBLE.

Appendix C – XRF composition table

	Compound Name	**Concentration wt(%)**	**Absolute Error**
1	SiO_2	*76.8*	*0.1*
2	AL_2O_3	*14.6*	*0.1*
3	Fe_2O_3	*3.26*	*0.05*
4	K_2O	*1.7*	*0.04*
5	MgO	*1.39*	*0.04*
6	TiO_2	*0.65*	*0.02*
7	Na_2O	*0.609*	*0.02*
8	CaO	*0.269*	*0.02*
9	P_2O_5	*0.218*	*0.01*
10	F	*0.198*	*0.02*
11	SO_3	*0.0687*	*0.008*
12	Cl	*0.0401*	*0.006*
13	ZrO_2	*0.0326*	*0.005*
14	Er_2O_3	*0.0301*	*0.005*
15	BaO	*0.0299*	*0.005*
16	Cr_2O_3	*0.0162*	*0.004*
17	MnO	*0.0144*	*0.004*
18	NiO	*0.00769*	*0.003*
19	ZnO	*0.00687*	*0.002*
20	Rb_2O	*0.0042*	*0.002*
21	SrO	*0.00418*	*0.002*
22	CuO	*0.00398*	*0.002*
23	PbO	*0.00353*	*0.002*

Table 2: Compounds found through XRF analysis.

Appendix D – Loss-on-Ignition values

Rock powder placed in 2 porcelain dishes: dish 1 and dish 2.

M_D= mass dry soil
M_{PDS}= mass porcelain dish + soil
M_P= mass of one empty porcelain dish
M_A= mass of ash (burned soil)
M_{PA}= mass porcelain dish +ash
M_O= mass of Organic matter

Values and Calculations

M_{P-1}: 62.0298 g M_{P-2}: 59.0730 g

M_{PDS-1}: 72.6670 g M_{PDS-2}: 70.3481 g

$M_D = M_{PDS} - M_P$

$M_{D-1} = M_{PDS-1} - M_{P-1} = 10.6372$ g

$M_{D-2} = M_{PDS-2} - M_{P-2} = 11.2751$ g

Heating to 440°C

M_{PA-1}: 72.5190 g M_{PA-2}: 70.1836 g

$M_A = M_{PA} - M_P$

$M_{A-1} = M_{PA-1} - M_{P-1} = 10.4892$ g

$M_{A-2} = M_{PA-2} - M_{P-2} = 11.1106$ g

$M_O = M_D - M_A$

$M_{O-1} = M_{D-1} - M_{A-1} = 0.1480$ g

$M_{O-2} = M_{D-2} - M_{A-2} = 0.1645$ g

Organic Matter content (OM):

Formula: $OM = (M_O / M_D) * 100$

$OM_{1-440} = (0.1480/10.6372) * 100 =$ **1.39 %**

$OM_{2-440} = (0.1645/11.2751) * 100 =$ **1.46 %**

Reheating to 550°C

$M_{PA-1-550}$: 72.4912 g $M_{PA-2-550}$: 70.1592 g

$M_A = M_{PA} - M_P$

$M_{A-1-550} = M_{PA-1-550} - M_{P-1} = 10.4614$ g

$M_{A-2-550} = M_{PA-2-550} - M_{P-2} = 11.0862$ g

$M_O = M_D - M_A$

$M_{O-1} = M_{D-1} - M_{A-1-550} = 0.1758$ g

$M_{O-2} = M_{D-2} - M_{A-2-550} = 0.1889$ g

Organic Matter content (OM):

Formula: $OM = (M_O / M_D) * 100$

$OM_{1-550} = (0.1758/10.6372) * 100 =$ **1.65 %**

$OM_{2-550} = (0.1889/11.2751) * 100 =$ **1.68 %**

Difference in Organic Matter content (OM) as result of reheating to 550°C:
Delta OM-1: 1.65 – 1.39 = **0.26 %**
Delta OM-2: 1.68 – 1.46 = **0.22 %**

Appendix E1 – Scanning Electron Microscope (SEM) EDEX results

SEM analysis was conducted on the following three polished thin-sections:

Thin-section 1

Thin-section 2

Thin-section 3

The presence, variation and amount of several elements are indicated in the elemental graphs corresponding to several areas and sub-areas of different samples (thin-sections). These areas and sub-areas are indicated for each thin-section.

Thin-section 1	
# areas analyzed:	*5*
Area:	Sub-areas:
1	*6*
2	*5*
3	*4*
4	*5*
5	*6*

Area 1:

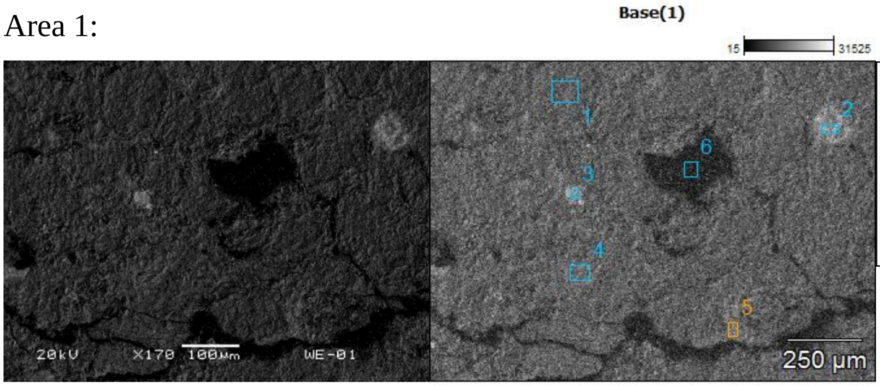

Image Name: Base(1)
Image Resolution: 512 by 384
Image Pixel Size: 2.91 µm
Acc. Voltage: 20.0 kV
Magnification: 85

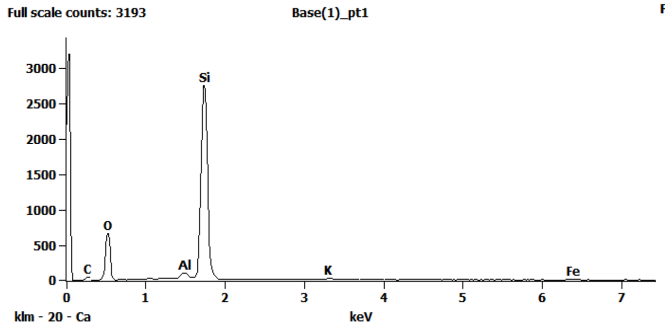

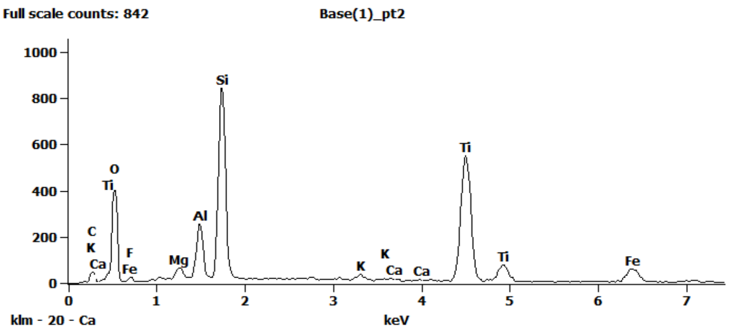

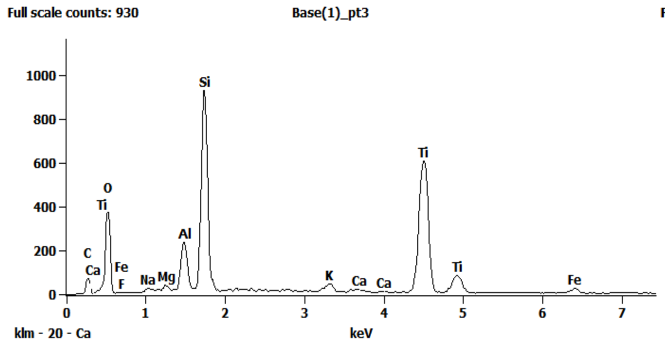

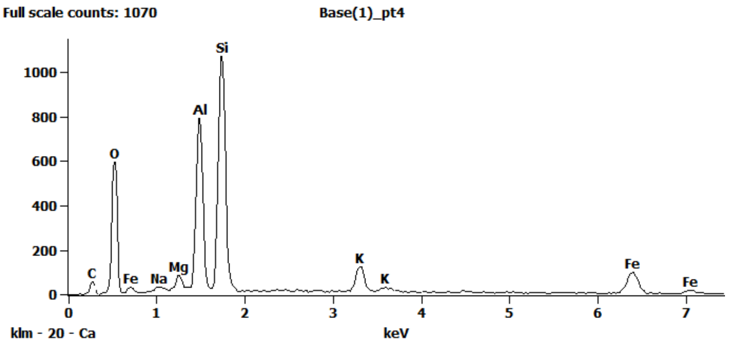

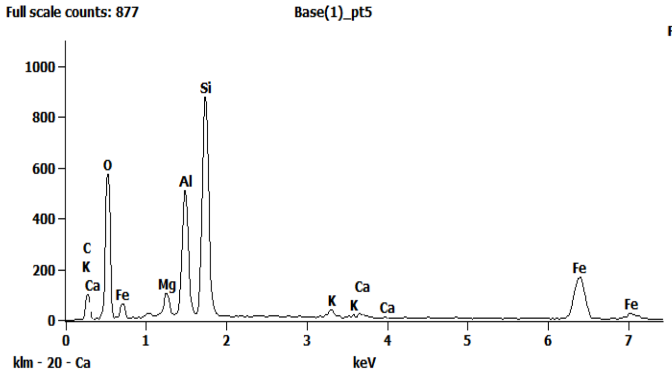

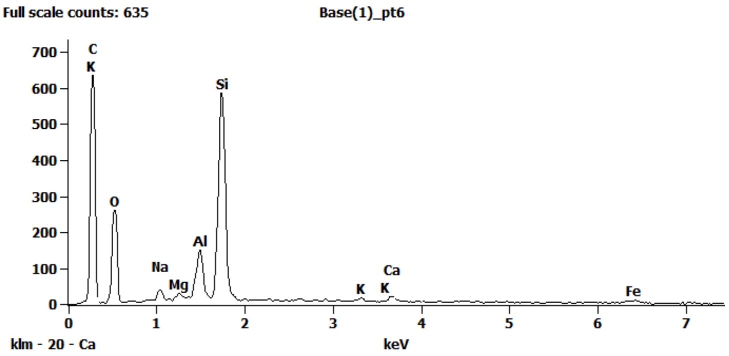

Area 2:

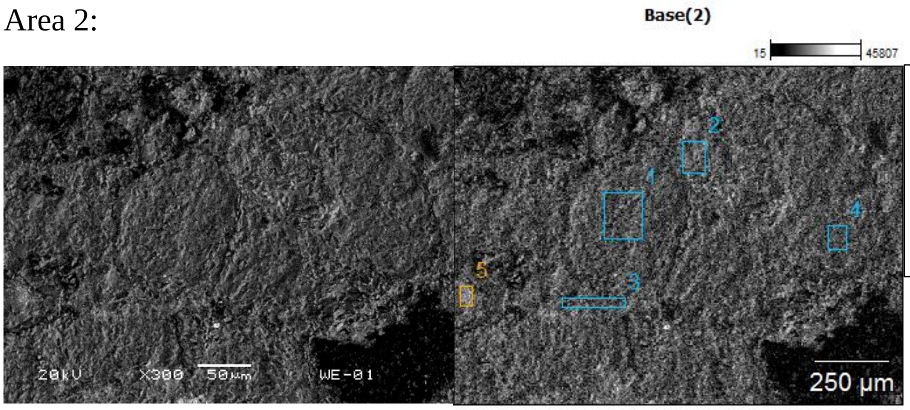

Image Name: Base(2)
Image Resolution: 512 by 384
Image Pixel Size: 2.91 μm
Acc. Voltage: 20.0 kV
Magnification: 85

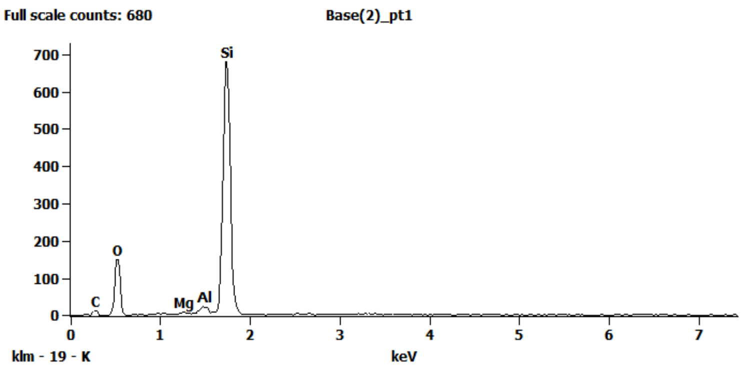

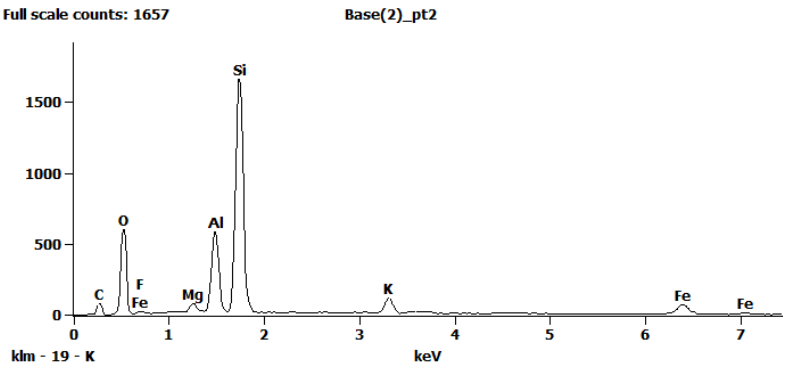

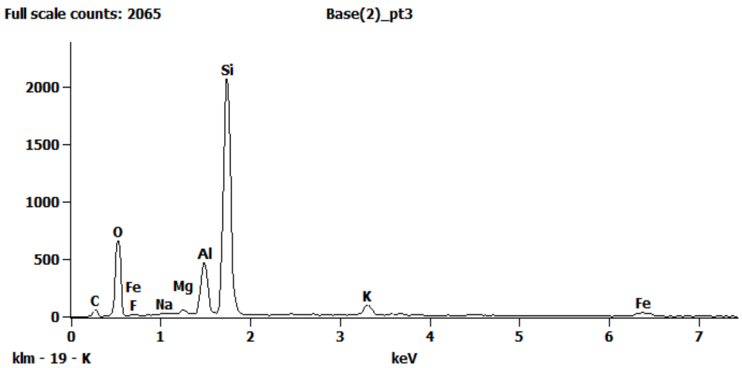

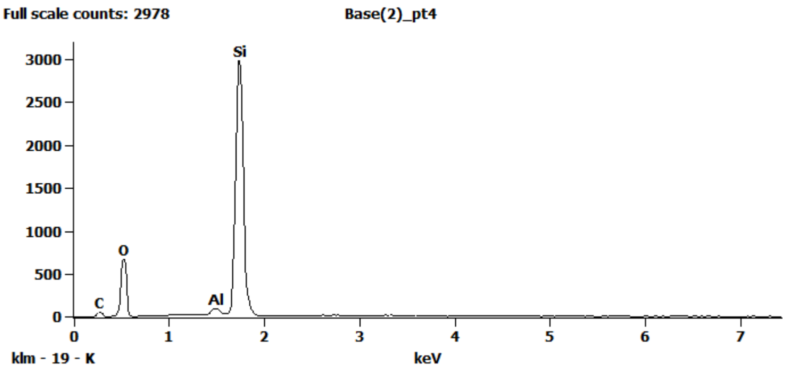

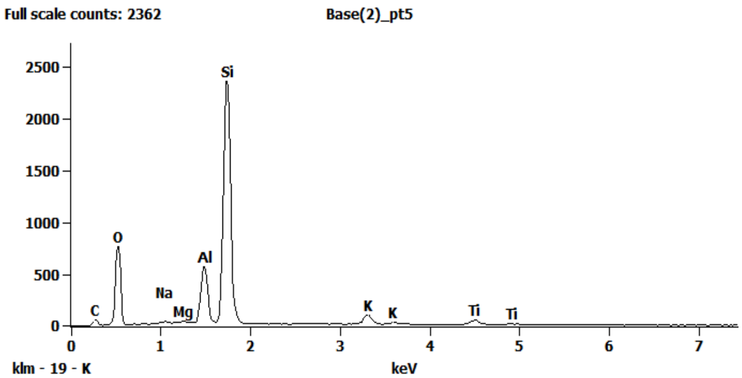

Base(4)

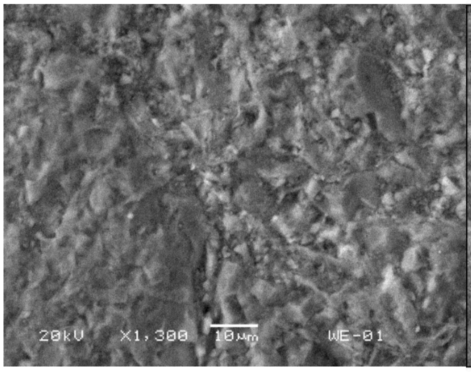

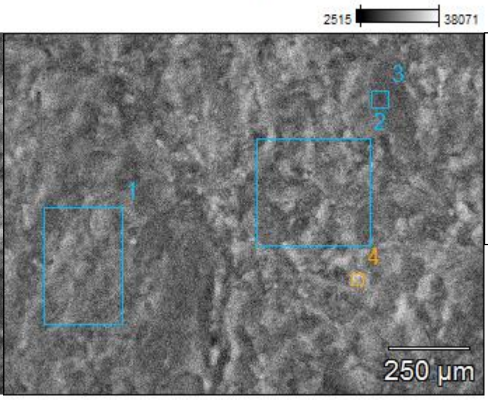

Image Name: Base(4)
Image Resolution: 512 by 384
Image Pixel Size: 2.91 µm
Acc. Voltage: 20.0 kV
Magnification: 85

Area 3:

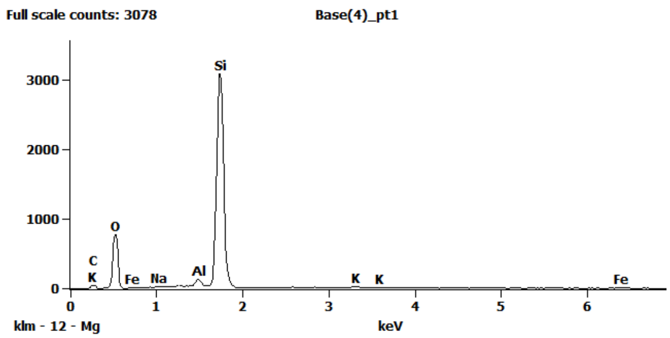

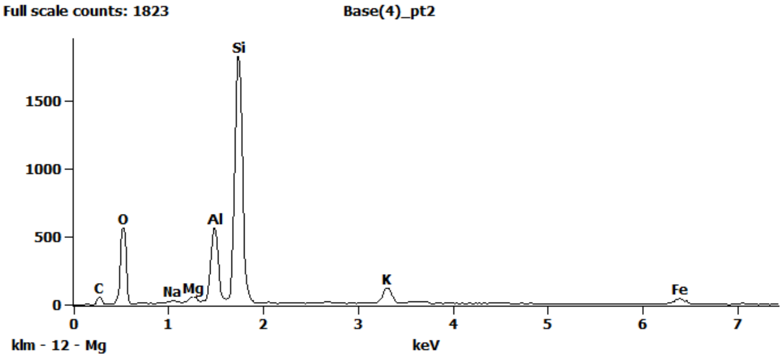

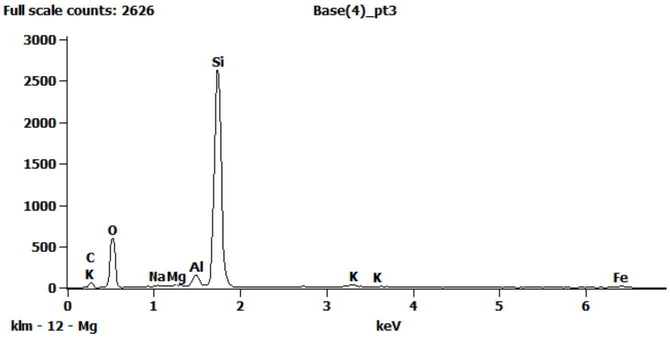

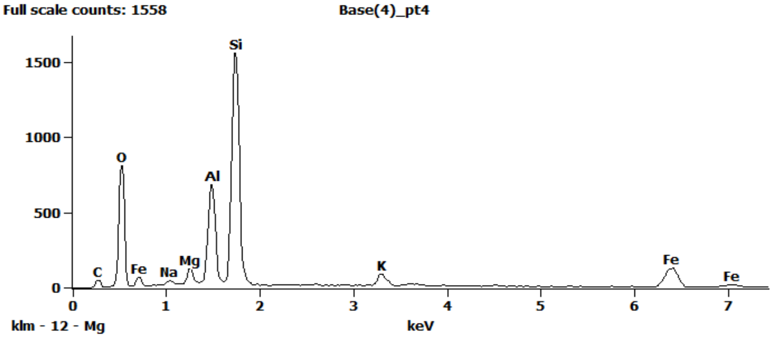

Area:4

Base(5)

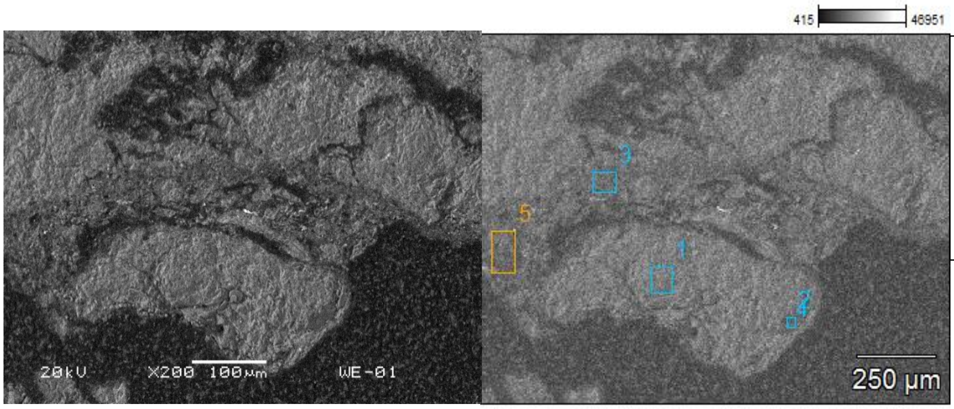

Image Name: Base(5)
Image Resolution: 512 by 384
Image Pixel Size: 2.91 µm
Acc. Voltage: 20.0 kV
Magnification: 85

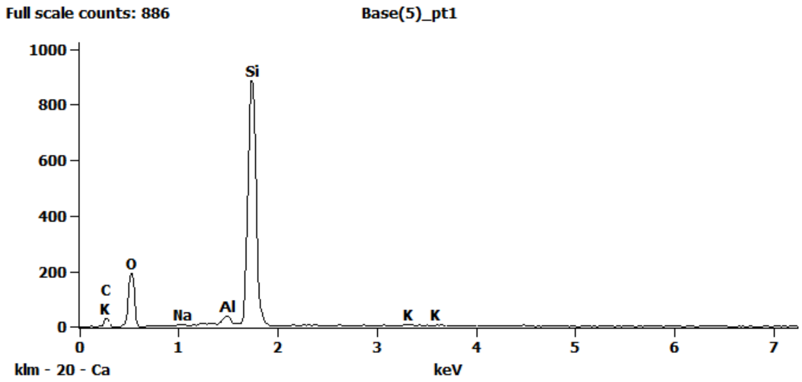
Full scale counts: 886
Base(5)_pt1
0
200
400
600
800
1000
C
K
O
Na
Al
Si
K
K
0
1
2
3
4
5
6
7
klm - 20 - Ca
keV

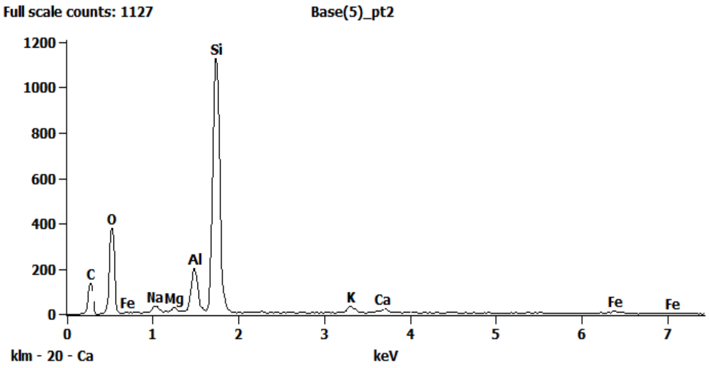
Full scale counts: 1127
Base(5)_pt2
0
200
400
600
800
1000
1200
C
O
Fe
Na
Mg
Al
Si
K
Ca
Fe
Fe
0
1
2
3
4
5
6
7
klm - 20 - Ca
keV

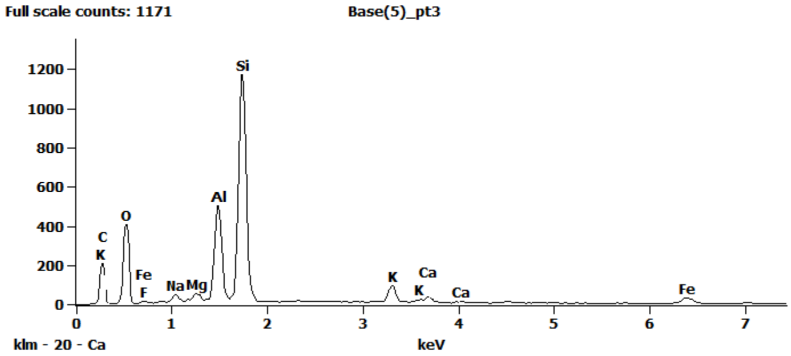
Full scale counts: 1171
Base(5)_pt3
0
200
400
600
800
1000
1200
C
K
O
Fe
F
Na
Mg
Al
Si
K
Ca
K
Ca
Fe
0
1
2
3
4
5
6
7
klm - 20 - Ca
keV

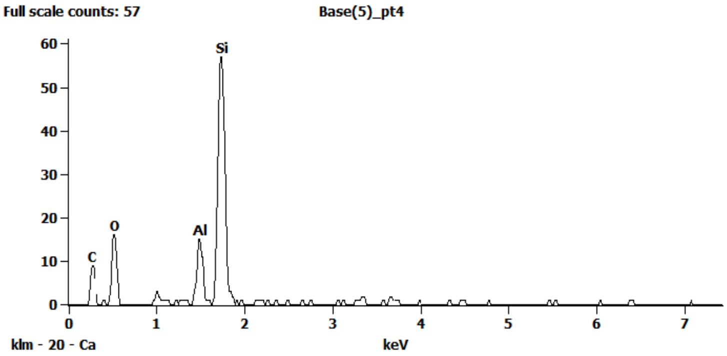
Full scale counts: 57
Base(5)_pt4
0
10
20
30
40
50
60
C
O
Al
Si
0
1
2
3
4
5
6
7
klm - 20 - Ca
keV

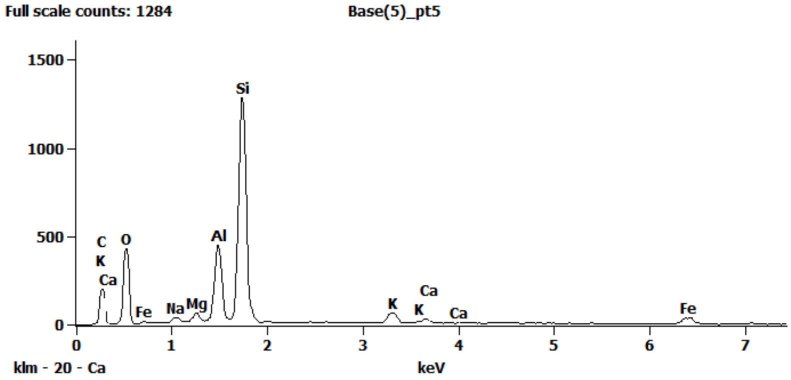
Full scale counts: 1284
Base(5)_pt5
0
500
1000
1500
C
K
Ca
O
Fe
Na
Mg
Al
Si
K
Ca
K
Ca
Fe
0
1
2
3
4
5
6
7
klm - 20 - Ca
keV

Area 5:

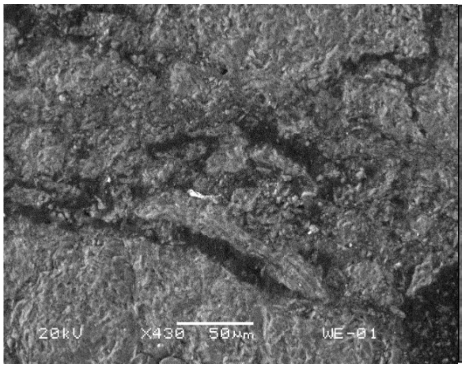

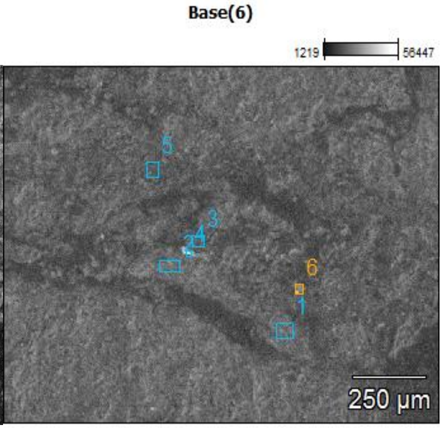

Image Name: Base(6)
Image Resolution: 512 by 384
Image Pixel Size: 2.91 µm
Acc. Voltage: 20.0 kV
Magnification: 85

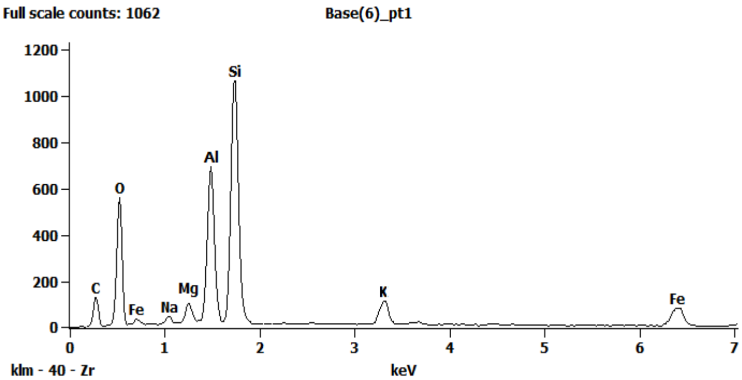

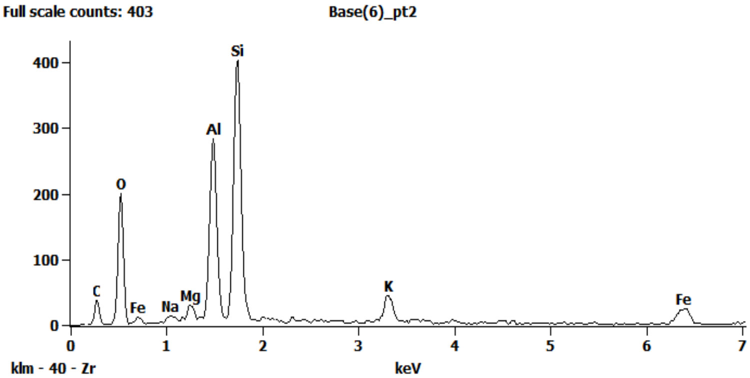

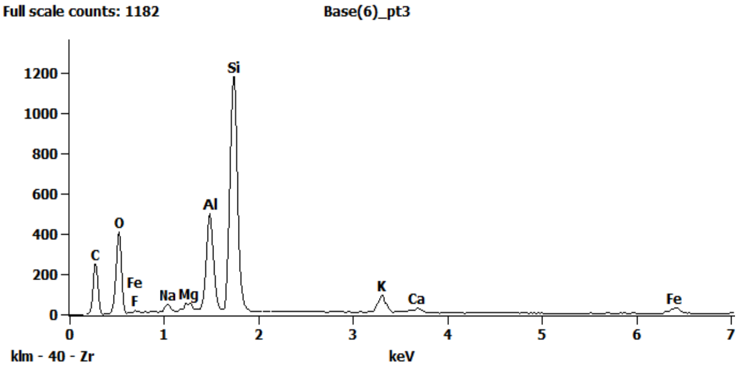

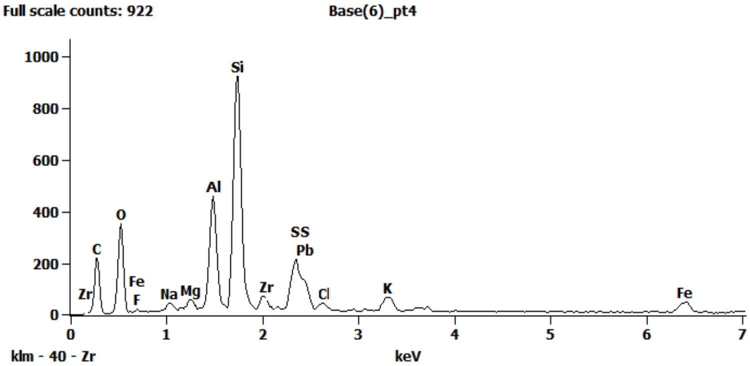

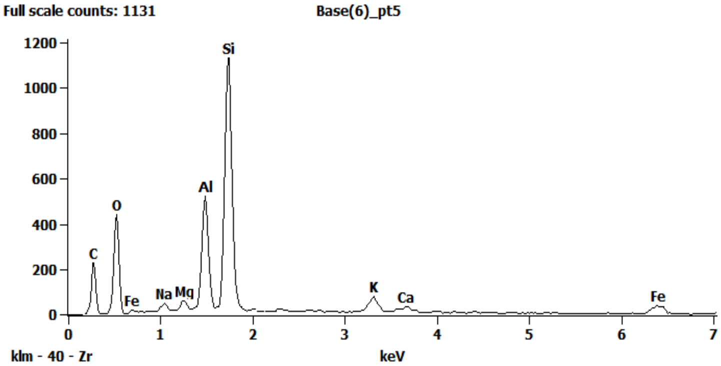

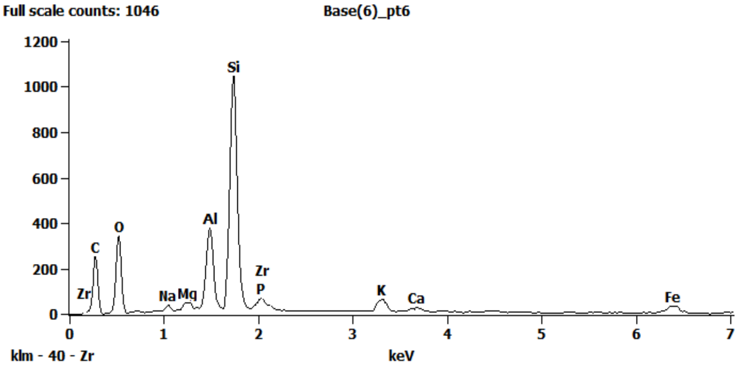

Thin-section 2	
# areas analyzed:	*3*
Area:	Sub-areas:
1	*5*
2	*3*
3	*3*

Area 1:

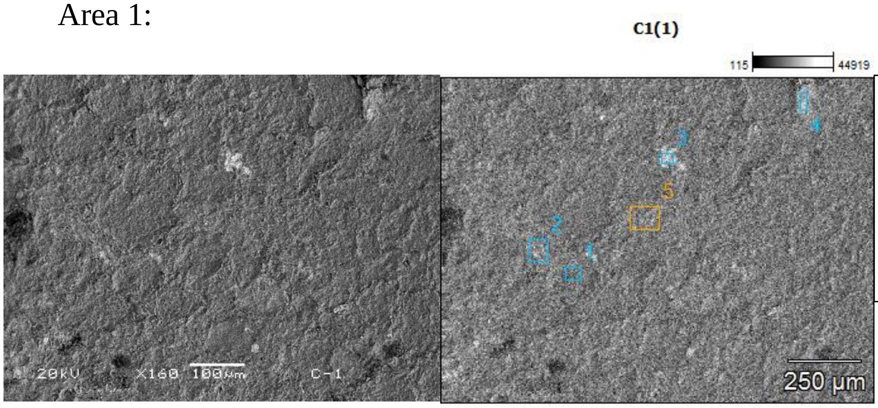

Image Name: C1(1)
Image Resolution: 512 by 384
Image Pixel Size: 2.91 µm
Acc. Voltage: 20.0 kV
Magnification: 85

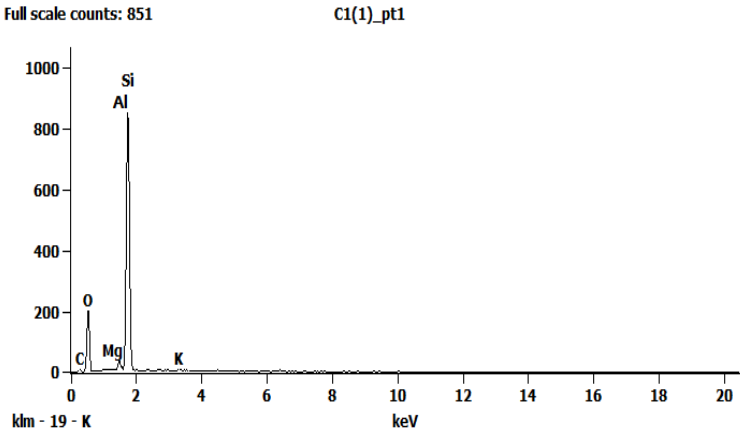

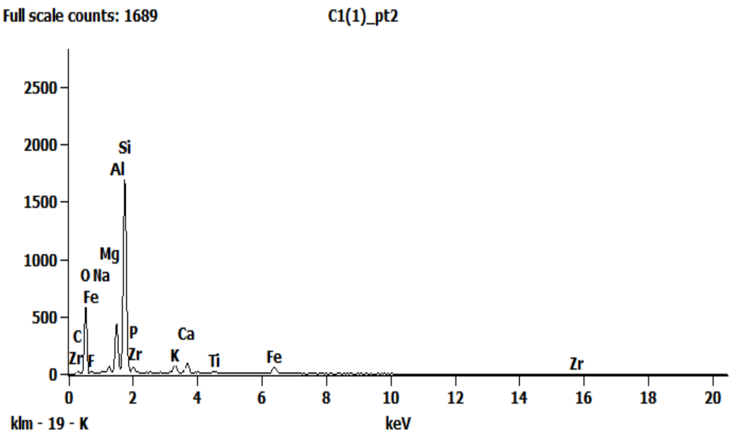

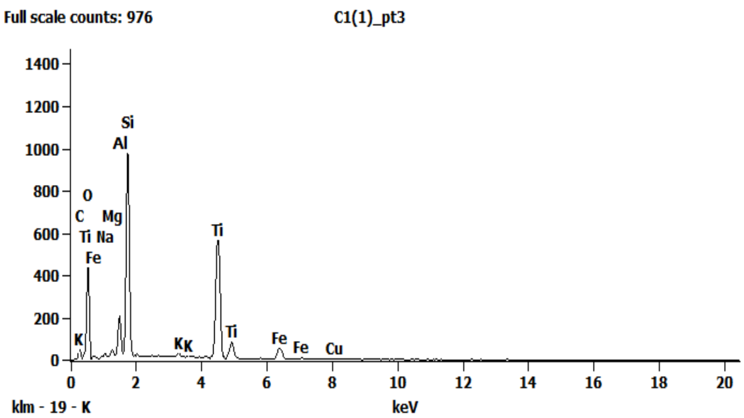

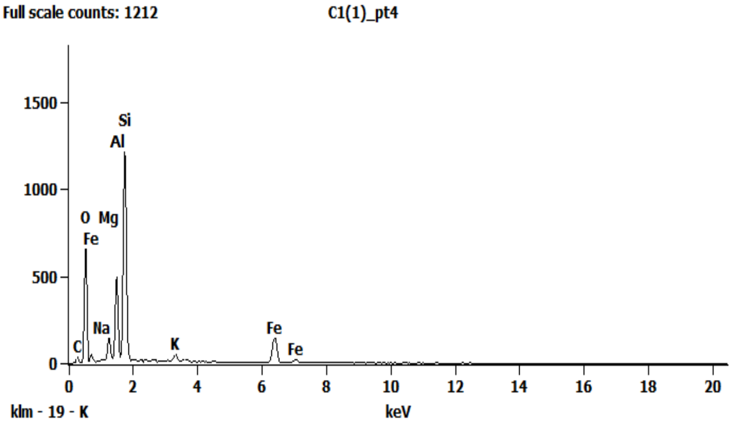

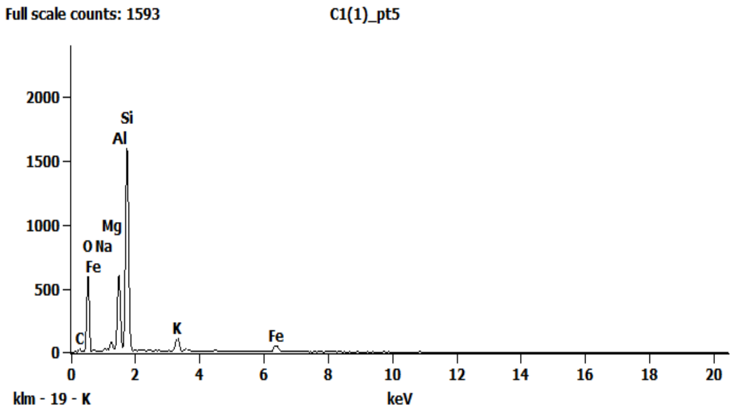

Area 2:

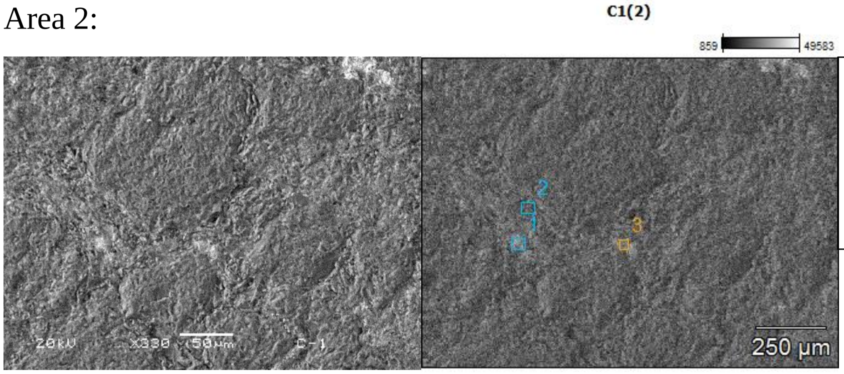

Image Name: C1(2)
Image Resolution: 512 by 384
Image Pixel Size: 2.91 µm
Acc. Voltage: 20.0 kV
Magnification: 85

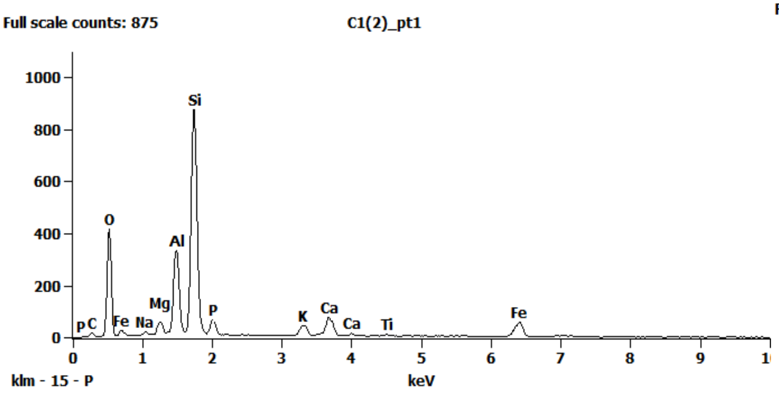

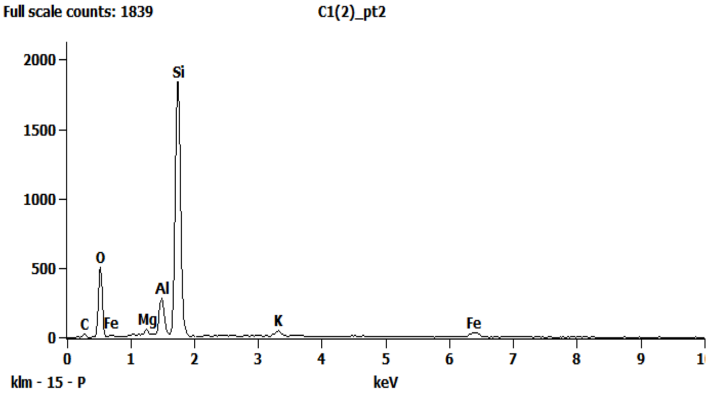

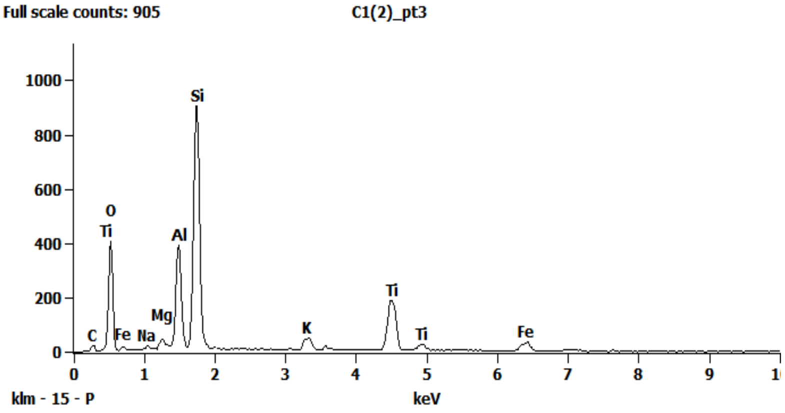

Area 3:

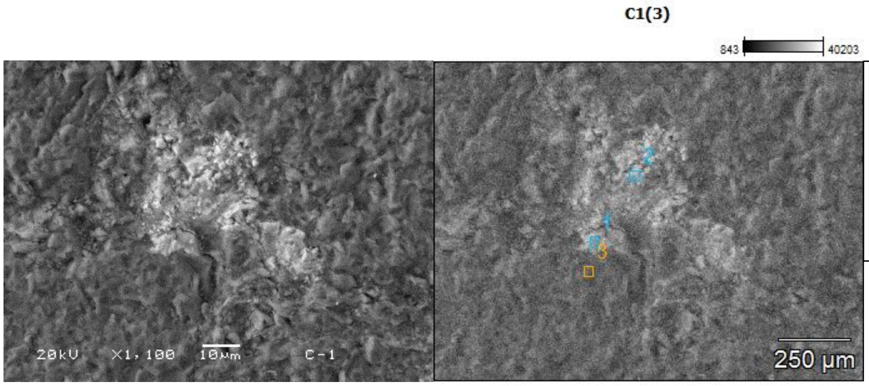

Image Name: C1(3)
Image Resolution: 512 by 384
Image Pixel Size: 2.91 µm
Acc. Voltage: 20.0 kV
Magnification: 85

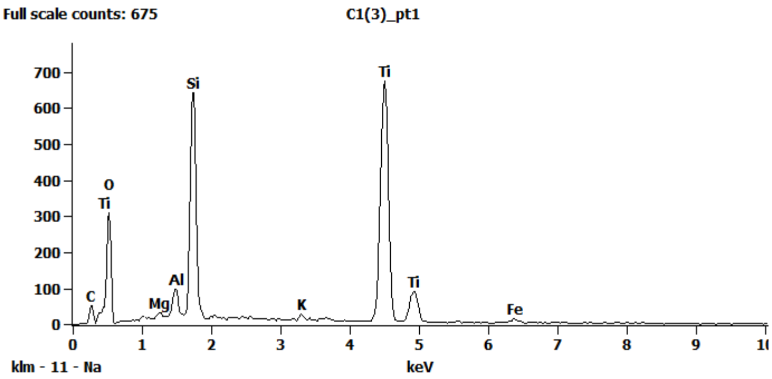

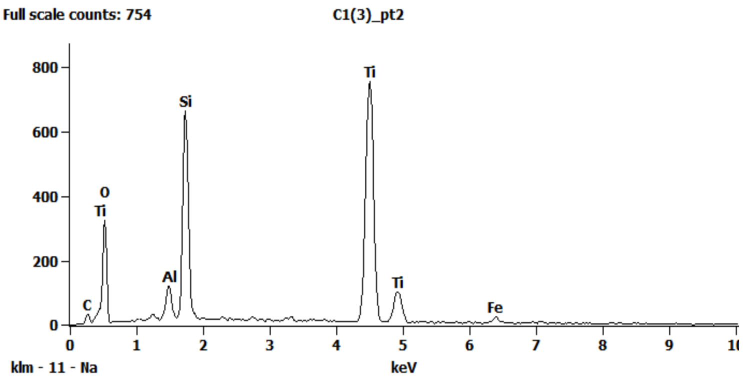

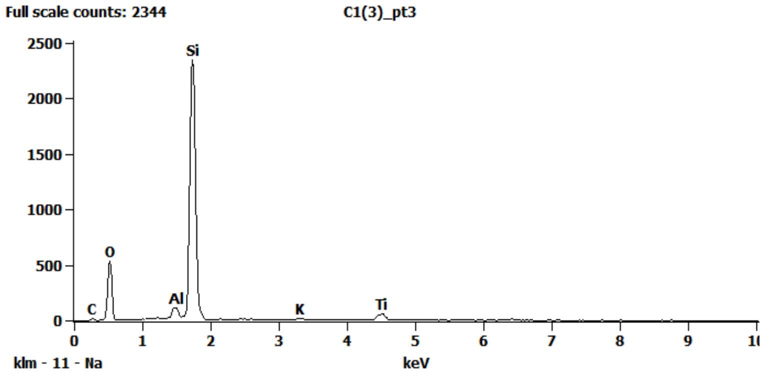

Thin-section 3	
# areas analyzed:	*8*
Area:	Sub-areas:
1	*2*
2	*1*
3	*4*
4	*6*
5	*3*
6	*3*
7	*1*
8	*3*

Area 1:

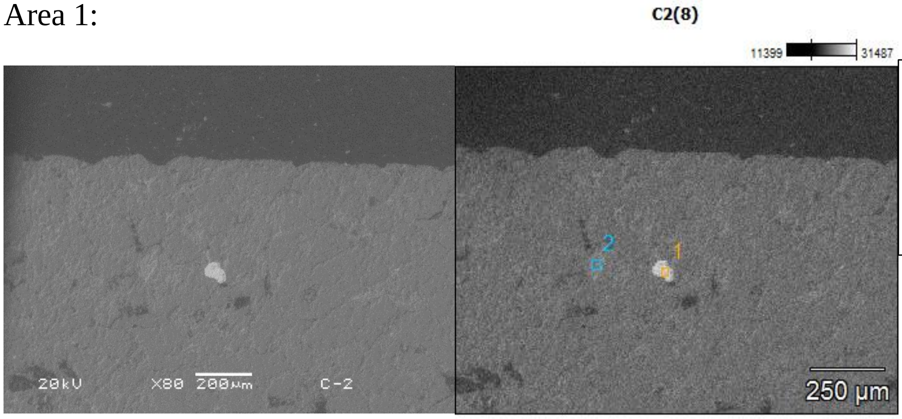

Image Name: C2(8)
Image Resolution: 512 by 384
Image Pixel Size: 2.91 µm
Acc. Voltage: 20.0 kV
Magnification: 85

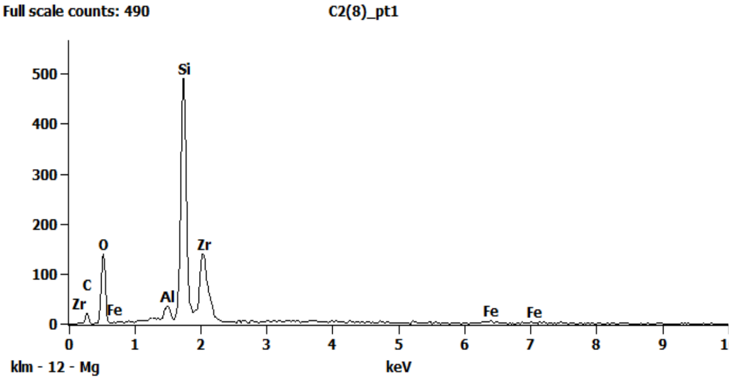

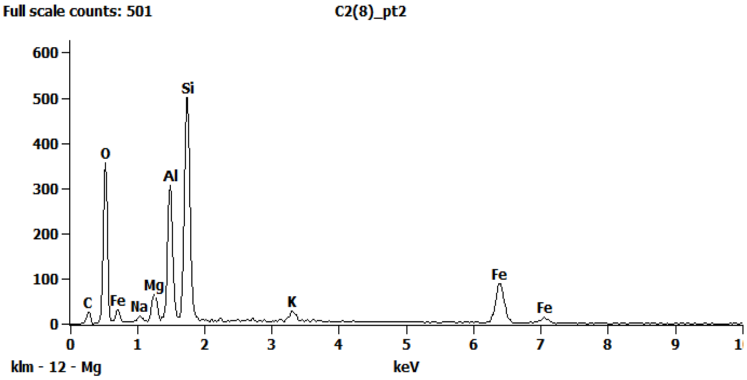

Area 2:

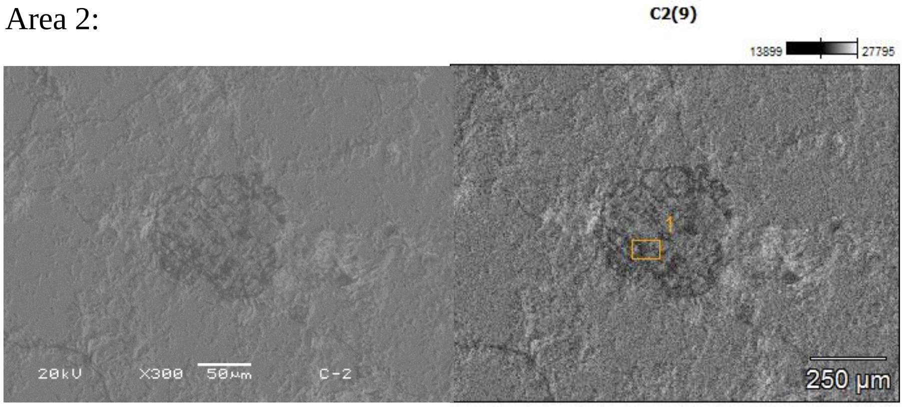

Image Name: C2(9)
Image Resolution: 512 by 384
Image Pixel Size: 2.91 µm
Acc. Voltage: 20.0 kV
Magnification: 85

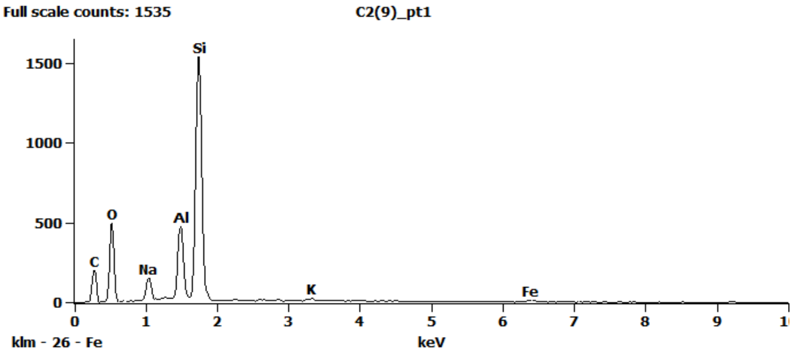

Area 3:

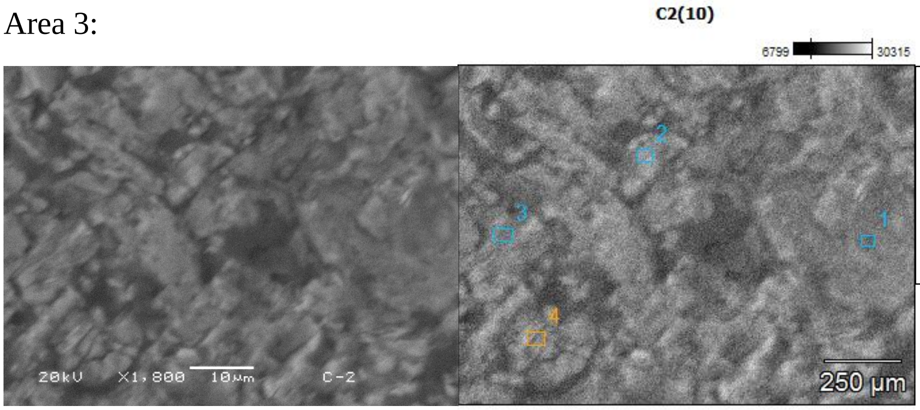

Image Name: C2(10)
Image Resolution: 512 by 384
Image Pixel Size: 2.91 µm
Acc. Voltage: 20.0 kV
Magnification: 85

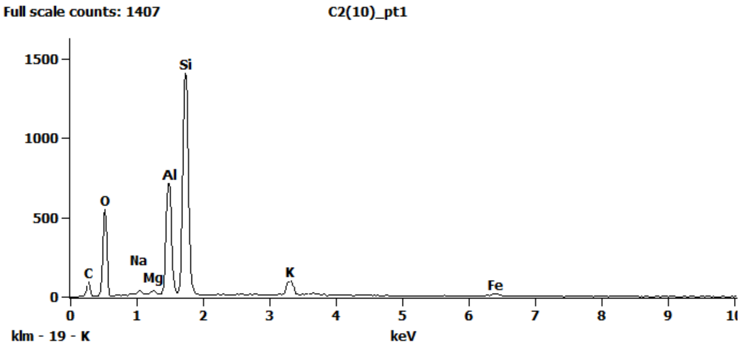

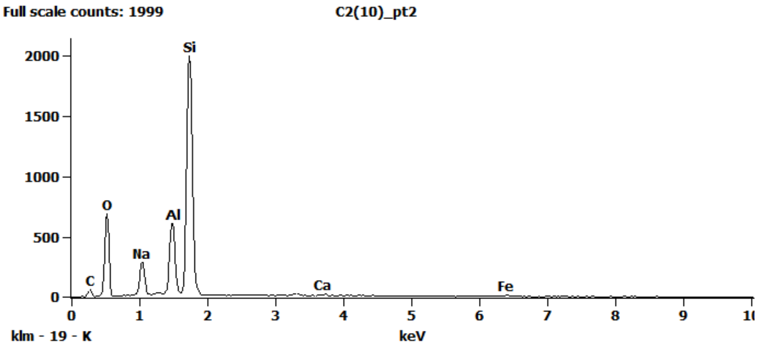

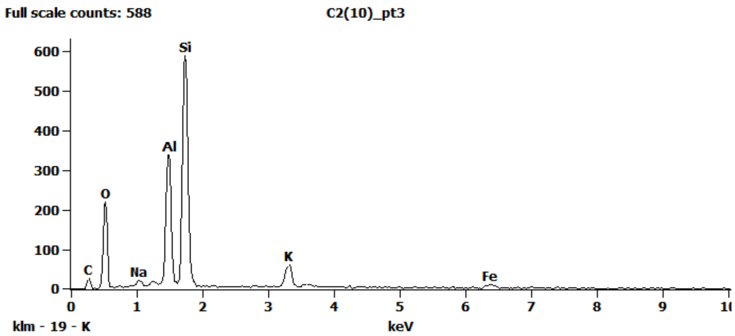

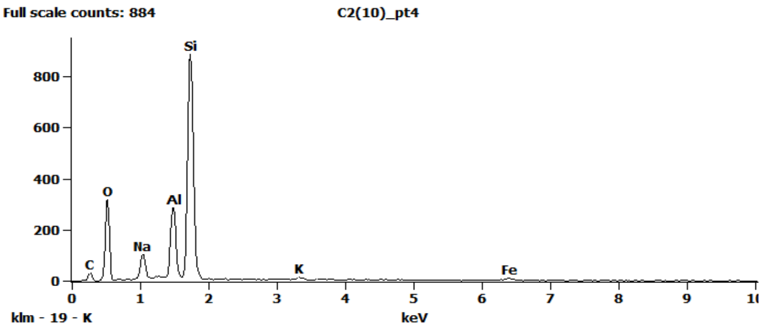

Area 4:

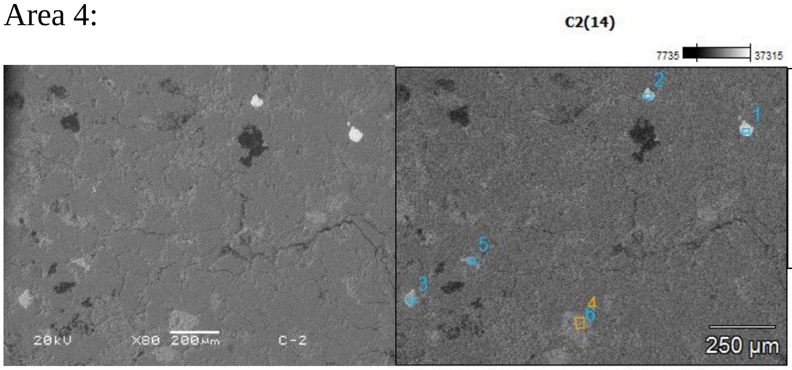

Image Name: C2(14)
Image Resolution: 512 by 384
Image Pixel Size: 2.91 µm
Acc. Voltage: 20.0 kV
Magnification: 85

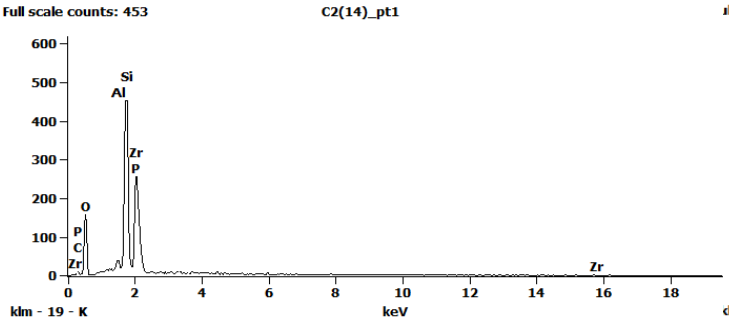

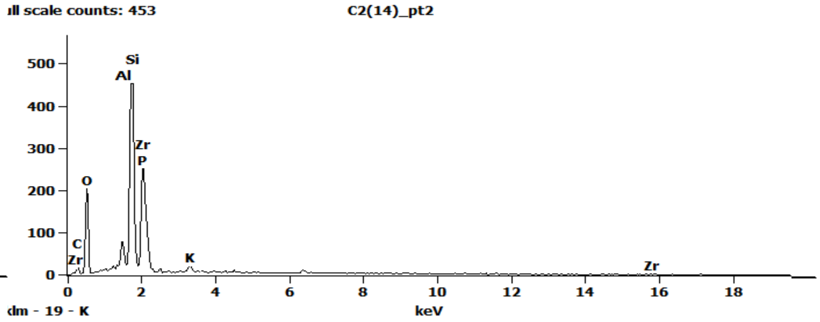

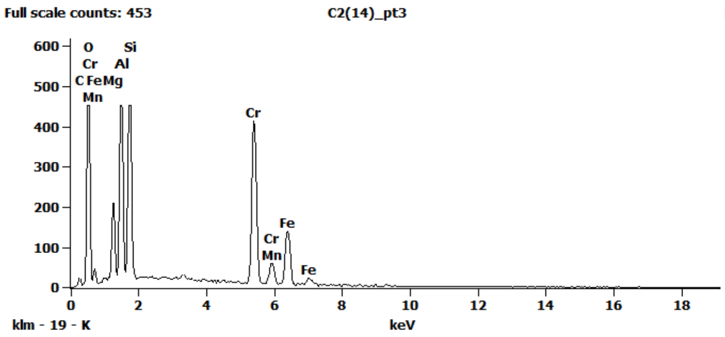

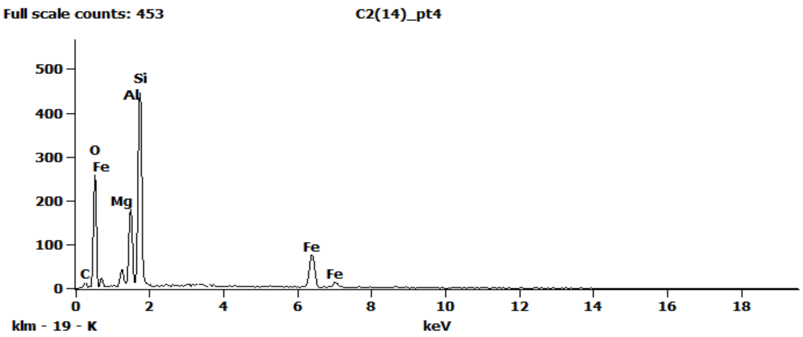

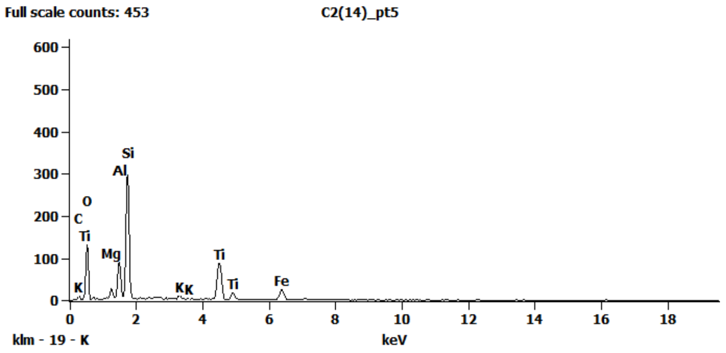

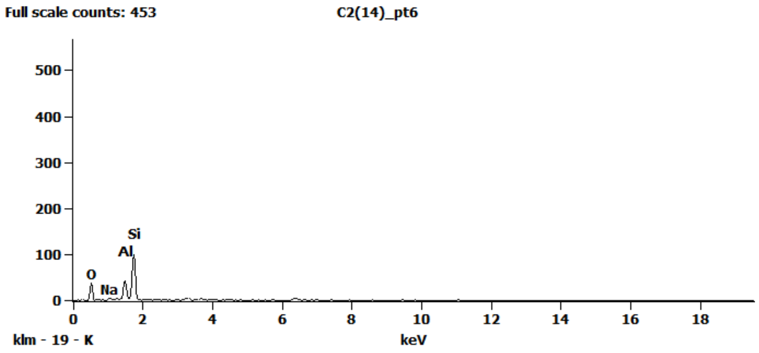

Area 5:

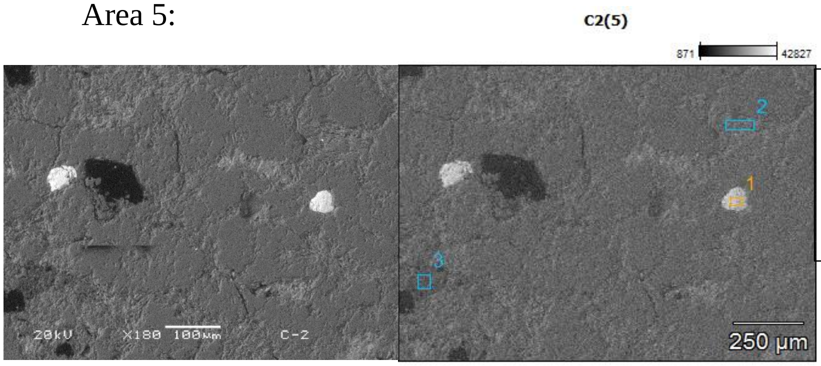

Image Name: C2(5)
Image Resolution: 512 by 384
Image Pixel Size: 2.91 µm
Acc. Voltage: 20.0 kV
Magnification: 85

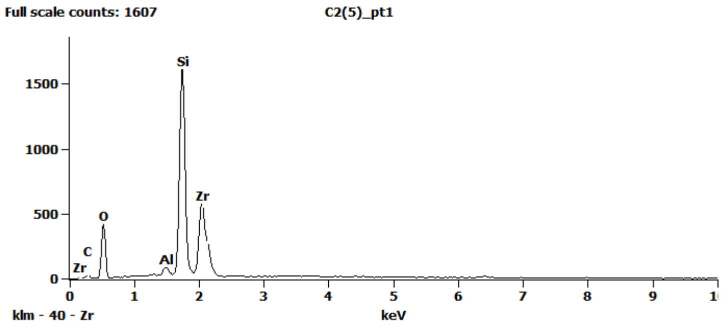

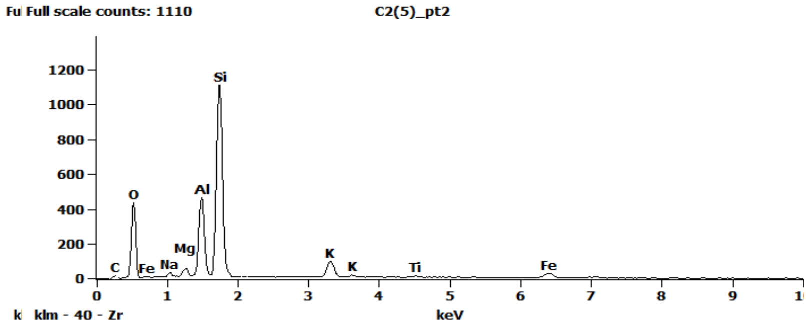

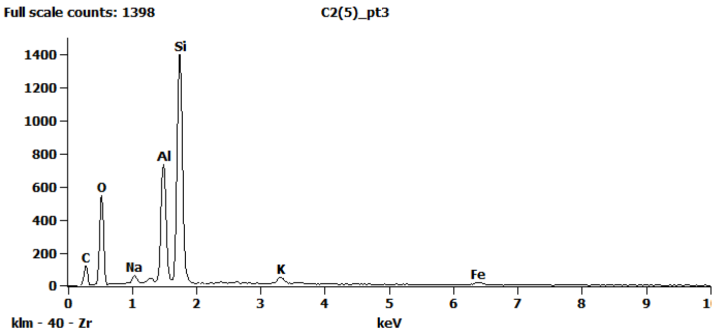

Area 6:

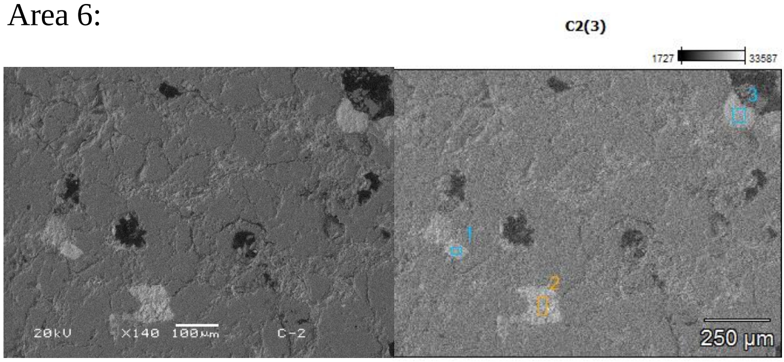

Image Name: C2(3)
Image Resolution: 512 by 384
Image Pixel Size: 2.91 µm
Acc. Voltage: 20.0 kV
Magnification: 85

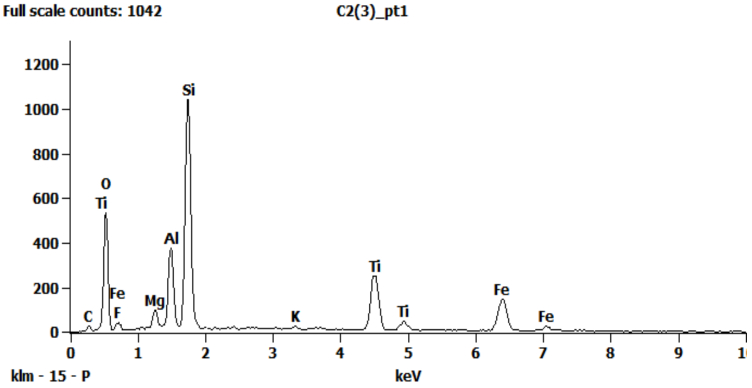

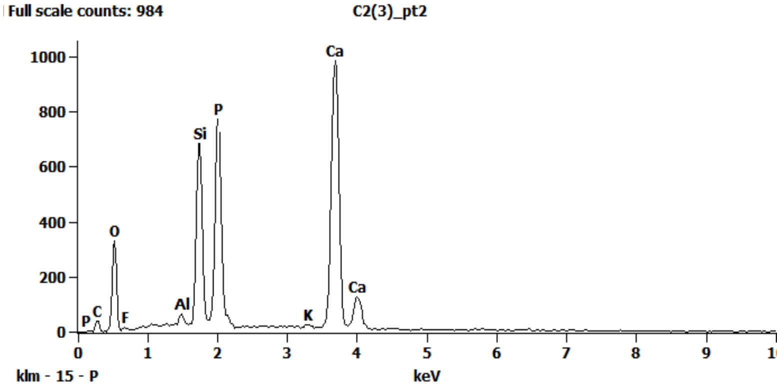

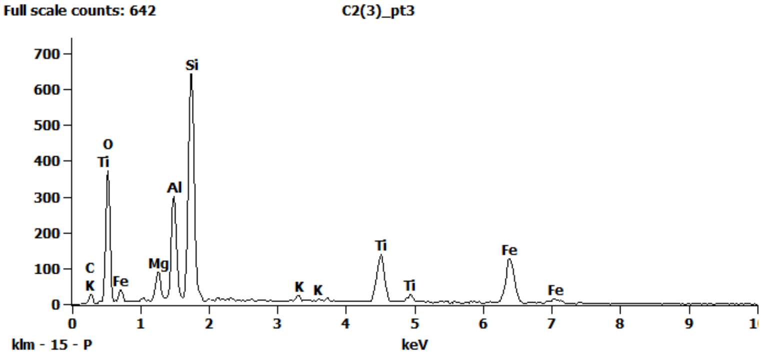

Area 7:

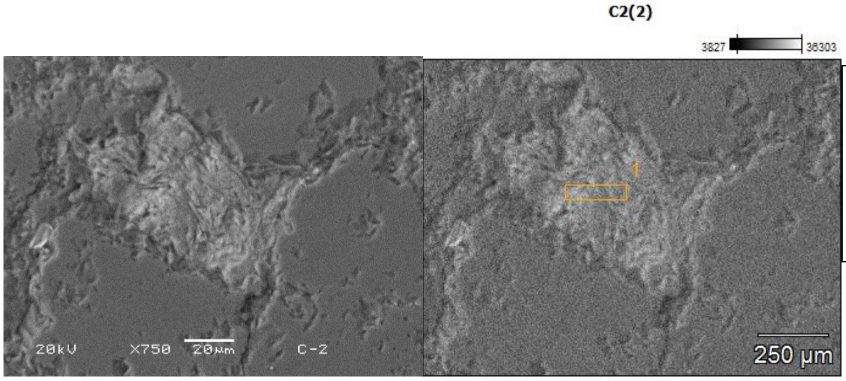

Image Name: C2(2)
Image Resolution: 512 by 384
Image Pixel Size: 2.91 µm
Acc. Voltage: 20.0 kV
Magnification: 85

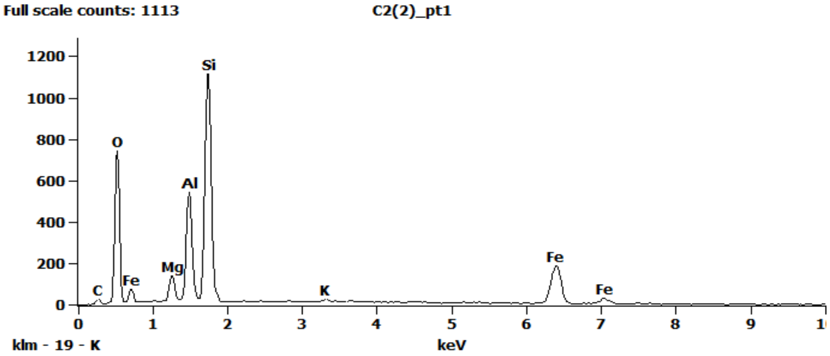

Area 8:

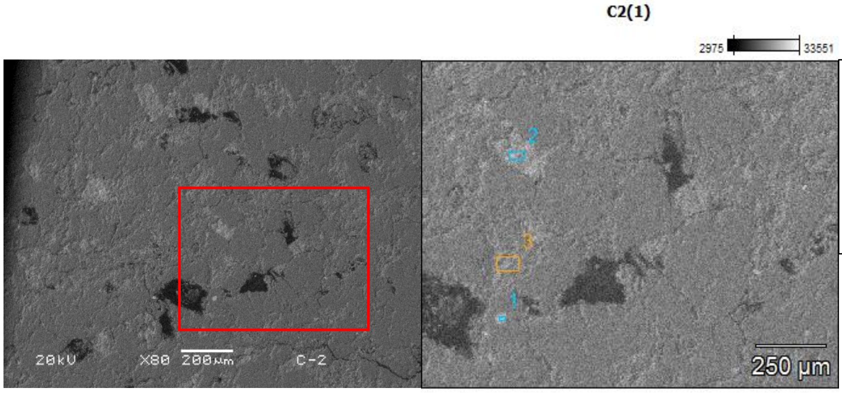

Image Name: C2(1)
Image Resolution: 512 by 384
Image Pixel Size: 2.91 µm
Acc. Voltage: 20.0 kV
Magnification: 85

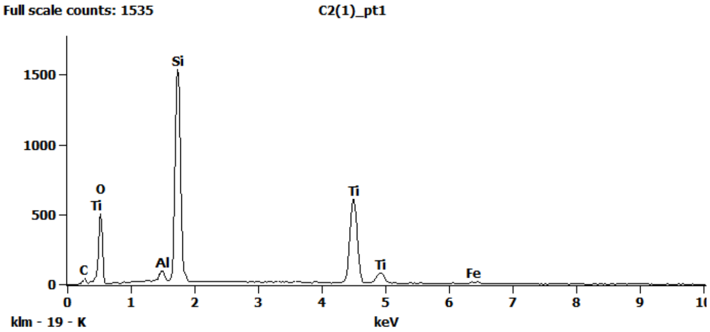

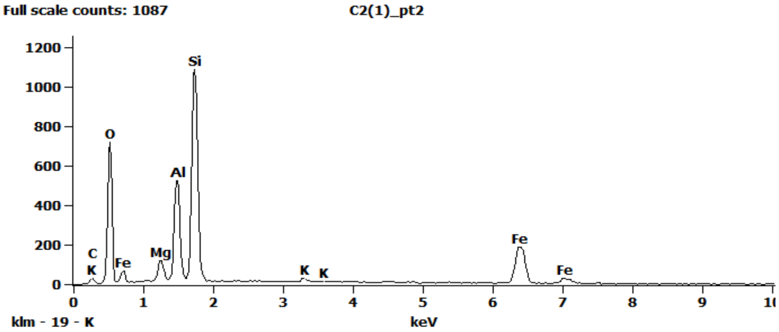

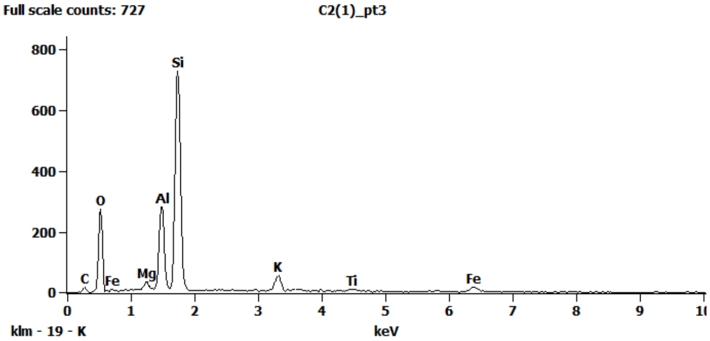

Appendix E2 – Elemental table of SEM analysis – sorted by weight

TABLE 3: THIS TABLE CONTAINS THE ELEMENTS THAT WERE FOUND IN SEVERAL AREAS WHICH WERE SUBJECTED TO SEM AND EDEX ANALYSIS.

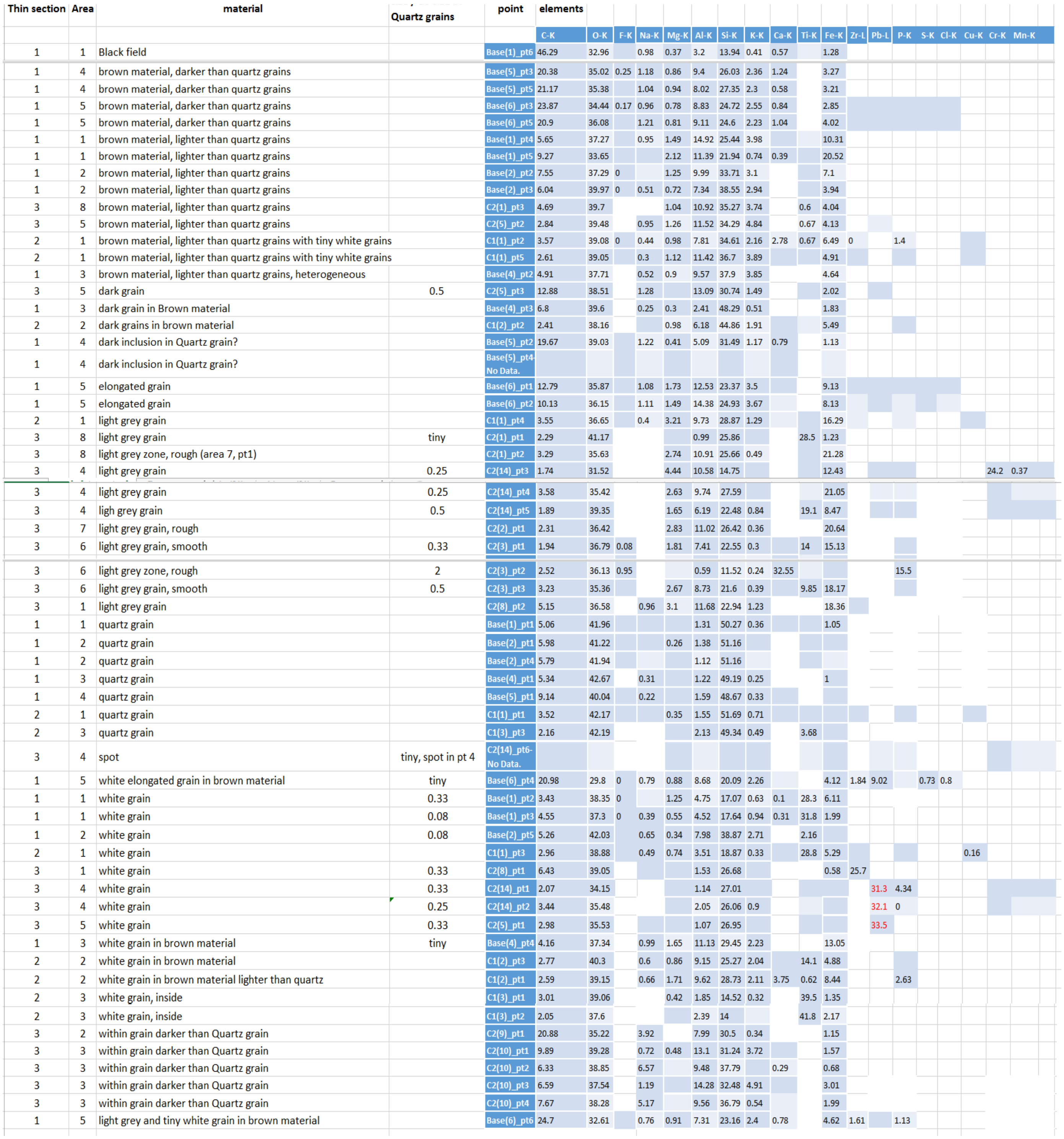

Thin section	Area	material	Quartz grains	point	elements																		
					C-K	O-K	F-K	Na-K	Mg-K	Al-K	Si-K	K-K	Ca-K	Ti-K	Fe-K	Zr-L	Pb-L	P-K	S-K	Cl-K	Cu-K	Cr-K	Mn-K
1	1	Black field		Base(1)_pt6	46.29	32.96		0.98	0.37	3.2	13.94	0.41	0.57		1.28								
1	4	brown material, darker than quartz grains		Base(5)_pt3	20.38	35.02	0.25	1.18	0.86	9.4	26.03	2.36	1.24		3.27								
1	4	brown material, darker than quartz grains		Base(5)_pt5	21.17	35.38		1.04	0.94	8.02	27.35	2.3	0.58		3.21								
1	5	brown material, darker than quartz grains		Base(6)_pt3	23.87	34.44	0.17	0.96	0.78	8.83	24.72	2.55	0.84		2.85								
1	5	brown material, darker than quartz grains		Base(6)_pt5	20.9	36.08		1.21	0.81	9.11	24.6	2.23	1.04		4.02								
1	1	brown material, lighter than quartz grains		Base(1)_pt4	5.65	37.27		0.95	1.49	14.92	25.44	3.98			10.31								
1	1	brown material, lighter than quartz grains		Base(1)_pt5	9.27	33.65			2.12	11.39	21.94	0.74	0.39		20.52								
1	2	brown material, lighter than quartz grains		Base(2)_pt2	7.55	37.29	0		1.25	9.99	33.71	3.1			7.1								
1	2	brown material, lighter than quartz grains		Base(2)_pt3	6.04	39.97	0	0.51	0.72	7.34	38.55	2.94			3.94								
3	8	brown material, lighter than quartz grains		C2(1)_pt3	4.69	39.7			1.04	10.92	35.27	3.74		0.6	4.04								
3	5	brown material, lighter than quartz grains		C2(5)_pt2	2.84	39.48		0.95	1.26	11.52	34.29	4.84		0.67	4.13								
2	1	brown material, lighter than quartz grains with tiny white grains		C1(1)_pt2	3.57	39.08	0	0.44	0.98	7.81	34.61	2.16	2.78	0.67	6.49	0		1.4					
2	1	brown material, lighter than quartz grains with tiny white grains		C1(1)_pt5	2.61	39.05		0.3	1.12	11.42	36.7	3.89			4.91								
1	3	brown material, lighter than quartz grains, heterogeneous		Base(4)_pt2	4.91	37.71		0.52	0.9	9.57	37.9	3.85			4.64								
3	5	dark grain	0.5	C2(5)_pt3	12.88	38.51		1.28		13.09	30.74	1.49			2.02								
1	3	dark grain in Brown material		Base(4)_pt3	6.8	39.6		0.25	0.3	2.41	48.29	0.51			1.83								
2	2	dark grains in brown material		C1(2)_pt2	2.41	38.16			0.98	6.18	44.86	1.91			5.49								
1	4	dark inclusion in Quartz grain?		Base(5)_pt2	19.67	39.03		1.22	0.41	5.09	31.49	1.17	0.79		1.13								
1	4	dark inclusion in Quartz grain?		Base(5)_pt4-No Data.																			
1	5	elongated grain		Base(6)_pt1	12.79	35.87		1.08	1.73	12.53	23.37	3.5			9.13								
1	5	elongated grain		Base(6)_pt2	10.13	36.15		1.11	1.49	14.38	24.93	3.67			8.13								
2	1	light grey grain		C1(1)_pt4	3.55	36.65		0.4	3.21	9.73	28.87	1.29			16.29								
3	8	light grey grain	tiny	C2(1)_pt1	2.29	41.17				0.99	25.86			28.5	1.23								
3	8	light grey zone, rough (area 7, pt1)		C2(1)_pt2	3.29	35.63			2.74	10.91	25.66	0.49			21.28								
3	4	light grey grain	0.25	C2(14)_pt3	1.74	31.52			4.44	10.58	14.75				12.43							24.2	0.37
3	4	light grey grain	0.25	C2(14)_pt4	3.58	35.42			2.63	9.74	27.59				21.05								
3	4	ligh grey grain	0.5	C2(14)_pt5	1.89	39.35			1.65	6.19	22.48	0.84		19.1	8.47								
3	7	light grey grain, rough		C2(2)_pt1	2.31	36.42			2.83	11.02	26.42	0.36			20.64								
3	6	light grey grain, smooth	0.33	C2(3)_pt1	1.94	36.79	0.08		1.81	7.41	22.55	0.3		14	15.13								
3	6	light grey zone, rough	2	C2(3)_pt2	2.52	36.13	0.95			0.59	11.52	0.24	32.55					15.5					
3	6	light grey grain, smooth	0.5	C2(3)_pt3	3.23	35.36			2.67	8.73	21.6	0.39		9.85	18.17								
3	1	light grey grain		C2(8)_pt2	5.15	36.58		0.96	3.1	11.68	22.94	1.23			18.36								
1	1	quartz grain		Base(1)_pt1	5.06	41.96				1.31	50.27	0.36			1.05								
1	2	quartz grain		Base(2)_pt1	5.98	41.22			0.26	1.38	51.16												
1	2	quartz grain		Base(2)_pt4	5.79	41.94				1.12	51.16												
1	3	quartz grain		Base(4)_pt1	5.34	42.67		0.31		1.22	49.19	0.25			1								
1	4	quartz grain		Base(5)_pt1	9.14	40.04		0.22		1.59	48.67	0.33											
2	1	quartz grain		C1(1)_pt1	3.52	42.17			0.35	1.55	51.69	0.71											
2	3	quartz grain		C1(3)_pt3	2.16	42.19				2.13	49.34	0.49		3.68									
3	4	spot	tiny, spot in pt 4	C2(14)_pt6-No Data.																			
1	5	white elongated grain in brown material	tiny	Base(6)_pt4	20.98	29.8	0	0.79	0.88	8.68	20.09	2.26			4.12	1.84	9.02		0.73	0.8			
1	1	white grain	0.33	Base(1)_pt2	3.43	38.35	0		1.25	4.75	17.07	0.63	0.1	28.3	6.11								
1	1	white grain	0.08	Base(1)_pt3	4.55	37.3	0	0.39	0.55	4.52	17.64	0.94	0.31	31.8	1.99								
1	2	white grain	0.08	Base(2)_pt5	5.26	42.03		0.65	0.34	7.98	38.87	2.71		2.16									
2	1	white grain		C1(1)_pt3	2.96	38.88		0.49	0.74	3.51	18.87	0.33		28.8	5.29						0.16		
3	1	white grain	0.33	C2(8)_pt1	6.43	39.05				1.53	26.68				0.58	25.7							
3	4	white grain	0.33	C2(14)_pt1	2.07	34.15				1.14	27.01						31.3	4.34					
3	4	white grain	0.25	C2(14)_pt2	3.44	35.48				2.05	26.06	0.9					32.1	0					
3	5	white grain	0.33	C2(5)_pt1	2.98	35.53				1.07	26.95						33.5						
1	3	white grain in brown material	tiny	Base(4)_pt4	4.16	37.34		0.99	1.65	11.13	29.45	2.23			13.05								
2	2	white grain in brown material		C1(2)_pt3	2.77	40.3		0.6	0.86	9.15	25.27	2.04		14.1	4.88								
2	2	white grain in brown material lighter than quartz		C1(2)_pt1	2.59	39.15		0.66	1.71	9.62	28.73	2.11	3.75	0.62	8.44			2.63					
2	3	white grain, inside		C1(3)_pt1	3.01	39.06			0.42	1.85	14.52	0.32		39.5	1.35								
2	3	white grain, inside		C1(3)_pt2	2.05	37.6				2.39	14			41.8	2.17								
3	2	within grain darker than Quartz grain		C2(9)_pt1	20.88	35.22		3.92		7.99	30.5	0.34			1.15								
3	3	within grain darker than Quartz grain		C2(10)_pt1	9.89	39.28		0.72	0.48	13.1	31.24	3.72			1.57								
3	3	within grain darker than Quartz grain		C2(10)_pt2	6.33	38.85		6.57		9.48	37.79		0.29		0.68								
3	3	within grain darker than Quartz grain		C2(10)_pt3	6.59	37.54		1.19		14.28	32.48	4.91			3.01								
3	3	within grain darker than Quartz grain		C2(10)_pt4	7.67	38.28		5.17		9.56	36.79	0.54			1.99								
1	5	light grey and tiny white grain in brown material		Base(6)_pt6	24.7	32.61		0.76	0.91	7.31	23.16	2.4	0.78		4.62	1.61		1.13					

Appendix F – Chemical names and formulas

Table 4: Mineral and elemental names and chemical formulas

Mineral	**Formula**
Aluminium (-oxide)	Al_2O_3
Apatite	$Ca_5(PO_4)_3(F,Cl,OH)$
Chlorite	ClO_2
Feldspar	$(KAlSi_3O_8 – NaAlSi_3O_8 – CaAl_2Si_2O_8$ (situation dependant)
Glauconite	$(K,Na)(Fe^{3+},Al,Mg)_2(Si,Al)_4O_{10}(OH)_2$
Hematite	Fe_2O_3
Ilmenite	$FeTiO_3$
Iron (-III-oxide)	Fe_2O_3
Mica	$AB_{2-3}(X, Si)_4O_{10}(O, F, OH)_2$ (situation dependant)
Quartz	SiO_2
Rutile	TiO_2
Zircon	$ZrSiO_4$
Element	**Formula**
Calcium	Ca
Fluor	F
Iron	Fe
Lead	Pb
Magnesium	Mg
Phosphorus	P
Potassium	K
Silicon	Si
Sodium	Na
Titanium	Ti
Zinc	Zn
Zirconium	Zr